Electronic components & applications

Vol. 5, N
June 19

ISSN 0141 – 6219

Electronic components & applications

Volume 5, No. 3 June 1983

Direct broadcast satellite tv is almost with us. After years of negotiation, cooperation and test flights, we will shortly see the launching of the first European direct broadcast television satellite. Poised about 36 000 km above the Earth, such satellites will bring a wider choice of programmes into European homes. Suddenly the world of professional components has been brought to our rooftops, if not our firesides. Components for frequencies of around 12 GHz are not new – but mass producing them is. The most important new component in the receiving aerial is the downconverter, which converts the 12 GHz satellite frequencies down to 1 GHz for transmission by coaxial cable into the house. Elcoma has been making components for the professional microwave industry for many years and has recently introduced new downconverters for private (and community antenna) satellite tv reception.

Contents

CMOS gate arrays – the fast way to semi-custom logic 130
R. Croes

Data communications 142
Alex Goldberger

The magnetoresistive sensor – a sensitive device for detecting magnetic field variations 148
U. Dibbern and A. Petersen

Circulators and isolators for reducing transmitter intermodulation 154
W. Golombek

A complete f.m. radio on a chip 159
W. H. A. van Dooremolen and M. Hufschmidt

Progress in SMPS magnetic component optimisation 171
L. P. M. Bracke

Data converters for robotics 181
Stephan Ohr

Brief items of interest 188

Abstracts and Authors 190

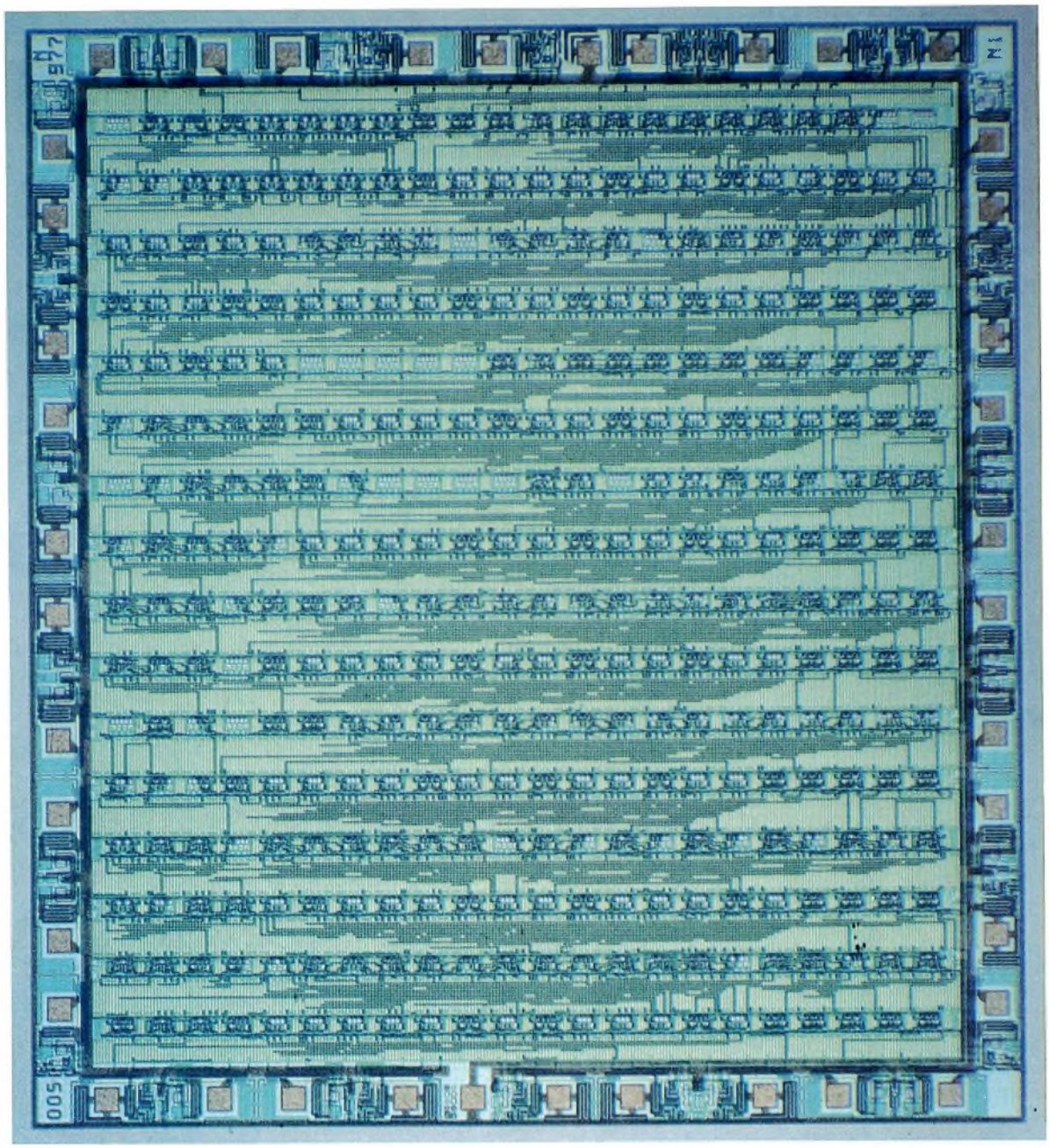

A PCF/PCC silicon-gate CMOS array of 352 cell units mask-programmed to form a semi-custom logic circuit

CMOS gate arrays – the fast way to semi-custom logic

R. CROES

Full custom logic ICs are compact, reliable and dissipate minimal power but they take a long time to develop and are expensive – too expensive if your production run is short. Discrete logic ICs cost less but they occupy more sockets and board space, cost more to assemble and test, and the overall system dissipates more power and is less reliable. An Uncommitted Logic Array (ULA) bridges the gap because it is an off-the-shelf chip which can be programmed to create a semi-custom IC that can reduce the component count of discrete IC logic by orders of magnitude and performs exactly the logic functions you need. Design and development times are much shorter, and development costs much lower, than for full custom logic.

One sort of ULA is the Field-Programmable type such as the Field Programmable Logic Array (FPLA) and Programmable Array Logic (PAL). These comprise arrays of logic elements in which initially, everything is connected to everything else via nichrome fuses. They can be field-programmed by selectively 'blowing' the fuses to leave only the required interconnections intact. Another type of ULA, with the advantage of variable architecture which allows more design flexibility and a higher gate utilisation factor than the FPLA or PAL, is the mask-programmable gate array as used for our PCF/PCC family of silicon-gate CMOS gate arrays.

Nearly all digital electronic systems and products can make beneficial use of PCF/PCC gate arrays. Most SSI and MSI circuits from today's standard TTL and CMOS logic families can be implemented. Even the functions performed by programmable array logic, field-programmable logic arrays, transistors and passive components can be incorporated. In the computer world they can be used in both mainframes and peripherals. In microprocessor-controlled systems, they can contain everything except the processor, memory and standard LSI peripherals.

INTRODUCTION TO THE PCF/PCC FAMILY

The advantages of silicon-gate CMOS

PCF/PCC gate arrays are made in Europe with the self-aligning silicon-gate CMOS process with local oxidation (LOCOS) to isolate the transistors (Fig.1). This process has been established for more than a decade and is used in preference to the bipolar, NMOS, PMOS or metal-gate CMOS process because it has the following important features:

– Low power dissipation in the static, dynamic or transitional state

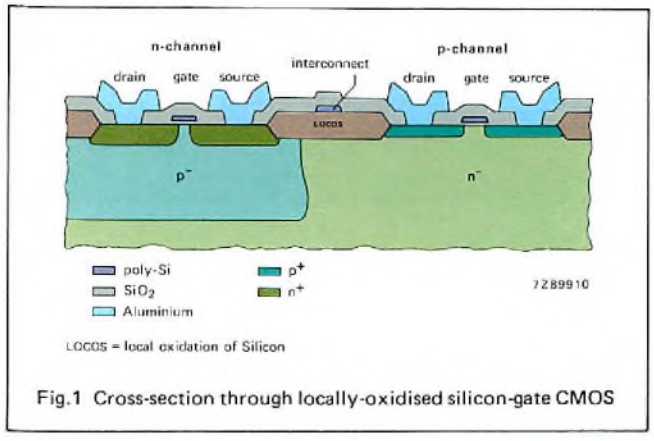

Fig.1 Cross-section through locally-oxidised silicon-gate CMOS

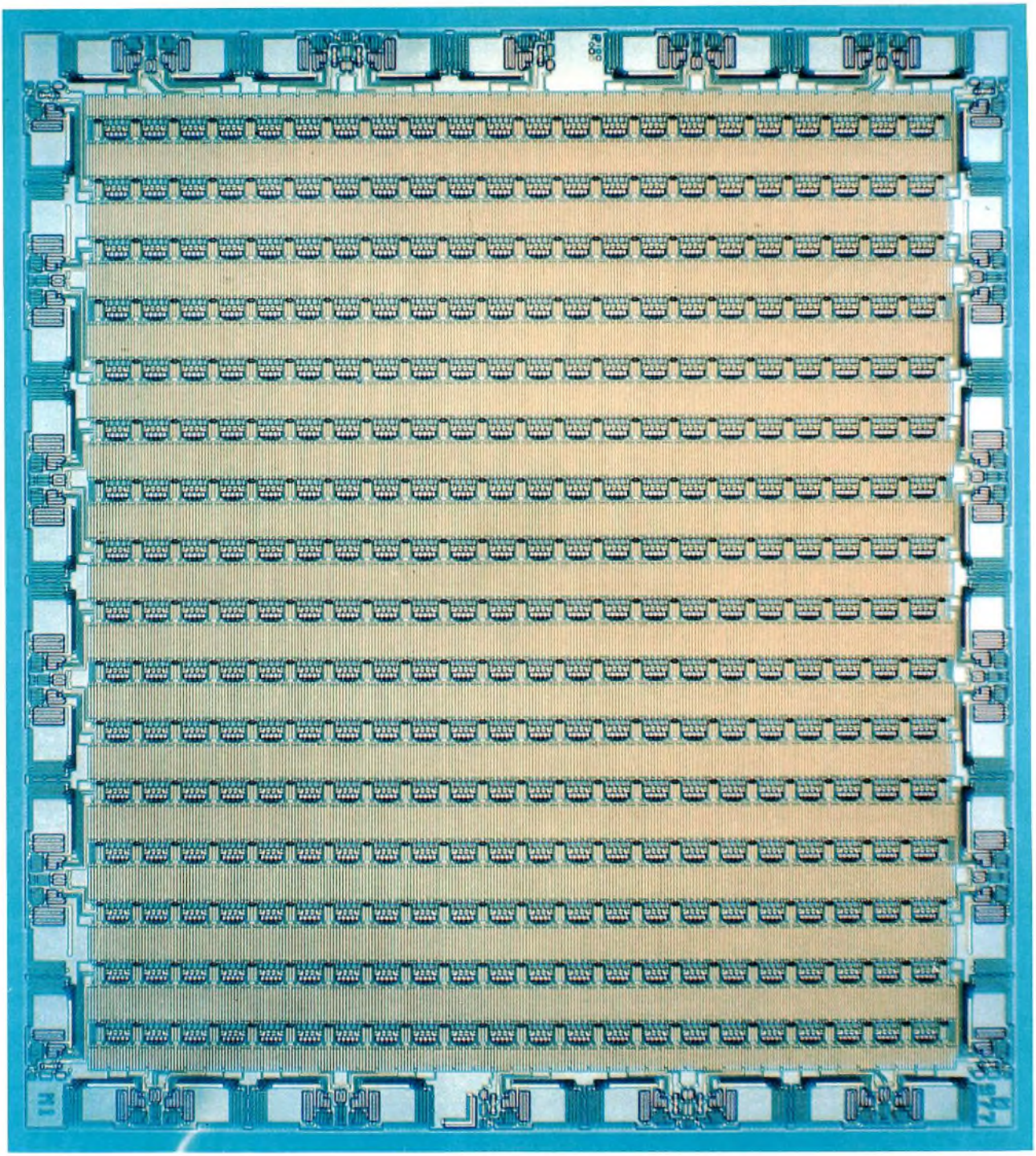

Fig.2 Typical pre-processed CMOS gate array chip with 352 cell units. Since the pre-processed chips are held in stock, turnround time for first samples after programming is very fast

- Single power supply with a wide operating voltage range of 3 V to 15 V. The low end of this range can be used to reduce power dissipation of 'slow' logic circuits
- High noise immunity
- High packing density by using local oxidation of silicon (LOCOS) to separate the n-channel and p-channel transistors and reduce node capacitance
- Highly doped low-resistance substrate prevents potentially destructive latch-up which can occur in conventional CMOS structures due to the application of voltages outside the V_{SS} to V_{DD} range
- Typical gate delay of 2 ns and a maximum flip-flop toggle frequency of 15 MHz with a 15 V supply
- Specification compatible with the HE4000B family of CMOS digital ICs
- Wide operating temperature range
  PCF (standard) −40 °C to +85 °C
  PCC (extended) −55 °C to +125 °C.

Gate array design principles

The PCF/PCC family of mask-programmable silicon-gate CMOS gate arrays comprises five types of pre-processed silicon chips consisting of a central rectangular matrix of 165, 224, 352, 588 or 864 cell units and a periphery of 38, 26, 38, 66 or 84 I/O devices with 40, 28, 40, 68 or 86 bonding pads. A typical array with 352 cell units (PCF/PCC0700) is shown in Fig.2. Each cell unit contains the uncommitted circuit elements equivalent to two 2-input NAND/NOR gates and can be mask-programmed to perform either one or two logic functions with up to four inputs and two outputs.

The PCF/PCC family is supported by a comprehensive computer-aided design (CAD) package which allows the gate arrays to be mask-programmed to perform the required functions without the need for tedious and error-prone tasks like breadboarding, digitising the layout and defining interconnections by hand. Since using the CAD facilities requires no knowledge of IC design and processing, it enables a logic system engineer to also retain direct control of his design throughout the integration phase.

As shown in Fig.3, the computer-aided design procedure starts with the preparation of a logic network description. This uses macro descriptions of a wide range of logic functions and types of I/O from a computer-based cell library to represent the required logic circuitry in terms that can be understood by the computer and to check its feasibility for integration. The logic behaviour of the network description can be tested by a logic simulation program SIMON which automatically calculates propagation delays and signals any departures from specification, race hazards or timing problems. This allows corrections to be incorporated before any hardware is committed. SIMON also generates test patterns for an automatic final test program. A cell placement program PLACE and an interconnection program INGATE use the verified logic network description to automatically determine which uncommitted elements of the gate array will be used and the most efficient manner of interconnecting them. The output from INGATE directly generates a control tape for interconnection and contact masks which open contact windows on the chip and deposit aluminium patterns which faultlessly wire the cell units and interconnect them with each other and the selected I/Os to form the desired logic circuit. Checking of the final interconnection patterns is not necessary. INGATE also calculates wiring loads which can be fed back to SIMON for automatic calculation of overall circuit delays.

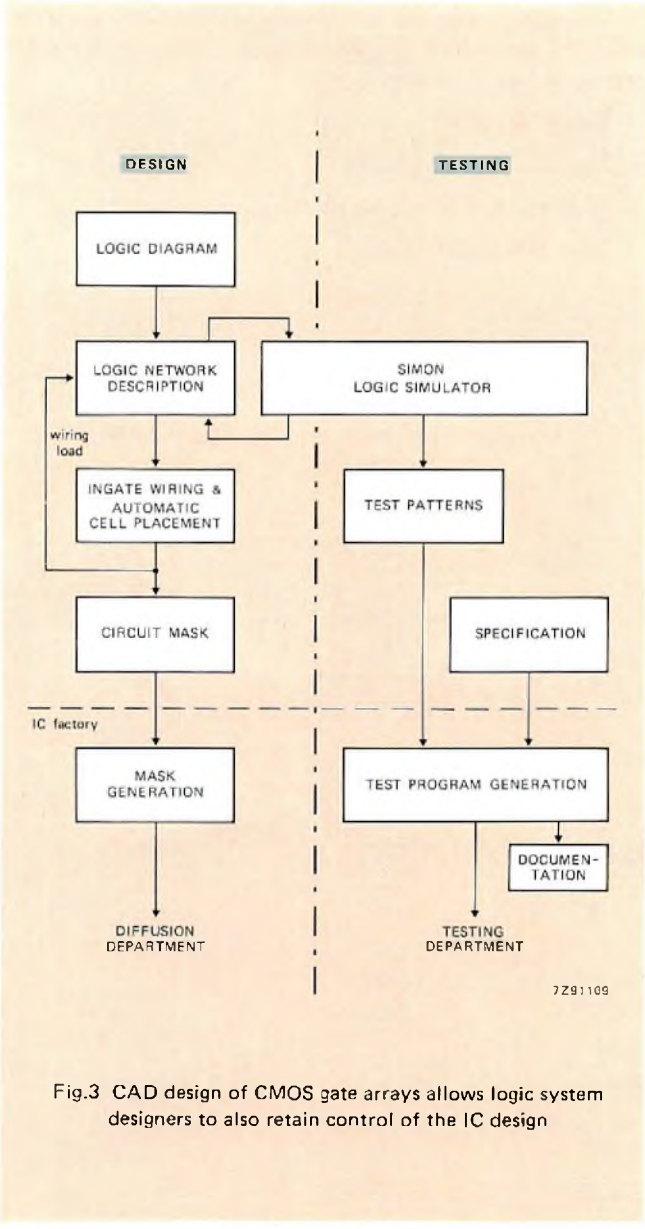

Fig.3 CAD design of CMOS gate arrays allows logic system designers to also retain control of the IC design

The automatic calculation of propagation delays during circuit simulation is particularly important because it determines the overall speed of the circuit and the number of elements that can be incorporated in each logic function block. The loading at each output node is evaluated by calculating the fanout and then adding the wiring load. The macro descriptions in the cell library include the delay figures for each logic function. SIMON adds these figures to the wiring load information fed back by INGATE. The HIGH to LOW and LOW to HIGH propagation delays are thus calculated during the logic simulation. For complex functions such as flip-flops, the different delay figures for each of the inputs are taken into account.

The verified test patterns from SIMON are derived from the customer's test sequences to verify adequate fault coverage before being used, together with a pin assignment list, as a basis for a final automatic test program. The final test program adds the d.c. parameter tests and generates control tapes which allow automatic testing on the CAD test equipment which includes:

- Sentry VII SS10
- Macrodata
- Philips LOCMOS testers 1650TG
- Tektronix S3260 series.

After the logic network description has been checked and approved, use of the CAD procedure to program the readily available pre-processed gate arrays is just as easy as designing a printed-wiring board by using a standard set of interconnection patterns which are guaranteed to be correct for performing a specific function. The turnround for first samples of the completed semi-custom IC is therefore very fast.

Design assistance and facilities

The computer-aided design of the gate arrays can be completely carried out in one of our design centres (Fig.4) or, if the user has the necessary facilities, he can do all or some of the design work himself. For example, a customer could simply deliver his logic diagram and circuit specification to one of our design centres and we would do the rest. At the other extreme, a customer with more extensive facilities could run our CAD software on his own computer and supply us with the final mask and test pattern tapes. Customers can of course also participate in the design at any intermediate stage between these two extremes, either by having a terminal connected to our computer via a modem, or by visiting one of our design centres and working alongside our gate array design specialists.

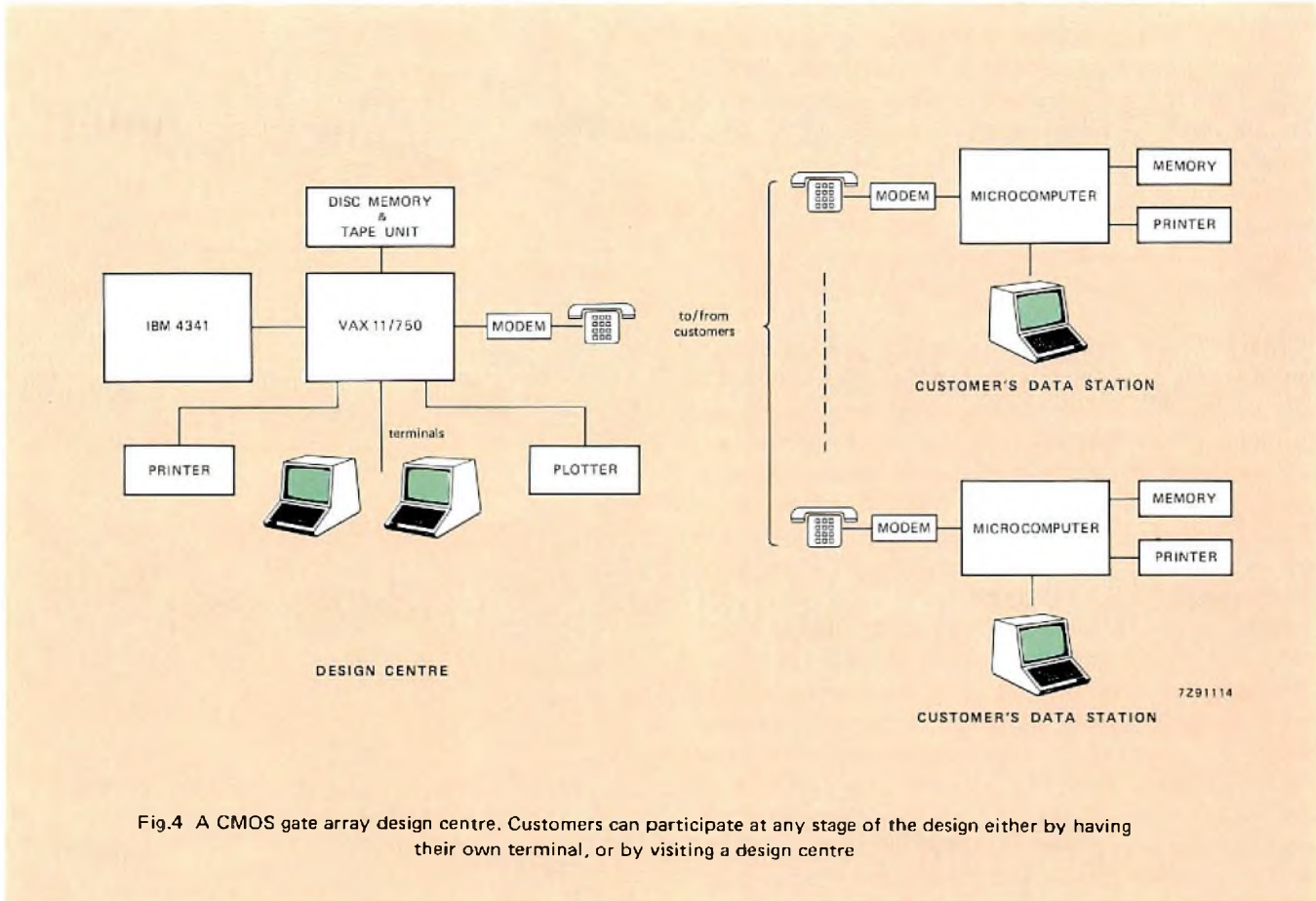

Fig.4 A CMOS gate array design centre. Customers can participate at any stage of the design either by having their own terminal, or by visiting a design centre

PCF/PCC family specification

RATINGS	limiting values in accordance with the Absolute Maximum System (IEC 134)	
supply voltage range	V_{DD}	−0.5 to +18 V
voltage on any input when pin pull up/down resistors are:		
used	V_I	−0.5 to V_{DD} +0.5 V
not used	V_I	−0.5 to +18 V
D.C. current into any input or output	±I	max. 10 mA
power dissipation per output	P	max. 100 mW
power dissipation per package		
for standard temperature range: −40 to +85 °C (PCF)		
plastic and ceramic DIL		
for T_{amb} = −40 to +60 °C	P_{tot}	max. 400 mW
for T_{amb} = +60 to +85 °C	P_{tot}	derate linearly by 8 mW/K to 200 mW
plastic mini-pack (SO)		
for T_{amb} = −40 to +70 °C	P_{tot}	max. 200 mW
for T_{amb} = +70 to +85 °C	P_{tot}	derate linearly by 5 mW/K to 125 mW
for extended temperature range: −55 to +125 °C (PCC)		
ceramic DIL		
for T_{amb} = −55 to +100 °C	P_{tot}	max. 400 mW
for T_{amb} = +100 to +125 °C	P_{tot}	derate linearly by 8 mW/K to 200 mW
storage temperature range	T_{stg}	−65 to +150 °C

DC characteristics — V_{SS} = 0 V

parameter	temp. range	V_{DD}	symbol	T_{amb} (°C)* low min.	low max.	+25 min.	+25 max.	high min.	high max.	unit	conditions
quiescent		5	I_{DD}	–	50	–	50	–	375	µA	
device	stand.	10	I_{DD}	–	100	–	100	–	750	µA	
current		15	I_{DD}	–	200	–	200	–	1500	µA	all valid input combinations
quiescent		5	I_{DD}	–	15	–	15	–	375	µA	$V_I = V_{SS}$ or V_{DD}
device	ext.	10	I_{DD}	–	25	–	25	–	750	µA	
current		15	I_{DD}	–	50	–	50	–	1500	µA	
input voltage		5	V_{IL}	–	1.5	–	1.5	–	1.5	V	
LOW:	all	10	V_{IL}	–	3.0	–	3.0	–	3.0	V	
INPI, INPB		15	V_{IL}	–	4.0	–	4.0	–	4.0	V	
input voltage		5	V_{IH}	3.5	–	3.5	–	3.5	–	V	**
HIGH:	all	10	V_{IH}	7.0	–	7.0	–	7.0	–	V	
INPI, INPB		15	V_{IH}	11.0	–	11.0	–	11.0	–	V	
input leakage		10	$\pm I_{IN}$	–	0.3	–	0.3	–	1.0	µA	V_I = 0 or 10 V
current	stand.	15	$\pm I_{IN}$	–	0.3	–	0.3	–	1.0	µA	V_I = 0 or 15 V

* T_{amb} low = −40 °C for standard, −55 °C for extended temperature range. T_{amb} high = +85 °C for standard, 125 °C for extended temperature range.

** for V_{DD} = 5 V, V_O = 0,5 V or 4.5 V; for V_{DD} = 10 V, V_O = 1.0 V or 9.0 V; for V_{DD} = 15 V, V_O = 1,5 V or 13,5 V; for all inputs $|I_O| < 1$ µA.

AC characteristics — V_{SS} = 0 V, T_{amb} = 25 °C

parameter	V_{DD}	symbol	min.	typ.	max.	unit
maximum toggle frequency	5	f_{max}	6	12	–	MHz
flip-flop GT00	10	f_{max}	12	24	–	MHz
	15	f_{max}	15	30	–	MHz
propagation delays	5	t_{PHL} and t_{PLH}	–	8	16	ns
2-input gate	10	t_{PHL} and t_{PLH}	–	3.2	6.4	ns
fan-out = 2	15	t_{PHL} and t_{PLH}	–	2	4	ns
output stage transition times					(input transition ≤20 ns, C_L = 50 pF)	
driver outputs	5	t_{THL}	–	60	120	ns
HIGH to LOW	10	t_{THL}	–	30	60	ns
	15	t_{THL}	–	20	40	ns
buffer outputs	5	t_{THL}	–	30	60	ns
HIGH to LOW	10	t_{THL}	–	15	30	ns
	15	t_{THL}	–	10	20	ns
buffer outputs	5	t_{TLH}	–	40	80	ns
LOW to HIGH	10	t_{TLH}	–	18	36	ns
	15	t_{TLH}	–	12	24	ns

System speed depends on number of gates in sequence. Average minimum frequencies are 3 MHz at V_{DD} = 5 V, 6 MHz at V_{DD} = 10 V, 9 MHz at V_{DD} = 15 V.

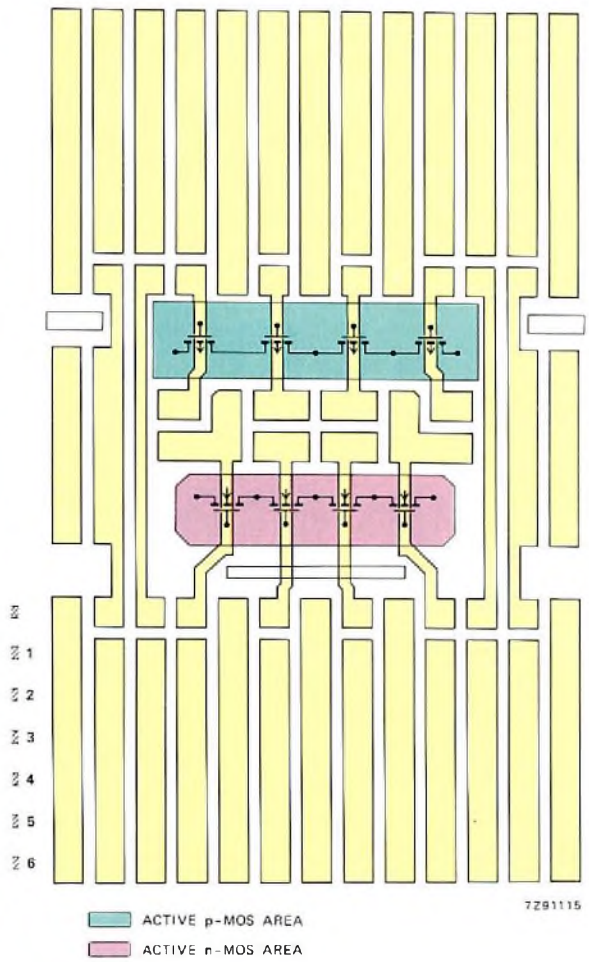

(a)

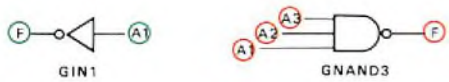

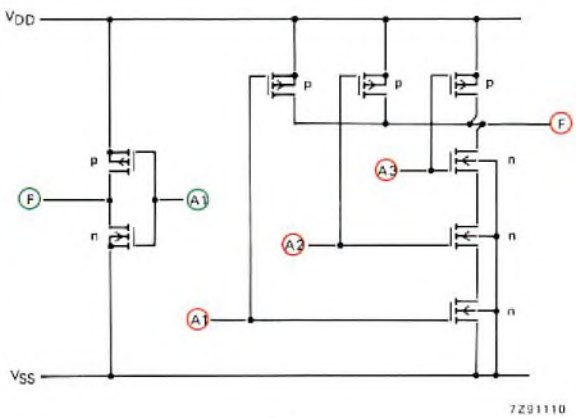

(b)

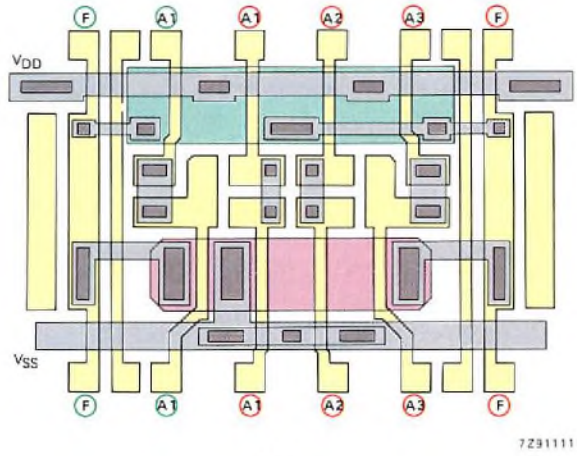

(c)

Fig.5 Structure of a CMOS gate array cell
(a) before programming
(b) the required logic circuit
(c) after programming

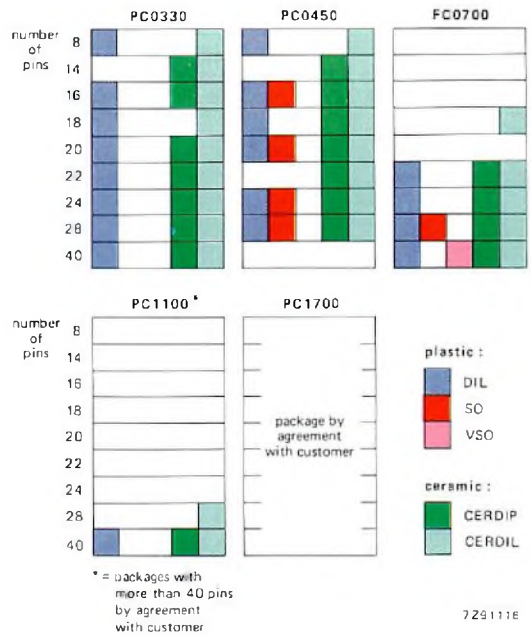

Fig.6 Packages for the PCF/PCC family

Summary

Outstanding advantages of PCF/PCC mask-programmable gate arrays are:

- Variable architecture allows over 90% of available gates to be programmed to perform up to 60 different functions
- 24 different I/Os and a range of pull-up/down resistors can be programmed. This allows interfacing with most other logic families
- The comprehensive Computer-Aided Design (CAD) system dramatically reduces development time and allows the designer of the original logic circuit to retain control of his own system throughout the final integration phase instead of relying on the expertise of a MOS IC designer
- The same data basis (the network description) is used for logic simulation, test pattern generation, cell placement, automatic interconnection routeing and mask generation
- Designing is as easy as with standard SSI or MSI
- Design changes can be easily incorporated
- The network description is made from a computer-based library of fully defined cell functions. The input/output list, dynamic characteristics and topology list of the input/output signals are part of the cell library macro descriptions. The SIMON program simulates the overall circuit, thoroughly tests it and allows modifications to be made before any hardware is committed
- After functions of the network description have been assigned to the array cell units and I/Os, by the PLACE program, a routeing program INGATE automatically specifies metallisation and contact mask patterns which are in accordance with the network description and are guaranteed to be correct for interconnecting bonding pads, I/Os, supply rails and cell transistors
- The final semi-custom logic IC protects proprietary rights because it is very difficult to copy.

THE PCF/PCC FAMILY IN DETAIL

Cell unit

As shown in Fig.5, a gate array cell unit contains four series-connected n-channel MOS transistors, four series-connected p-channel MOS transistors, and eleven vertical polysilicon interconnection strips above and below the transistors. Each interconnection strip area can accommodate five completely independent horizontal rows of CAD routed aluminium interconnections. On each side of the transistors, there is a polysilicon feedthrough strip for making connections across the cell unit or to other rows of cell units. There are also two input/output feedthrough strips. The substrates of the four p-channel MOS transistors are connected to the positive supply bus (V_{DD}), and the p-well of the four n-channel MOS transistors are connected to the negative supply bus (V_{SS}). Contact points are available for all sources, drains and gates and are automatically connected as required when cell library functions are allocated to the cell unit. The gates of the complementary transistors are not initially connected to each other so that they can be connected to different potentials. This allows transmission gates to be programmed so that packing density and speed can be increased. Since each cell unit has a maximum of two output strips, it cannot accommodate more than two cell library functions.

I/O periphery

The I/O periphery consists of uncommitted bonding pads with anti-static protection, and I/O cells consisting of several uncommitted complementary pairs of MOS transistors. A pull-up/down resistor with a choice of eight values can be assigned to each bonding pad. The I/O cells can be assigned to the bonding pads and mask-programmed as 3-state outputs, drivers, buffers, Schmitt triggers or oscillators from the cell library. I/Os can be designated as transceivers by combining a 3-state output with any input stage. Bonding pads can also be assigned as direct inputs to the cell units in the core of the gate array. This flexible range of I/Os allows the final semi-custom circuit to interface directly with most other logic families.

TABLE 1
Survey of PCF/PCC gate array facilities

type number: PCF.... or PCC....	0330	0450	0700	1100	1700
2-input gate equivalents	330	448	704	1116	1728
cell units	165	224	352	558	864
rows of cell units	11	14	16	18	24
cell units per row	15	16	22	31	36
horizontal mask-programmable interconnection strips (max):					
above top row of cell units	5	5	5	6	7
between cell units	10	9	10	13	14
below bottom row of cell units	5	5	5	6	7
bonding pads	40	28	40	68	86
inputs/outputs (max) consisting of:					
3-state I/Os (max)	34	26	38	66	84
drivers (max)	38	14	22	66	84
buffers (max)	38	12	16	66	84
Schmitt-triggers (max)	34	8	10	66	84
pull-up/down resistors (max)	34	26	34	66	84

Packages

PCF/PCC gate arrays are available in a wide range of plastic and ceramic packages as shown in Fig.6.

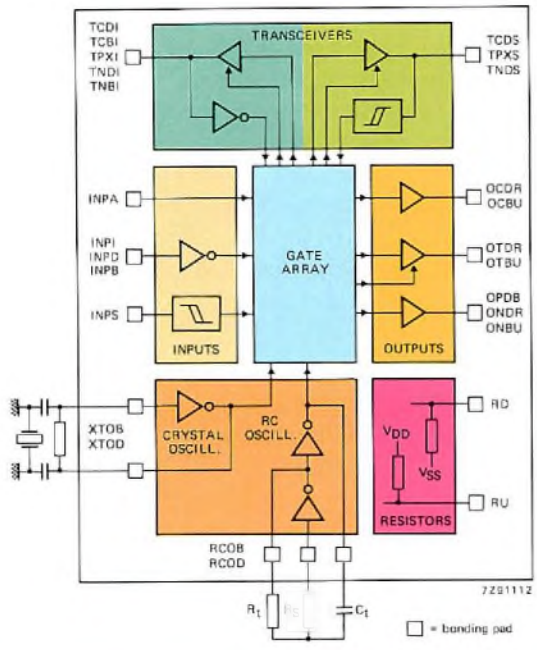

transceivers with inverter input	
TCDI	complementary driver output
TCBI	complementary buffer output
TPXI	open drain p-channel driver output
TNDI	open drain n-channel driver output
TNBI	open drain n-channel buffer output
transceiver with Schmitt trigger input	
TCDS	complementary driver output
TPXS	open drain p-channel driver output
TNDS	open drain n-channel driver output
inputs	
INPA	direct access to array
INPI	inverter
INPD	driver
INPB	buffer
INPS	Schmitt trigger
outputs	*fanout: driver = 2 LSTTL loads, buffer = 4 LSTTL loads*
OCDR	complementary driver
OCBU	complementary buffer
OTDR	3-state driver
OTBU	3-state buffer
OPDB	open drain p-channel driver
ONDR	open drain n-channel driver
ONBU	open drain n-channel buffer
oscillators	
XTOD	crystal oscillator with driver stage
XTOB	crystal oscillator with buffer stage
RCOD	RC oscillator with driver stage
RCOB	RC oscillator with buffer stage
resistors	
RD	pull-down resistors
RU	pull-up resistors

Fig.7 The PCF/PCC I/O cell library is versatile enough to allow interfacing with most other logic families

The cell library

The cell function library contains about 60 different functions for the cell units of the gate arrays (Table 2), 24 different functions for the peripheral I/O cells (Fig.7), and a range of pull-up/down resistors which can be assigned to the bonding pads. The cell library contains a macro description for each logic function. The descriptions include an input/output list for converting the customer's logic diagram into a logic network description which can be understood by the SIMON program, the delay specification, and topology of input and output signals for the INGATE program. Some examples of library cell functions and their physical interpretation by the INGATE program are shown in Fig.5. Figure 8 shows the cell unit occupation of some of the functions from the library.

EVALUATION/TEST CIRCUIT PCF0700/005

This evaluation/test circuit is a 704-gate array type PCF0700 which has been programmed with all the gate array functions from the CAD cell function library, together with a number of complex logic circuits which also incorporate most of the I/O cell library functions. The circuit is used for testing and/or demonstrating the logic function and a.c. characteristics of the PCF/PCC family of CMOS gate arrays. It can also be used to evaluate parameters which are not specified in the published data (e.g. the behaviour of linear functions). Since there are insufficient pins available on the PCF0700 to access all the gate array cell functions individually, the evaluation circuit includes nine output multiplexers. Functions are selected by programming six input selection pins. By using the CMOS gate array design rules laid down in the gate array design manual, a utilisation factor of 92% has been achieved. The circuits available in addition to the cell library functions are:

- 4-bit static shift register which is compatible with HEF4015B and uses transmission gate master/slave flip-flops GT00
- transmission gate master/slave flip-flop GT00 which can be activated by clock and $\overline{\text{clock}}$ inputs so that propagation delay can be measured between the clock pulse and output transitions
- inverter input INPI connected directly to a complementary buffer output OCBU
- 4-stage asynchronous binary ripple counter which is compatible with HEF4024B and uses transmission gate master/slave flip-flops GT00
- RC or crystal-controlled oscillator
- two Schmitt-triggers assembled from NAND/NOR gates for evaluating hysterisis due to the different switching levels of the two types of gate

– 5-stage Johnson counter which is compatible with HEF4017B and uses transmission gate master/slave flip-flops GTRRP

– ring oscillator comprising one chain of 13 NAND gates and one chain of 7 NAND gates. This circuit is for measuring maximum operating frequency and propagation delay times of sequential logic. Since all the interconnections have been executed by the CAD automatic routeing program INGATE, the resulting propagation delays include the effect of wiring loads that would occur in a practical circuit.

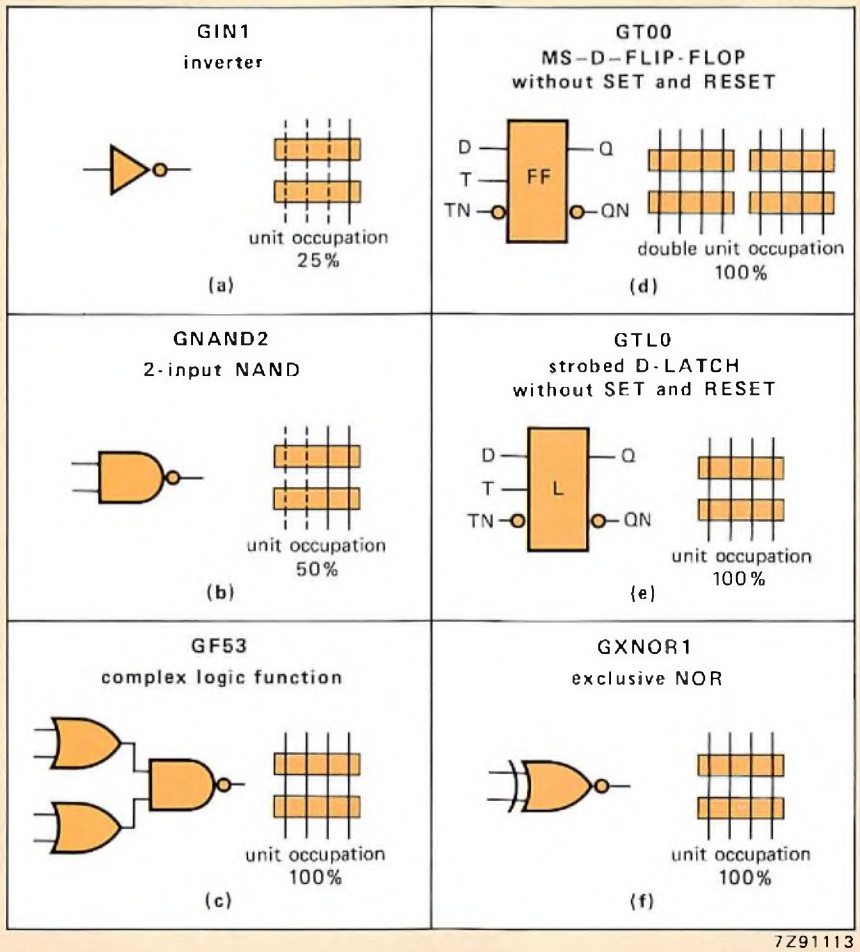

Fig.8 Examples of a few of the gate array logic functions showing the cell occupation

TABLE 2
The PCF/PCC gate array cell library

library identification code	logic element	function	number of units	number of equiv. gates	remarks
inverters/buffers					
GIN1	inverter	$\overline{A}$	¼	½	max. 2 in one unit
GIN2	array driver inverting	$\overline{A}$	½	1	2 times GIN1
GIN3	array driver inverting	$\overline{A}$	¾	1 + ½	3 times GIN1
GIN4	array driver inverting	$\overline{A}$	1	2	4 times GIN1
GIN6	array driver inverting	$\overline{A}$	1 + ½	3	6 times GIN1
GIN8	array driver inverting	$\overline{A}$	2	4	8 times GIN1
GIN12	array driver inverting	$\overline{A}$	3	6	12 times GIN1
GB12	array buffer non-inverting	A	1	2	2 times GIN1
GB13	array buffer non-inverting	A	1	2	3 times GIN1
NAND/AND gates					
GNAND2	2-input NAND	$\overline{A1 \cdot A2}$	½	1	
GNAND3	3-input NAND	$\overline{A1 \cdot A2 \cdot A3}$	¾	1 + ½	
GNAND4	4-input NAND	$\overline{A1 \cdot A2 \cdot A3 \cdot A4}$	1	2	
GAND2	2-input AND	$A1 \cdot A2$	1	2	output GIN2
GAND3	3-input AND	$A1 \cdot A2 \cdot A3$	1	2	
OR/NOR gates					
GNOR2	2-input NOR	$\overline{A1 + A2}$	½	1	
GNOR3	3-input NOR	$\overline{A1 + A2 + A3}$	¾	1 + ½	
GNOR4	4-input NOR	$\overline{A1 + A2 + A3 + A4}$	1	2	
GOR2	2-input OR	$A1 + A2$	1	2	output GIN2
GOR3	3-input OR	$A1 + A2 + A3$	1	2	
complex logic functions					
GF01	complex function	$\overline{A1 + B1 \cdot B2}$	1	2	
GF02		$\overline{A1 + B1 \cdot B1 \cdot B3}$	1	2	
GF03		$\overline{A1 \cdot A2 + B1 \cdot B2}$	1	2	
GF06		$\overline{A1 + A2 + B1 \cdot B2}$	1	2	
GF15		$\overline{A1 + B1 \cdot (C1 + C2)}$	1	2	
GF51		$\overline{A1 \cdot (B1 + B2)}$	1	2	
GF52		$\overline{A1 \cdot (B1 + B2 + B3)}$	1	2	
GF53		$\overline{(A1 + A2) \cdot (B1 + B2)}$	1	2	
GF56		$\overline{A1 \cdot A2 \cdot (B1 + B2)}$	1	2	
GF65		$\overline{A1 \cdot (B1 + C1 \cdot C2)}$	1	2	
GXOR1	EXCLUSIVE-OR	$\overline{A \cdot B + \overline{A} \cdot \overline{B}}$	1	2	unbuffered
GXNOR1	EXCLUSIVE-NOR	$A \cdot B + \overline{A} \cdot \overline{B}$	1	2	unbuffered
GXOR2	EXCLUSIVE-OR	$\overline{A \cdot B + \overline{A} \cdot \overline{B}}$	1	2	buffered
GXNOR2	EXCLUSIVE-NOR	$A \cdot B + \overline{A} \cdot \overline{B}$	1	2	buffered
GXOR3	EXCLUSIVE-OR	$\overline{A \cdot B + \overline{A} \cdot \overline{B}}$	2	4	

TABLE 2 *(continued)*
The PCF/PCC gate array cell library

library identification code	logic element	number of units	number of equiv. gates	remarks
transmission gate latches				
GTL0	strobed D-LATCH without SET and RESET	1	2	
GTLRP	strobed D-LATCH with RESET	1 + ½	3	positive triggered
GTLRN	strobed D-LATCH with RESET	1 + ½	3	negative triggered
GTLSP	strobed D-LATCH with SET	1 + ½	3	positive triggered
GTLSN	strobed D-LATCH with SET	1 + ½	3	negative triggered
GTL2	strobed D-LATCH with SET and RESET	1 + ½	3	
compound latches				
GGM0	MASTER module without SET and RESET	2	4	all positive triggered
GGMR	MASTER module with RESET	2	4	
GGMS	MASTER module with SET	2	4	
GGM2	MASTER module with SET and RESET	2	4	
GGS0	SLAVE module without SET and RESET	2	4	all negative triggered
GGSR	SLAVE module with RESET	2	4	
GGSS	SLAVE module with SET	2	4	
GGS2	SLAVE module with SET and RESET	2	4	
transmission gate master-slave flip-flop (MS-D-FF)				
GT00	MS-D-FF without SET and RESET	2	4	
GTR0P	MS-D-FF with RESET on MASTER	2 + ½	5	positive triggered
GTR0N	MS-D-FF with RESET on MASTER	2 + ½	5	negative triggered
GTRRP	MS-D-FF with RESET on MASTER and SLAVE	3	6	positive triggered
GTRRN	MS-D-FF with RESET on MASTER and SLAVE	3	6	negative triggered
GTSSP	MS-D-FF with SET on MASTER and SLAVE	3	6	positive triggered
GTSSN	MS-D-FF with SET on MASTER and SLAVE	3	6	negative triggered
GT22	MS-D-FF with SET and RESET on MASTER and SLAVE	3	6	
compound master-slave flip-flops				
GG00	MS-RS-FF without SET and RESET	4	8	all negative triggered
GGR0	MS-RS-FF with RESET on MASTER	4	8	
GGRR	MS-RS-FF with RESET on MASTER and SLAVE	4	8	

Data communications

ALEX GOLDBERGER

Recent developments in information systems and computer and microcomputer hardware have highlighted the need for efficient data communications. The data communication process generally requires at least five elements: a transmitter or source of information, a message, a binary serial interface, a communication channel or link, and a receiver of transmitted information (Fig.1). The range of channels includes private wire, wideband, Digital Data Service, limited distance, voice grade, subvoice grade, and telegraph (Table 1). A data communications interface is often needed to make the binary serial data compatible with the communication channel.

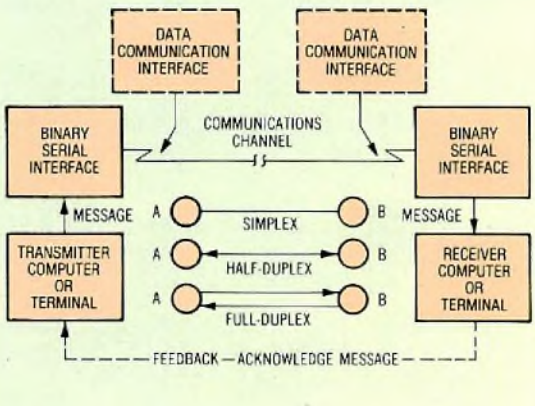

Fig.1 Elements of data communications process. Five major elements are source, message, interface channel, and receiver. Channel can be any of three basic types

COMMUNICATION CHANNELS AND FACILITIES

There are three basic types of channels: simplex, half-duplex, and full-duplex. As an example of each, consider transmission between points A and B in Fig.1. Transmission from A to B only (and not from B to A) requires a *simplex* channel. Simplex channels are used in loop mode confifurations such as supermarket checkout terminals. Transmission from A to B and then from B to A, but not simultaneously, requires a *half-duplex* channel. If a 2-wire circuit is used, the line must be turned around to reverse the direction of transmission. A 4-wire circuit eliminates line turnaround. Transmission from A to B and from B to A simultaneously describes a *full-duplex* channel. Although four wires are most often used, a 2-wire circuit can support full-duplex communications if the frequency spectrum is subdivided into receive and transmit channels.

A channel is characterised by its bandwidth. In general, the greater the bandwidth of the channel, the higher the possible transmission speed. This speed is usually measured in terms of the number of signal elements per second, the *baud rate*. If a signal element represents one of two binary states, the baud rate is equal to the bit rate. When more than two states are represented, as in multilevel modulation, the bit rate exceeds the baud rate.

Digital vs analog transmission

Digital transmission can be applied to digital data or to voice signals. In either case, information is sent over the communications channel as a stream of pulses. Pulses transmitted over a communication line are distorted by line capacitance, inductance, and leakage. The longer the line or the

TABLE 1
Communication channel characteristics

channel type	channel interface	data rates (bits/s)	applications
fibre optics	fibre optic connector	up to 10M	computer-computer, computer-high speed peripheral
private wire or cable	line drivers and receivers modem eliminators limited distance modems	1M to 2M	in-plant data communications
wideband analog	wideband Bell 300-series modems, CCITT V-series wideband modems	19.2k to 230.4k	telephone channel multiplexing
Dataphone Digital Service	Data Service Unit Digital Station Terminal	2.4k, 4.8k, 9.6k, 56k, 1.544M	private terminal-coumputer, geographically dispersed links
switched telephone network (DDD)	2-wire modems	0 to 2k (async), 2k to 4.8k (sync)	terminals, data collection stations, other interactive communications
	acoustic couplers	300, 450, 600, 1.2k (async)	
leased voice-grade lines (with or without conditioning)	2/4 wire modems	0 to 2.4k (async) 2k to 9.6k (sync)	remote batch, private communitions networks
subvoice grade	narrowband modems	150 to 200	teletypes, A-D converters, telemetry
telegraph	dc signaling	45 to 75	TWX, TELEX

faster the pulse rate, the more difficult it is to interpret the received signal. This signal degradation is the reason for the closely spaced regenerative repeaters used in digital data transmission facilities. When noise and distortion threaten to corrupt the pulse stream, the pulses are detected and regenerated. If the regeneration process is repeated properly, the received signal will be an exact replica of the transmitted signal. It is possible to transmit pulses over short distances using privately owned cable or common-carrier wire pairs. This is *baseband transmission* and usually requires line drivers and receivers on each end of the line. Longer distance communication must use the digital transmission facilities of the common carriers.

In analog transmission, a continuous range of signal amplitudes or frequencies is sent over the communications line. Linear amplifiers maintain signal quality. The voice telephone network supplied by the common carriers uses analog transmission facilities to service most data communications users. To interface the analog voice channels to digital terminals and computers, a modulator-demodulator (modem) is used. In a modem, digital information modulates a carrier signal, which passes through the telephone network just as does a voice signal. At the receiving end, the signal is demodulated back into digital form.

Voice grade lines

Voice grade telephone lines are available through the public switched network (Direct Distance Dialed or DDD); as private leased lines without conditioning; and as private, conditioned, leased lines. Although the bandwidth is the same for all three, the effective data rates vary because of different specifications for signal noise, amplitude attenuation, and envelope delay distortion. Voice grade telephone lines with a bandwidth of 2700 Hz (300 to 3000 Hz) are by far the most common medium used for data communications.

Dial-up lines are the 2-wire pairs supplied by the common carriers on the public switched telephone network. Most often these lines are used for half-duplex operation, although frequency band splitting modems can facilitate full-duplex at 1200 bits/s. A major advantage of dial-up lines is that any point on a worldwide telephone network can be reached. Furthermore, communication costs are limited to the time the lines are actually in use.

Four major problems are associated with the switched telephone network. First, the lines may be noisy. The human brain can interpret what is being said desprite the interference that plagues many calls, but computers and terminals can easily lose or misinterpret data because of noise. Second, delay distortion is caused by the various frequency components of a signal being transmitted at a nonuniform speed through the transmission medium. This may result in received data that are erroneous. Third, the switched network requires relatively long connect, disconnect, and turnaround times, which limit the system data throughput. Fourth, the reliability of telephone switching equipment is relatively low.

Although more costly than dial-up lines, private leased lines largely circumvent the problems that afflict the switched network. Their basic advantages are ready availability and freedom from busy signals, fixed monthly

charges, and conditioning for better data quality, as well as higher transmission rates and throughput. Leased lines are generally 4-wire circuits usable for half or full-duplex operation. Simultaneous transmission and reception is possible, and line turnaround is eliminated. The basic disadvantages of leased lines are higher cost and the line's connection to only one location. However, if telecommunication demands entail high-volume, high-quality, high-speed traffic between two points, a leased line is the best choice.

MODEMS

Modems are devices that convert digital data from a computer or terminal to a modulated carrier wave required by the communication channel. One modem is needed at each end of the channel, as shown in Fig.2. Modems are also known as data sets and are designed for specific kinds of service and for specific bandwidths or data rates. Those discussed here accept a binary serial input from the transmitter and provide a binary serial output to the receiver. Parallel input modems (used mostly for paper tape transmission) and analog input machines (used primarily for facsimile transmission) are not considered. The three types that are considered are short haul, wideband, and voice grade (Table 2).

Short haul modems operate over relatively short distances – generally less than 16 km – on solid conductor, non-limited, non-loaded lines. In some cases, they are not true modems but are line drivers and line receivers that transmit and receive digital data. Although the communication line must be carefully chosen, the cost can often be one-tenth that of a voice grade modem rated at the speed. Other advantages are higher speed and reliability and easier maintenance.

Wideband modems operate over telephone transmission facilities at speeds of 19.2k bits/s to 230.4k bits/s. This class of data set is supplied almost exclusively by the common carrier and requires the bandwidth of 6 to 60 dedicated voice grade channels. Examples are the Bell 303B, C, and D for 19.2k, 50k and 230.4k-bit/s full-duplex operation.

A voice grade modem, designed for use on voice grade lines, should be selected on the basis of the type of service (dial-up or leased), the required data rate, and an acceptable level of error performance. The two broad categories of voice grade modems are asynchronous and synchronous. Asynchronous modems operate at a maximum data rate of 1800 bits/s over dial-up facilities and 2000 bits/s on conditioned leased lines. Acoustic couplers are asynchronous modems designed for dial-up use that are generally limited to speeds of 600 bits/s or less. Synchronous modems operate at a maximum data rate of 4800 bits/s over dial-up and 9600 bits/s on conditioned leased lines.

TABLE 2
Modem characteristics

modem type	communications channel	data rate (bits/s)	use
1. voice-grade (vg)			
a. high-speed synchronous	leased line (3002) dial-up	4.8k, 7.2k, 9.6k 4.8k	high-volume machine-to-machine communications. 600 to 1200 bits/s
b. medium-speed synchronous medium-speed asynchronous	leased line/dial-up leased line	2.4k, 3.6k 1.8k, 2k	interactive or low-speed remote batch operations. 150 to 300 bits/s
c. low-speed asynchronous	dial-up	300, 600	interactive teleprinters and teletype-writers, data acquisition and collection. 30 to 60 bits/s
2. wideband			
a. super group (60 vg)	5700, 5800 (TELPAK)	230.4k	large-volume telephone line multiplexing, dedicated computer to computer links
b. group (12 vg)	8801	40.8k, 50k, 56k	
c. half group (6 vg)	8803	19.2k	
d. lineplexer (2 vg)	2 leased lines	19.2k	
3. short-haul			
a. limited distance (<16 km)	private wire/cable nonloaded, non-conditioned non-carrier line	2k to 1M 2k to 19.2k	data communications in plant (private wire) or off premises where distance is <16 km (leased line)
b. medium distance (<80 km)	leased line	2k to 9.6k	intermediate distance (16 to 80 km)
4. modem eliminators and line drivers/receivers	private wire/cable	2k to 1.544M	on-premises data communications. typical distances are 150 m to 3.0 km

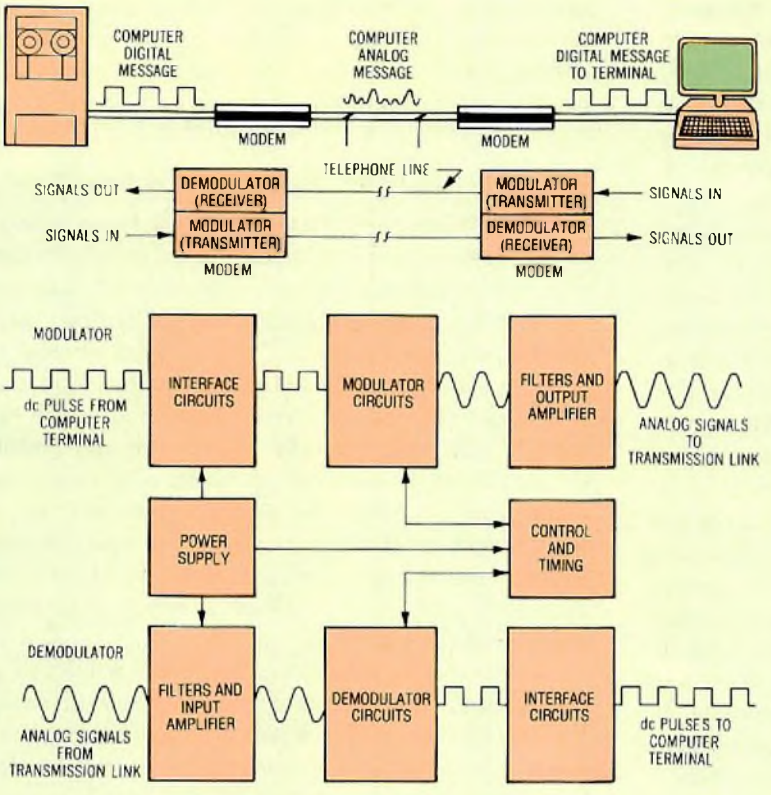

Fig.2 Analog transmission using modems. Each modem is divided into two functional segments: modulator and demodulator. The modulator accepts digital input in the form of squared pulses and converts them to analog, audio-frequency signals which are sent over the transmission link. At the end of the link, the demodulator of the second modem reconverts the analog signals to digital output

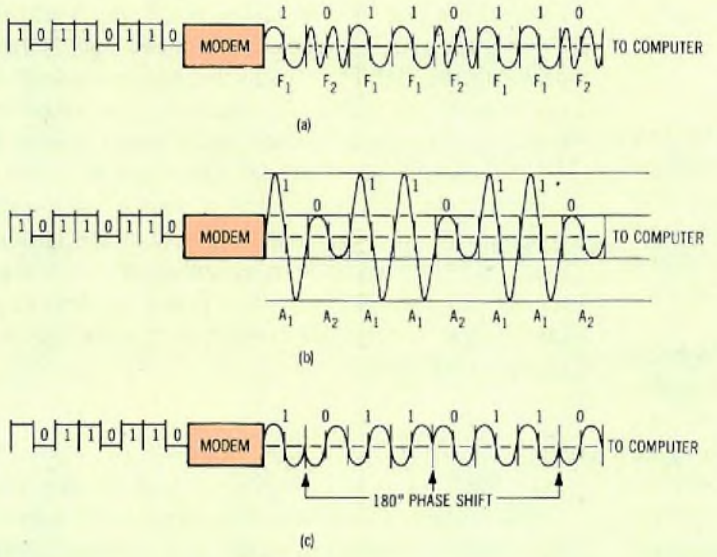

Fig.3 Modulation techniques. In frequency-shift keying (a) the modem shifts the frequency of an audio-frequency carrier up or down to represent binary 1s and 0s. In amplitude modulation (b) one carrier amplitude level (A_1) represents binary 1 and the other (A_2) binary 0. In phase modulation (c) the modem shifts the carrier phase 180° every time a binary 0 occurs; for a binary 1 there is no change of phase.

Modulation techniques

Whether to use the dial-up network or leased lines depends on how the modem modulates data for transmission. Certain modulation techniques permit higher transmission rates than others, and all modulation techniques directly affect the maximum data rate and the error performance. The three basic modulation techniques are frequency modulation (FM), amplitude modulation (AM), and phase modulation (PM) (Fig.3).

The most popular form of frequency modulation is frequency-shift keying, FSK, in which the carrier frequency (operating at, say, 1700 Hz) is modulated ±500 Hz to represent binary 1 or binary 0. Thus, a frequency of 1200 Hz represents a zero, while a frequency of 2200 Hz represents a binary 1. FSK techniques are generally quite suitable for low speed devices like teleprinters and allow operation at speeds as high as 1800 bits/s.

Amplitude modulation enables a modem to transmit and receive the analog equivalents of binary 1s and 0s. This technique involves varying the amplitude of the line's carrier frequency. Several levels of amplitude modulation are possible, allowing twice as much data to be sent in the same time frame. Both AM and FSK are quite suitable for data transmission; FSK has a noise advantage over AM, but AM allows more efficient use of the available bandwidth.

Phase modulation modems are generally described in terms of the number of phase shifts generated, and operate at speeds of 2000 bits/s and above. In this technique, the transmitted signal is shifted a certain number of degrees in response to the pattern of bits coming from the terminal or computer. For example, in a 2-phase PM modem, if the analog signal generated by the transmitting modem is shifted 180°, a binary 1 (or 0 if desired) is indicated. If there is no shift, then the signal will be interpreted as a series of zeros (or ones) until such a shift is sensed. Generally, PM modems operate in four and eight phases, permitting up to two or three times the data to be sent over the line in the same bandwidth. Most 4800 and 9600-bits/s modems use PM.

Conditioning and equalisation

As data in the form of analog signals are sent down the line between modems, they suffer from the effects of envelope delay and amplitude distortion. Signals of different frequencies are delayed or attenuated by varying amounts as they are transmitted. To compensate for these effects, two techniques are employed: line conditioning and modem equalisation.

Line conditioning is the process by which the telephone company maintains the quality of a specific, privately leased line to a certain standard of permissible delay distortion and signal attenuation. AT&T has two types of conditioning referred to as C and D. There are five categories of C conditioning (C1 to C5) and two categories of D conditioning (D1 and D2). C conditioning tempts to equalise the drop in signal voltage and envelope delay for all frequenices transmitted; D conditioning controls the signal-to-noise ratio and harmonic distortion. Both may be used on the same communication channel.

Modem equalisation refers to compensation for amplitude and envelope delay distortion of the line. Equalisation is seldom required in lower-speed modems attached to a leased line, since minimum line conditioning is sufficient. However, conditioning and equalisation are required when higher speed modems (4.8k and 9.6k bits/s) are attached. Modems used for high speed transmission over the dial-up network must have equalisation, since it is never certain exactly which unconditioned telephone line will be used.

Communication line sharing and modem sharing

When several input/output devices are required at one end of a communication link, a multiplexer or modem sharing unit, which enables these devices to share one communication line, can be used to reduce costs. Multiplexers take low speed inputs from a number of terminals and combine them into one high speed data stream for simultaneous transmission on a single channel. At the other end of the link, a second multiplexer (actually a demultiplexer) reconverts the high speed data stream into a series of low speed inputs to the host computer. The channel is split into time slots (time division multiplexing) or frequency bands (frequency division multiplexing). Intelligent or statistical multiplexers increase line utilisation by allocating time slots on the basis of a line activity algorithm.

Modem sharing units enable multiple terminals to share one modem. They are particularly valuable in networks that require clusters of terminals at remote sites because the number of modems and transmission lines are reduced. Operation is polled half-duplex. Multiport modems can split a high speed channel (e.g., 9600 bits/s) into various medium speed channels (e.g., two 2400 bits/s and one 4800 bits/s), thus permitting several medium speed terminals to share a 9600 bit/s line. A multiplexer is a device that performs channel splitting; a lineplexer or biplexer splits 19.2k bit/s data into two 9600 bit/s paths that can be transmitted over two conditioned full-duplex channels. This eliminates the need for a wideband channel to send and receive data at 19.2k bits/s. A port sharing unit connects to a communication controller or central processing unit port and transmits or receives data from two to six terminals or modems. Less costly than a multiplexer, it reduces the number of controller ports in a polled terminal data communications configuration and makes more efficient use of connected ports.

Synchronisation techniques

Four kinds of synchronisation – bit, character, block and message – must be distinguished when using synchronous transmission. Bit synchronisation is achieved through a received clock signal which is coincident with the received serial data stream. Most modems or 'business machines' (i.e., terminals) derive this clock by means of phase-locked loops from the 0 to 1 and 1 to 0 transitions occurring in the received data. This technique, called self-clocking, overcomes the effect of propagation delay between distant stations and the tendency of electronic circuits within the modem to drift.

Character synchronisation is accomplished by recognising one or two 'phasing' characters, often called SYN or sync characters. The receiver senses these SYN characters and phases its receive logic to recognise, by bit count, the beginning and end of each subsequent character. To ensure character synchronisation throughout a message, SYN sequences are sometimes inserted in the transmitted data stream at 1 or 2-second intervals. This permits receiving stations to verify that they are in sync.

Request for retransmission

Data-link control protocols include an error checking field to allow the receiving station to validate the message. When errors are detected, the receiving station issues a request for retransmission (ARQ). The two types of ARQs are *stop and wait* and *continuous*. Each provides defined methods for acknowledging correct (error-free) reception of transmitted blocks of information.

When a connection is established in the stop and wait ARQ, the transmitter sends one block and then stops. Eventually, the receiver acquires that block, subjects the block to an error check, and then sends an ACK control character to the transmitter to acknowledge that the block is correct, or a NAK control character to indicate an error. If an ACK is returned, the transmitter sends the next block in sequence. If a NAK is returned, that block is retransmitted. Thus, the stop and wait mode involves periods of idleness, including propagation delays between each block, so that the line is not communicating nearly at its rated capacity.

In continuous ARQ, the transmitter keeps sending one block after another without stopping. The receiver and transmitter retain individual counts of the blocks outstanding and provide buffer storage to retain those blocks. Only when an erroneous block is detected does the receiver tell the transmitter to resend that block and all subsequent in-transit, but unacknowledged, blocks.

Standards and protection

The electrical, functional, and physical interface to data terminal equipment provided by modems is compatible with Electronics Industries Association (EIA) or International Consultative Committee for Telephone and Telegraph (CCITT) standards. Most commercial modems conform to EIA RS-232, and plug-to-plug compatibility via a 25-pin connector is ensured between modems and data terminal equipment that subscribe to this standard. CCITT V.26 is the electrical equivalent of RS-232-C, while V.24 is the U.S. standard's functional pin equivalent. CCITT V.35, a current-mode, 34-pin connector interface standard for serial data transmission up to 56k bits/s, is used by wideband European modems and in the Bell System DDs Data Service Unit at 56k bits/s. Military standard MIL-STD 188 is a U.S. government standard for military communications equipment. An improved EIA functional standard, RS-449, was approved in November 1977. Although not yet implemented in U.S. modems, it is being incorporated into modems used in Germany and in the CCITT V.36 modem.

Common carrier equipment on the switched telephone network must be protected. A device called a data access arrangement (DAA) limits the attached modem's signaling power to prevent it from exceeding the power level restrictions of the communication channel. In 1977, the FCC ruled that modem manufacturers can incorporate equivalent protective circuitry in their products, register them with the FCC, and connect them directly to the telephone network. DAAs are available from FCC-certified independent suppliers and can be leased from the Bell System. Modems rented from the Bell System or those used on leased lines do not require a DAA.

ACKNOWLEDGEMENT

This article is based on one that was published in Computer Design, May 1981, copyright 1981 by Computer Design Publishing Co.: permission to reprint is gratefully acknowledged.

The magnetoresistive sensor – a sensitive device for detecting magnetic field variations

U. DIBBERN and A. PETERSEN

Magnetic-field sensors provide a highly effective means of measuring both linear and angular displacement. This is because even quite small movement of actuating components in machinery (metal rods, cogs, cams etc.) can create measurable changes in magnetic field. Examples where this property is put to good effect can be found in instrumentation and control equipment, which often require position sensors capable of detecting displacements in the region of tenths of a millimetre, and in electronic ignition systems, which must be able to determine the angular position of an internal combustion engine with great accuracy.

The magnetoresistive sensor (MRS) is one of the more recent developments for detecting magnetic field variations, and in many applications provides an attractive alternative to the conventional Hall-effect sensor. For example, the MRS is more sensitive than the Hall-effect sensor and can operate over a much wider temperature range. Moreover, its frequency range is much wider – from d.c. up to several megahertz.

The device makes use of the well-known property of a magnetic material to change its resistivity in the presence of an external magnetic field. This change is brought about by rotation of the magnetization relative to the current direction. In the case of permalloy for example (a ferromagnetic alloy containing 20% iron and 80% nickel), a 90° rotation of the magnetization (due to the application of a magnetic field normal to the current direction) will result in a 2 to 3% change in resistivity.

The MRS consists of four permalloy strips arranged in a meander pattern (Fig.1) on a silicon substrate, and connected to form the four arms of a Wheatstone bridge configuration. The degree of bridge imbalance is then used to indicate the magnetic field strength, or more precisely, the variation in magnetic field normal to the permalloy strips. As detailed below, the device characteristic (resistivity versus magnetic-field) is linearized using a special set-up known as a 'barber-pole' configuration.

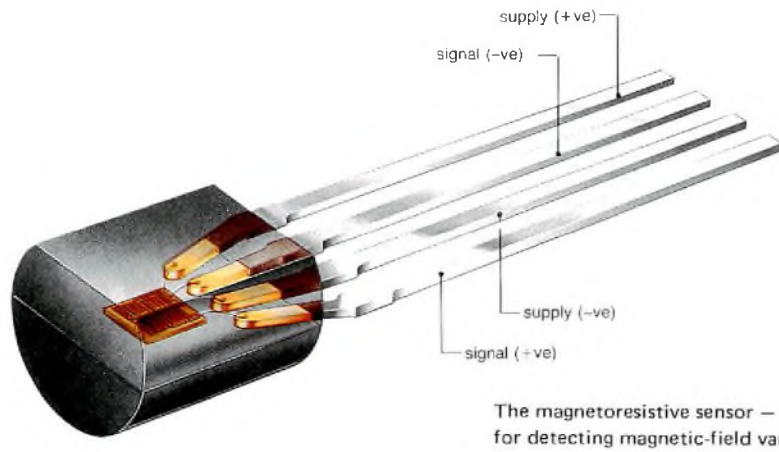

The magnetoresistive sensor – a recent development for detecting magnetic-field variations.

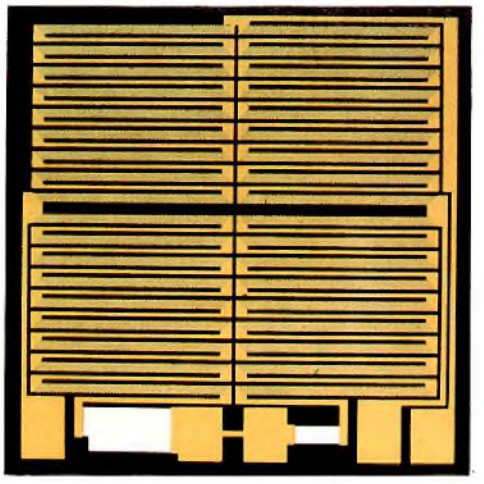

Fig.1 The MRS chip is made up of four permalloy strips arranged in a meander pattern and connected to form the four arms of a Wheatstone bridge. The chip incorporates special resistors that are trimmed during manufacture to give zero offset at 25 °C

LINEARISING SENSOR CHARACTERISTICS – THE 'BARBER-POLE' CONFIGURATION

The resistivity of a polycrystalline ferromagnetic alloy such as permalloy is related to the angle θ that the magnetization makes with the current direction by

$$\rho = \rho_0 + \Delta\rho_{max} \cos^2\theta \qquad (1)$$

where ρ_0 is the isotropic resistivity, and $\Delta\rho_{max}$ is the change in resistivity resulting from a 90° rotation of the magnetization (from the direction of current flow).

If this rotation is caused by a magnetic field H normal to the direction of current, and if the field tending to align the magnetization with the current is H_0 (comprising the demagnetizing and anisotropic fields), then $\sin\theta = H/H_0$, and

$$\rho = \rho_0 + \Delta\rho_{max}\,[1 - H^2/H_0^2] \qquad \text{for } H < H_0$$

and (2)

$$\rho = \rho_0 \qquad \text{for } H \geqslant H_0$$

It's obvious from this quadratic expression that the resistivity/magnetic-field characteristic is non-linear, and moreover, that the set-up will not furnish a unique value for H.

There are, however, several ways of linearizing the characteristic. One is to provide a uniform biasing field H_{bias} in the direction of the field H. Then, provided $H \ll H_{bias}$, ρ will be proportional to H. The MRS employs another method that uses gold stripes secured to the top of each permalloy strip at an angle of 45° to its axis (Fig.2). This has been termed the 'barber-pole' configuration owing to its resemblance to the poles commonly seen outside barber shops.

Since gold has a much higher conductivity than permalloy, the effect of these stripes is to rotate the net current direction through 45° (Fig.2), i.e. to reduce θ to $\theta - 45°$. Relation (1) then becomes

$$\rho = \rho_0 + \Delta\rho_{max}/2 + \Delta\rho_{max}\, H/H_0\sqrt{[1 - H^2/H_0^2]} \qquad (3)$$

As Fig.3 illustrates, for small values of H (relative to H_0) ρ increases linearly with H.

With the complementary barber-pole configuration to that shown in Fig.2, i.e. with the gold stripes inclined at

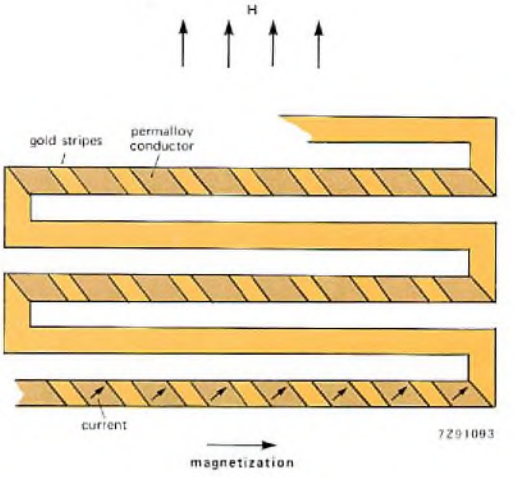

Fig.2 Gold stripes on the permalloy surface rotate the current direction through 45°. This linearizes the resistivity/magnetic-field characteristics of the MRS

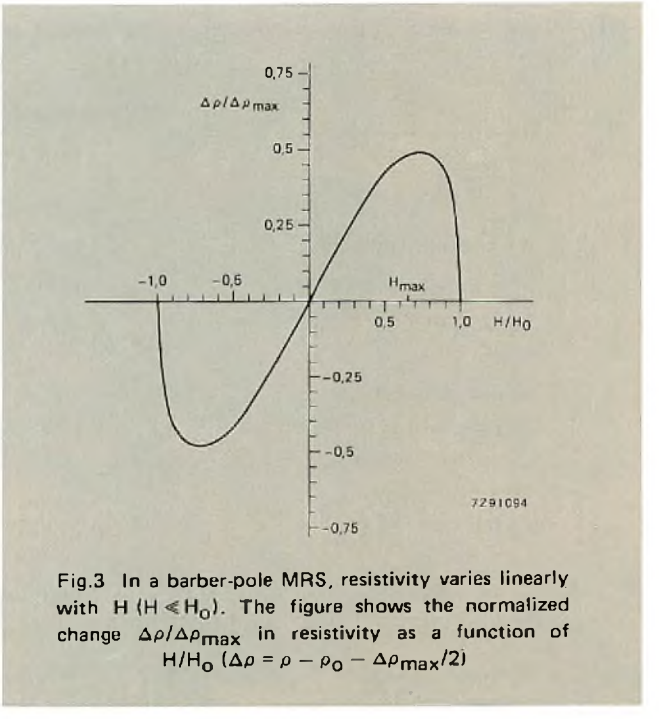

Fig.3 In a barber-pole MRS, resistivity varies linearly with H ($H \ll H_0$). The figure shows the normalized change $\Delta\rho/\Delta\rho_{max}$ in resistivity as a function of H/H_0 ($\Delta\rho = \rho - \rho_0 - \Delta\rho_{max}/2$)

$-45°$ to the axis of the permalloy strip, θ increases to $\theta + 45°$ and (1) becomes

$$\rho = \rho_0 + \Delta\rho_{max}/2 - \Delta\rho_{max}\, H/H_0\sqrt{[1 - H^2/H_0^2]}$$

i.e. ρ decreases linearly with H.

The MRS itself comprises two (diagonally opposed) elements in which ρ increases with H, and two in which it decreases. This largely eliminates the effects of ambient variations (temperature etc.) on the individual elements, and, moreover, magnifies the degree of bridge imbalance, thereby increasing the sensitivity of the device.

MANUFACTURE

The devices are manufactured in thin-film technology using established photo-lithographic processes. Major steps in the fabrication process are as follows:

- Surface oxidation of silicon substrates (dimensions 1,6 × 1,63 mm²)
- Sputter deposition of a titanium adhesive layer (0,1 μm thick) and then of permalloy
- Formation of permalloy strips using subtractive photo-lithographic process
- Baking at high temperature and application of a strong magnetic field parallel to the strip axis. The field imparts a preferred magnetization direction to the permalloy strips
- Sputter deposition of a titanium/tungsten adhesive layer (0,1 μm thick) on the surface of the permalloy strips
- Formation of gold barber-pole pattern on the surface of the permalloy strips
- Trimming of MRS bridge to give zero offset voltage at 25 °C.

SENSITIVITY – GOVERNING FACTORS

One of the major advantages the MRS has over other devices like the Hall-effect sensor is the ease with which its sensitivity can be set during manufacture. For small field variations, the sensitivity of the MRS is, from (3), given by $\Delta\rho/H = \Delta\rho_{max}/H_0$. $\Delta\rho_{max}$ is determined by the material properties; H_0 by, among other things, the strip geometry.

Fig.4 illustrates how the strip geometry governs sensitivity. For a given field, the thicker the permalloy strip, the less the magnetization is rotated. So by using different strip geometries, it's possible to produce a range of devices with different sensitivities and measuring ranges. At present, four types are produced – designated types A to D. A comparison of these types is provided in the table below.

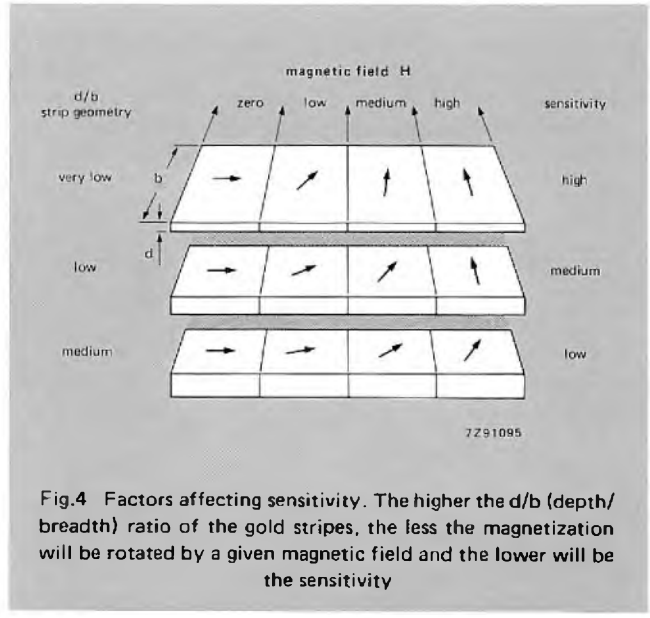

Fig.4 Factors affecting sensitivity. The higher the d/b (depth/breadth) ratio of the gold stripes, the less the magnetization will be rotated by a given magnetic field and the lower will be the sensitivity

MRS characteristics (at T_{amb} = 25 °C)

	MRS/A	MRS/B	MRS/C	MRS/D
H_{max}	±1000 A/m	±3000 A/m	±7000 A/m	±20000 A/m
open-circuit sensitivity	2,5 μVm/A	2,7 μVm/A	0,43 μVm/A	0,06 μVm/A
open-circuit voltage @H_{max}	40 mV	80 mV	50 mV	24 mV
bridge current	16 mA	10 mA	16 mA	20 mA
bridge resistance	250 Ω	800 Ω	300 Ω	120 Ω
temperature coefficient				
constant voltage	−0,4%/K	−0,4%/K	−0,4%/K	−0,4%/K
constant current	−0,12%/K	−0,12%/K	−0,12%/K	−0,12%/K
linearity				
full scale	3%	3%	3%	3%
half scale	1%	1%	1%	1%
offset voltage	±0,05 mV	±0,16 mV	±0,06 mV	±0,024 mV
offset drift between −40 and 120 °C	0,015%/K	0,015%/K	0,015%/K	0,015%/K
sensitvity drift between −40 and 120 °C	0,1%/K	0,1%/K	0,1%/K	0,1%/K

The sensitivity of the MRS falls with increasing operating temperature. This isn't a major problem, however, since it is relatively easy to incorporate effective compensating networks in the operating circuitry. In fact, as the next section shows, the linear temperature variation of bridge resistance is itself used to compensate variations of sensitivity with temperature.

USING THE MRS

The MRS in circuit

For some applications it's not necessary to compensate for temperature dependence of the bridge characteristics, and it's sufficient to operate the MRS from a simple constant-voltage source. A constant-current source could also be used, at the cost, however, of lower sensitivity.

For many applications, however, temperature compensation is essential, and Fig.5 shows a simple set-up in which this can be realized.

The output of the bridge, which indicates the degree of imbalance, is amplified by opamp A_0 – common-mode rejection being provided by a feedback network incorporating opamp A_1.

A negative-impedance converter (NIC) incorporating opamp A_2 provides a temperature dependent voltage source for the bridge. This set-up has the advantage of providing a ready means of correcting for temperature effects using the bridge resistance itself as the controlling parameter. Any change in bridge resistance (caused by a change in operating temperature) will affect the voltage across the bridge. The output signal of A_2 then acts to restore this voltage to its original value (V_{ref}).

Figure 6 shows a more extensive circuit, embodying the functions of Fig.5 and including an output comparator stage to provide a step-function output (e.g. for counting purposes). This circuit is designed to operate from a single 12 V d.c. supply.

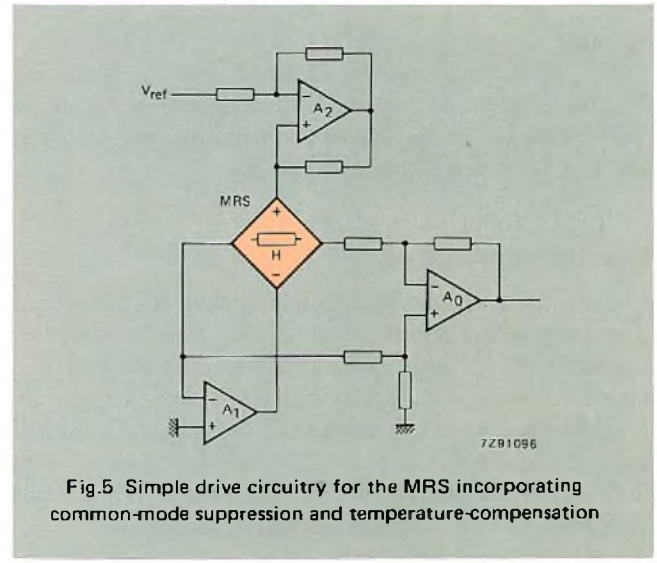

Fig.5 Simple drive circuitry for the MRS incorporating common-mode suppression and temperature-compensation

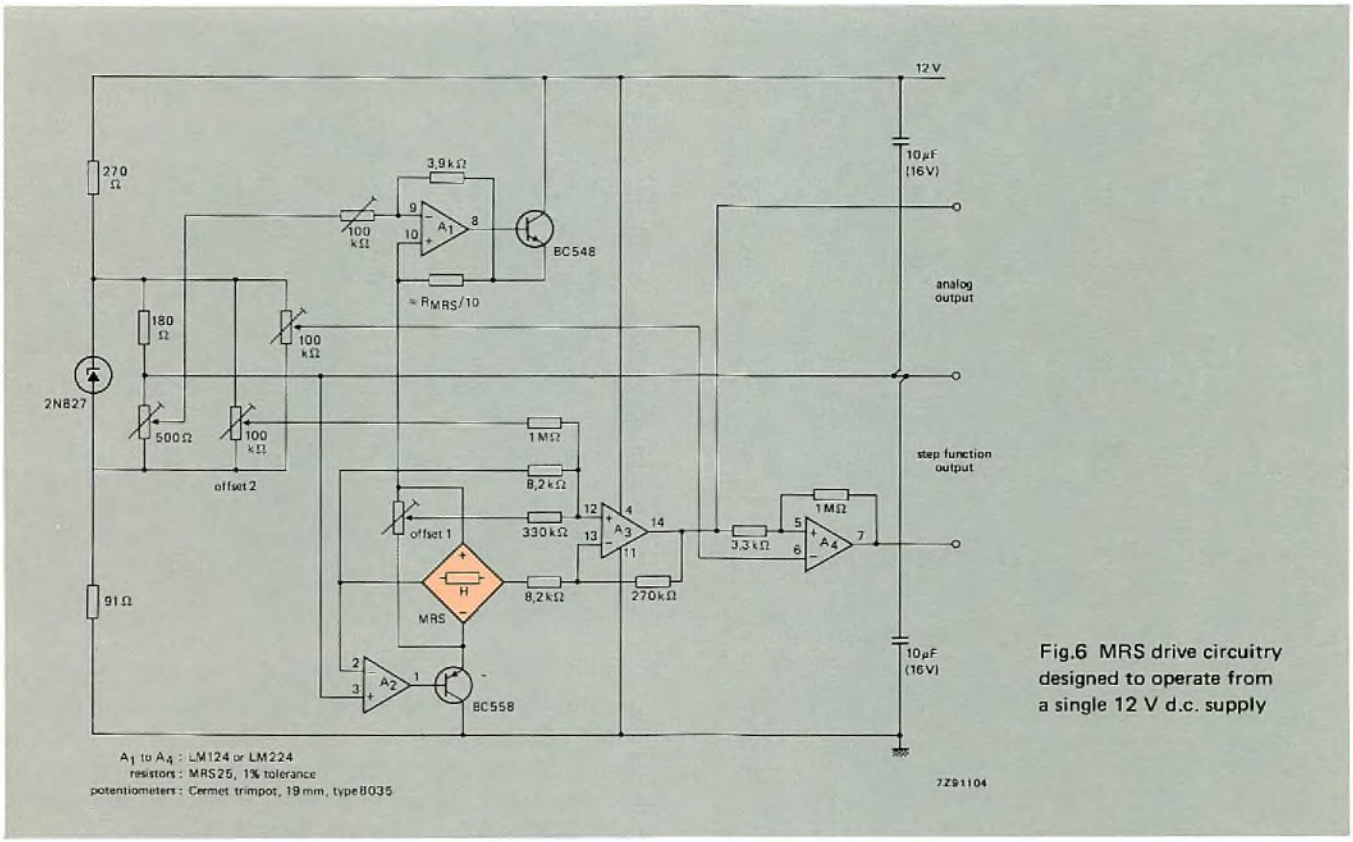

Fig.6 MRS drive circuitry designed to operate from a single 12 V d.c. supply

Internal magnetization

In the absence of a magnetic field normal to the permalloy strips, H_0 aligns the magnetization with the strip axis. If, for any reason, the sensor should come under the influence of a powerful magnetic field opposing H_0, the magnetization may flip 180° and the strips become magnetized in the opposite direction. This leads to drastic changes in sensor characteristics. As a precaution, therefore, the sensor should be provided with a stabilizing magnetic field parallel to H_0. Note, however, that the stabilizing field reduces sensitivity slightly, but since it need not to be too strong, the effect is minimal.

This field should not be confused with the linearising field H_{bias} referred to above, which is unnecessary with the MRS owing to the barberpole configuration, and which in any case, is applied perpendicular to H_0.

Practical applications

Linear position sensor. The MRS is ideally suited for use as a linear position sensor. Fig.7 shows a simple set-up for measuring linear displacement. Here a Ferroxdure disc magnet (magnetized axially) is located with its axis approximately normal to the plane of the sensor. The axis is inclined slightly to the normal to provide the sensor with the necessary stabilizing field. As Fig.8 shows, this set-up is highly sensitive to axial displacement of the magnet.

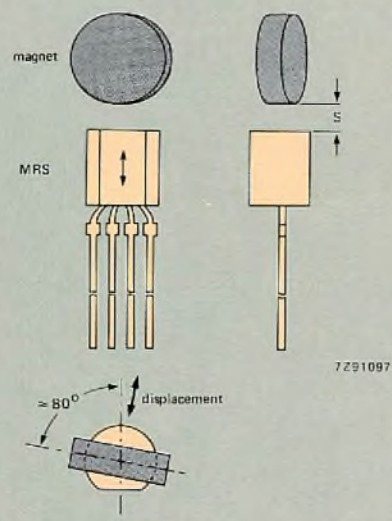

Fig.7 A highly sensitive position sensor using the MRS. A Ferroxdure disc magnet located with its axis approximately normal to the plane of the sensor chip, will, when moved axially, produce relatively large variations in the magnetic field passing through the sensor. The magnet axis is inclined slightly to the normal to provide the sensor with the necessary stabilizing field

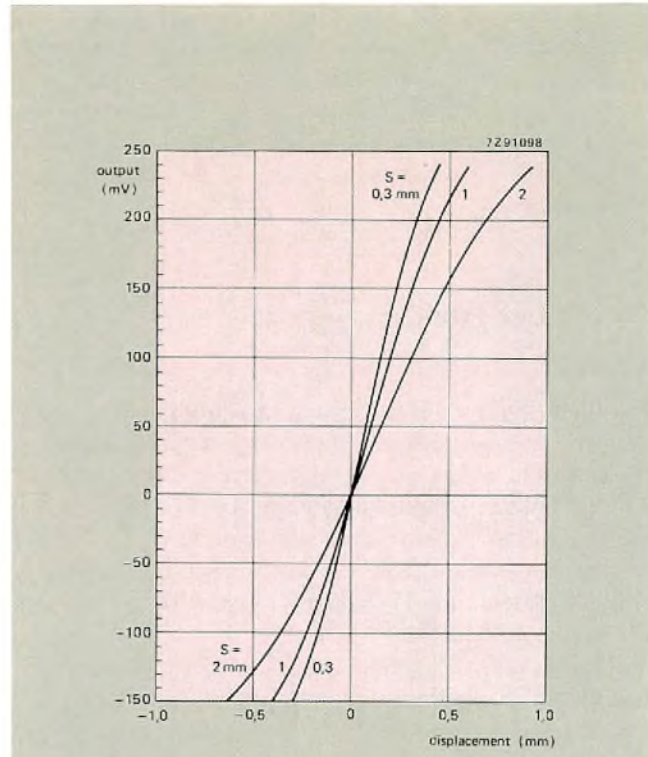

Fig.8 Sensor output versus magnet displacement for the set-up of Fig.7

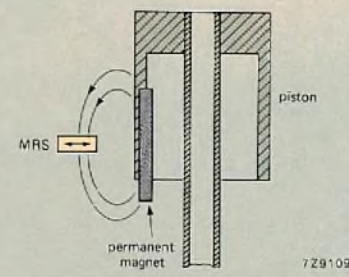

Fig.9 The MRS monitoring the axial position of a piston. The double-headed arrow indicates the sensitive direction of the MRS. A permanent magnet embedded in the piston body produces a field through the MRS whose vertical component forms the stabilizing field, and whose horizontal component varies with piston displacement

Fig.9 shows an example in which the MRS is used to monitor the axial position of a piston. A permanent magnet is embedded in the body of the piston, and the sensor is located off axis between its poles. The sensitive direction of the MRS (the direction in which it is sensitive to magnetic field variations) is indicated in Fig.9 by the arrows.

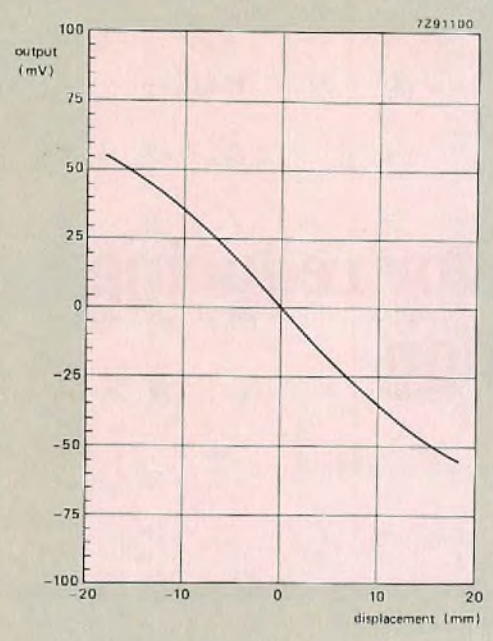

Fig.10 MRS output versus piston displacement

In this set-up, as in the one shown in Fig.7, both the stabilizing field and the varying field are produced by the same magnet. The vertical field passing through the MRS varies only slightly over the axial travel of the magnet and can be regarded as a constant stabilizing field. As the piston and magnet move axially, variations in the horizontal off-axis field are detected by the sensor, which produces a d.c. signal (Fig.10) proportional to piston displacement.

Angular position sensor. Fig.11(a) shows an experimental set-up in which the MRS is used to detect the angular position of a toothed iron wheel. The set-up could find application in, for example, electronic ignition systems. The sensor is located between a rotating iron wheel and a permanent magnet oriented with its magnetic axis parallel to the axis of the wheel. To provide the biasing field, the magnet centre is displaced slightly relative to the MRS.

Figure 12 shows the time varying output from the sensor, for sensor/wheel spacings S of 0,1 mm, 0,4 mm and 0,8 mm. The output is approximately sinusoidal with an amplitude strongly influenced by the spacing S. However, the interesting point emerging from Fig.12 is that the crossover point of the sinusoid is independent of S, and could therefore be used as the trigger point in an electronic ignition system.

Figure 11(b) shows a variation on the set-up of Fig.11(a) in which a non-metallic wheel bearing a steel tab rotates beneath an MRS. This set-up produces a similar output to that of Fig.11, again with the crossover point independent of sensor/wheel spacing.

The obvious advantage of both these set-ups lies in the fact that precise location of the sensor/magnet combination is unimportant as far as ignition timing is concerned, so adjustment procedures in a practical device would be greatly simplified.

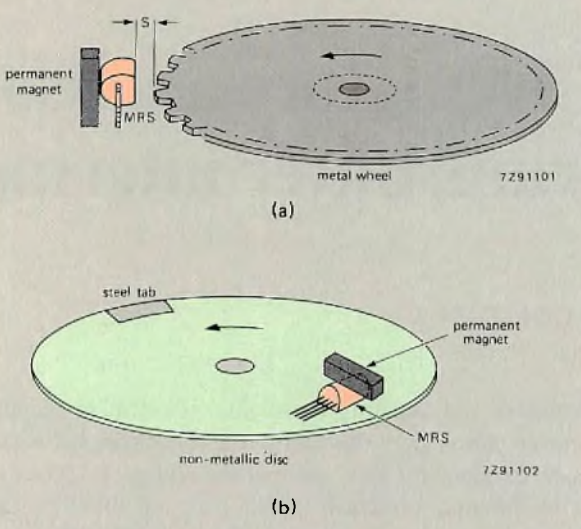

Fig.11 An MRS monitoring the angular position of (a) a rotating toothed iron wheel and (b) a rotating non-metallic wheel bearing a steel tab. Both these set-ups may find important applications in electronic ignition systems

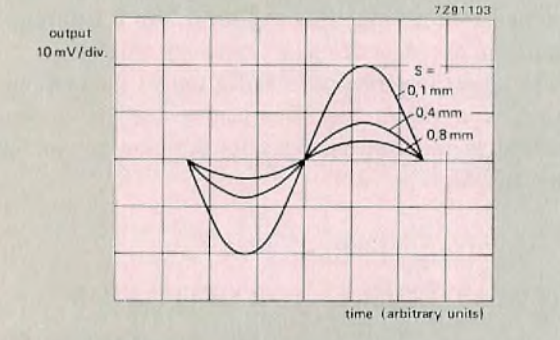

Fig.12 Time varying output of the MRS for the set-up of Fig.11(a), for different values of sensor/wheel spacing S. The output is approximately sinusoidal with an amplitude strongly influenced by S, but with a crossover point independent of S

These examples serve only to illustrate the many roles the MRS can fill. Other uses will become apparent as the device becomes more readily available. It's already quite possible to produce devices sufficiently sensitive to detect variations in the Earth's magnetic field. Such devices could be used to monitor traffic flow for example. Or they could be used to monitor electric current in, say, car-headlight circuitry, and to trigger a warning signal if the lights should fail.

Circulators and isolators for reducing transmitter intermodulation

W. GOLOMBEK

Circulators and isolators are highly effective in reducing intermodulation between transmitters operating on closely spaced frequencies. They are particularly useful when the intermodulation products fall in parts of the frequency spectrum removed by kilohertz rather than megahertz from the wanted frequencies. In these circumstances the commonly used coaxial cavity filters lose their effectiveness through severely reduced rejection efficiency, and – when used in cascade for better rejection – increased insertion loss. A circulator on the other hand, between transmitter and antenna, can reduce intermodulation by 20 dB or more, at the expense of no more than about 0,2 to 0,6 dB increase in insertion loss (depending on frequency range).

This article describes the operation of circulators and isolators, and shows how they can be used to maximum advantage in transmitting systems operating on communal transmitter sites.

CIRCULATOR/ISOLATOR OPERATION

The circulator (Fig.1) is a passive non-reciprocal device, consisting of three or more ports, coupled to a ferrite core magnetised along its axis by a pair of permanent magnets. The biasing field produced by these magnets orients the electron spins within the core to produce a gyromagnetic effect, with electrons precessing about the magnetic field direction.

An r.f. signal entering via port 1 say, interacts with the precessing electrons to produce a standing-wave pattern within the core (which acts as a low-Q resonator). This pattern is governed by the magnitude of the biasing field, so with suitable choice of permanent magnets, a nodal point can be made to occur at one of the other ports, e.g. port 3, which is thus isolated from the input (port 1). In the example shown in Fig.1, energy entering via port 1, exits via port 2, energy entering via port 2, exits via port 3, and so on in cyclic order.

The isolator is basically a three-port circulator with one of its ports, port 3 say, terminated with a matching load able to absorb all the energy directed to it. In the forward direction, r.f. energy can pass from port 1 to port 2, but energy passing in the reverse direction, i.e. into port 2, will be absorbed by the matching load. Note: the value of this load is critical. A mismatch producing appreciable v.s.w.r. will result in power being reflected by the load, and this power will emerge from port 1, thus negating some of the isolation possible with these devices.

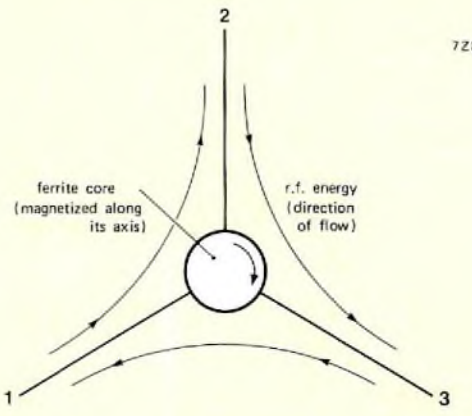

Fig.1 Three port circulator. The circulator has a circular ferrite core magnetised along its axis. When r.f. energy enters via port 1, a standing wave pattern is set up within the core which behaves effectively as a low-Q resonator. With proper adjustment of the magnetic field, a nodal point occurs at port 3 which is thus isolated from port 1. So all energy entering via port 1 exits via port 2, energy entering via port 2, exits via port 3, and so on

Circulators/Isolators/Isoductors for transmitter applications

frequency range[1]) (MHz)	cat. no. 2722 162...	type circ. C isol. I	max cw power (W) forw.	refl.	isolation (dB) min.	typ.	insertion loss (dB) max.	typ.	v.s.w.r. max.	typ.	temperature range (°C)	connector type[1])	approx. mass (g)
Mobile and fixed radio communication													
72-73	02911	I	25	20	20	23	0,7	0,6	1,25	1,2	0-55	Nfem	350
73-74	02731	I	25	20	20	23	0,7	0,6	1,25	1,2	0-55	Nfem	350
83-84	02721	I	25	20	20	23	0,7	0,6	1,25	1,2	0-55	Nfem	350
86,5-87,5	02861	I	25	20	20	23	0,7	0,6	1,25	1,2	0-55	Nfem	350
138-141	02901	I	25	20	22	24	0,4	0,3	1,2	1,15	0-55	Nfem	350
	05001	C	110		22	24	0,4	0,3	1,2	1,15	0-55	Nfem	350
144,5-147,5	02951	I	25	20	22	24	0,4	0,3	1,2	1,15	0-55	Nfem	350
153,5-156,5	02961	I	25	20	22	24	0,4	0,3	1,2	1,15	0-55	Nfem	350
156,9-162,1	03831	C	110		22	24	0,4	0,3	1,2	1,15	0-55	Nfem	350
157,9-163,1	03841	C	110		22	24	0,4	0,3	1,2	1,15	0-55	Nfem	350
165,4-170,6	03851	C	110		22	24	0,4	0,3	1,2	1,15	0-55	Nfem	350
160-178	01871	C	500		20	24	0,35	0,3	1,25	1,15	−10-60	Nfem	2100
	01901	C	1000		20	24	0,35	0,3	1,25	1,15	−10-40[2])	HF7/16fem	2150
225-400	03732	C	60		16	19	1,4	0,9	1,5	1,3	−40-80	Nfem	400
	03722	C	60		16	19	1,4	0,9	1,5	1,3	−40-80	SMAfem	380
225-270	01931	C	150		18	21	0,35	0,2	1,35	1,25	0-70	Nfem	725
	03171	C	500		20	24	0,35	0,3	1,25	1,15	−10-60	Nfem	2100
	03181	C	1000		20	24	0,35	0,3	1,25	1,15	−10-40[2])	HF7/16fem	2150
270-330	03421	C	60		18	21	0,35	0,2	1,25	1,25	0-70	SMAfem	725
	01941	C	150		18	21	0,35	0,2	1,35	1,25	0-70	Nfem	725
330-400	01951	C	150		18	21	0,35	0,3	1,35	1,25	0-70	Nfem	725
400-470	02711	I	25	20	20	25	0,5	0,35	1,25	1,15	−10-60	Nfem	350
	03411	C	100		20	25	0,5	0,35	1,25	1,15	−10-60	Nfem	400
	01572	C	300		20	25	0,35	0,20	1,25	1,15	−10-60	Nfem	1200
406-414	02931	I/C[3])	70	70	45	55	0,8	0,5	1,25	1,2	−10-60	Nfem	800
450-458	02981	I/C[3])	70	70	45	55	0,8	0,5	1,25	1,2	−10-60	Nfem	800
460-468	02851	I/C[3])	70	70	45	55	0,8	0,5	1,25	1,2	−10-60	Nfem	800
462-468	01555	C	60	60	25	30	0,5	0,3	1,2	1,1	−10-60	Nfem	400
510-514	02921	I/C[3])	70	70	45	55	0,8	0,5	1,25	1,2	−10-60	Nfem	800
600-960	05171	C	10		16	20	1,3	0,8	1,4	1,25	−25-65	SMAfem	400
	06011	I	10	1	16	20	1,3	0,8	1,4	1,25	−25-65	SMAfem	400
790-1000	03811	C	100		20	25	0,5	0,3	1,25	1,14	−10-60	SMAfem	400
	02741	I	50	10	20	25	0,5	0,35	1,25	1,15	−25-65	SMAfem	400
	03261	C	100		20	25	0,5	0,3	1,25	1,14	−10-60	Nfem	400
	03263[4])	C	100		20	25	0,5	0,3	1,25	1,14	−10-60	Nfem	400
Isoductors													
68-150	09001		25		20		0,9 or 0,7[5])		1,22		0-60		40
140-260	09011		25		20		0,6		1,22		0-60		40
230-470	09021		25		20		0,5		1,22		0-60		40

[1]) Other frequency ranges, and other connectors are available on request.

[2]) If the devices are air cooled, dry-air should be used as a pressure of 25 mm water column and with a maximum intake temperature of 40 °C. The connector temperature should then not exceed 55 °C.

[3]) I/C denotes a 4-port device with one port terminated with a matched load.

[4]) Ultra-low-noise version of type 03261.

[5]) Depending on whether frequency is ⩽ 100 MHz or > 100 MHz.

Circulators/isolators are designed to operate in a specific frequency range (see Table). They are dedicated, packaged devices, available in waveguide or triplate technology, and with a choice of coaxial or waveguide terminations. For radio and TV transmission, however, the choice of terminations is usually limited to coaxial.

A range of isoductors is also available. These unpackaged devices are printed-circuit compatible. They function as either circulators or isolators, and can easily be tuned to the desired frequency with the aid of trimming capacitors.

Bandwidth

Figure 2 shows how the isolation, v.s.w.r. and insertion loss of a typical narrow band isolator varies with frequency. At the centre f_c of its range, the device can provide up to 30 dB isolation, but this drops off rapidly either side of f_c. Usually, the bandwidth covers about 3% of f_c, the isolation falling by some 15 to 20 dB at the band edges. So a 150 MHz device could conceivably be used from 147 MHz to 153 MHz. If maximum isolation is essential, however, i.e. more than 25 dB, a more realistic bandwidth might extend from 148 MHz to 151 MHz (±1% of f_c).

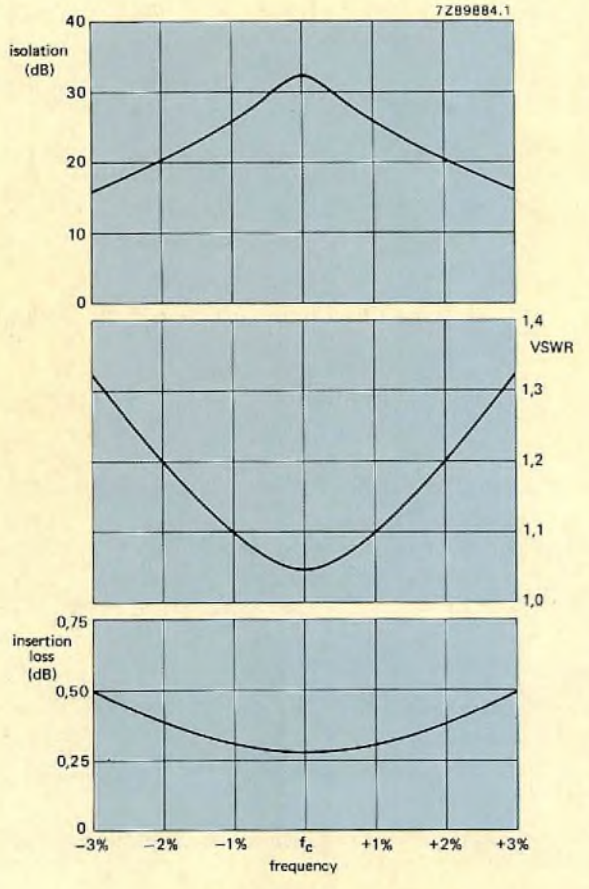

Fig.2 Isolation, v.s.w.r. and insertion loss of a typical narrow band isolator as functions of frequency

With this narrower bandwidth, the performance at the band edges roughly equates with that of a fairly standard coaxial filter. So for a bandwidth greater than about ±2% the coaxial filter is definitely favoured.

Two or more isolators in series, each covering a discrete but adjacent 1% section of the band, would provide a greater overall bandwidth, but the insertion losses might then be excessive. As an alternative, a broadband circulator/isolator could be used. These devices have a bandwidth of 20% or more, with a minimum isolation of about 20 dB. Normally, they cover the whole frequency band of interest, and no special tuning is required.

ISOLATING ON-SITE TRANSMITTERS

Figure 3(a) shows a basic setup for two on-site transmitters operating with separate antennas.

If the antenna systems connected to each transmitter are mounted on a common structure, then provided care is taken with feeder runs, polarisation, spacing etc., you could expect intrinsic isolation of about 35 dB. Anything less than this would certainly lead to excessive levels of spurious radiation. For, say, 25 W transmitter power, this will result in 3rd order products at around the 5 mW level, and in 5th order products at a slightly lower level. Such power levels are quite capable of providing a receiver signal of around 5 μV at a distance of 2 km.

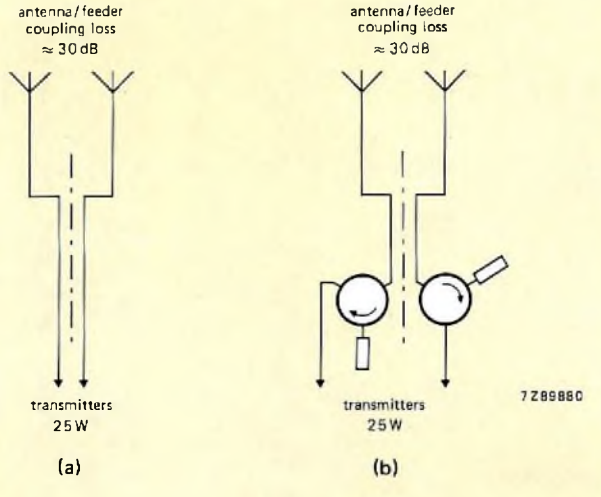

Fig.3 (a) Two closely spaced transmitters operating with separate antennas. Total isolation between the transmitters would be around 35 dB which for a 25 W transmitter will result in 3rd and 5th order products at around the 5 mW level. This is sufficient to produce a spurious signal of around 5 μV at a distance of 2 km; (b) isolators in the antenna circuit, giving some 20 dB isolation (at the expense of only about 1 dB power loss), reduce the intermodulation level from 5 mW to around 50 μW, and cut the range of interference from 2 km to under 200 m for the same receiver signal.

This level of spurious radiation is not serious in itself if the transmitting frequencies are properly planned, i.e. to allow the spurious signals to fall on unoccupied frequencies. Usually, however, this is not the case, and to prevent excessive interference on occupied frequencies, an isolator is essential.

Figure 3(b) shows the system with an isolator in each antenna circuit. These leave the output signals relatively unaffected (less than 1 dB power loss), whilst reducing reverse power by some 20 dB. This reduces the intermodulation level in the setup described above from 5 mW to 50 μW, and cuts the range of interference from 2 km to under 200 m for the same receiver signal.

Note: for better intermodulation suppression, two isolators in series can be inserted between each transmitter and its associated antenna.

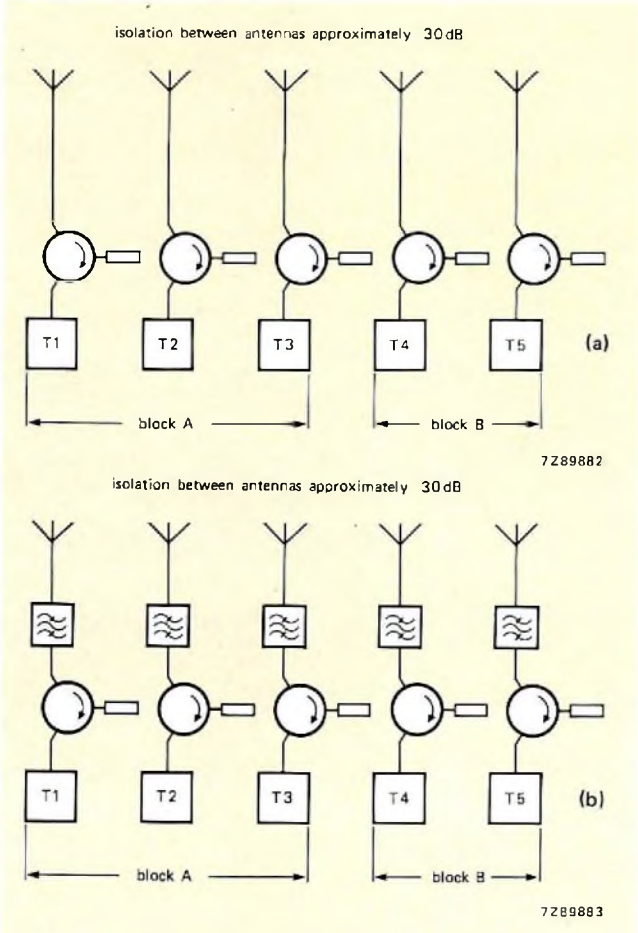

Fig.4 (a) Two blocks of transmitters – T1, T2, T3 operating on 1500, 1501, 1504 MHz and T4, T5 operating on 1525 and 1527 MHz. Isolators in the antenna circuits give 20 dB increase in isolation between transmitters within each block, but owing to limited bandwidth, only 10 dB increase in isolation between blocks. So with say 30 dB intrinsic antenna isolation, total isolation will be only 40 dB; (b) coaxial bandpass filters in the antenna circuits add about 30 dB to the interblock isolation, giving a total interblock isolation of around 70 dB

COMBINING ISOLATORS AND FILTERS

Circumstances may exist on communal transmitter sites where several frequencies are instrumental in causing intermodulation problems. Some of these frequencies may be separated from the others by several megahertz, and for these, normal (narrow band) circulators/isolators will be ineffective.

Figure 4(a) illustrates the problem. Here two blocks of transmitters: T1, T2, T3 operating on 1500, 1501 and 1504 MHz, and T4, T5 operating on 1525 and 1527 MHz have isolators in their antenna circuits. Suppose these provide 20 dB isolation. The total isolation between transmitters within each block, including say 30 dB intrinsic antenna isolation, will then be around 50 dB. Because of their limited bandwidth, however, the isolators will only provide about 10 dB isolation between each block, so the total isolation will be only 40 dB.

Figure 4(b) shows how the use of filters can overcome this problem. Coaxial bandpass filters in the antenna circuits, whilst having no effect on the isolation between transmitters in each block, can add 30 dB to the interblock isolation, giving a total isolation of around 70 dB.

In the above example (i.e. with only about 25 MHz separation between blocks), the problem could be solved just as easily with broad band isolators. In many instances, however, this would not be practicable.

OPERATING RECOMMENDATIONS

- *Unit power rating.* Do not exceed the rated power of a circulator or isolator.
- *Terminating load – power rating.* The terminating load of an isolator must be capable of dissipating the full rated output power of the transmitter. Otherwise, severe mismatch, caused for example by snow or ice on the antenna, could damage or destroy the isolator and lead ultimately to transmitter failure. It should be noted that the load rating will fall with increasing ambient temperature. If several isolators in series are used, only the isolator nearest the antenna is subject to the above requirement.
- *Unit 'hop-over'.* An isolator is only effective in reducing spurious signals that arrive via the antenna. Any equipment coupling will negate some of the isolation gained. So to gain maximum benefit from using an isolator, the effect of surrounding units (hop-over) should be minimized, either by screening the units, or by keeping them well separated. Other likely sources of 'hop-over' that should be looked for, and eliminated if possible are: common earthing of feeder lines within the same cabinet, poor quality feeder lines, and badly made coaxial joints.
- *Magnetic effects.* Keep the units away from stray magnetic fields, produced for example by loudspeakers, transformers etc.

TUNING ISODUCTORS

1. Tune the transmitter to the required frequency and reduce its power to around 1/10th of its normal output power (or less if possible).
2. Connect the isoductor to the transmitter in the forward direction i.e. arrow pointing away from the transmitter (Fig.5) and tune the parallel capacitor at the input of the isoductor and then the series capacitor at the input for maximum forward power (measured on a power meter connected to the output of the isoductor). Repeat for the output capacitors.
3. Reverse the isoductor in the transmission line so that the arrow points towards the transmitter, and adjust the parallel capacitor at the terminated port and then the series capacitor for minimum reverse power (measured on the power meter).
4. Return to step (2) and re-adjust if necessary.

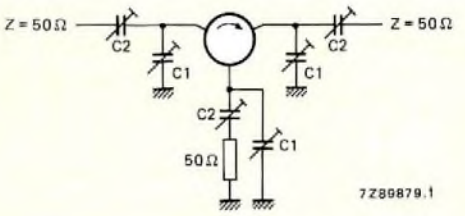

type	C1 (pF)	C2 (pF)
2722 162 09001	25 to 200	20 to 150
2722 162 09011	5,5 to 65	5,5 to 65
2722 162 09021	2 to 16,5	2 to 16,5

Fig.5 Isoductor circuit. Only low temperature coefficient trimming capacitors should be used

REFERENCE

For a more detailed discussion of isolators and circulators and their uses, consult Philips Application book 'Isolators and Circulators', 1974, published by Philips Electronic Components and Materials Division.

A complete f.m. radio on a chip

W. H. A. VAN DOOREMOLEN and M. HUFSCHMIDT

Until now, the almost total integration of an f.m. radio has been prevented by the need for LC tuned circuits in the r.f., i.f., local-oscillator and demodulator stages. An obvious way to eliminate the coils in the i.f. and demodulator stages is to reduce the normally used intermediate frequency of 10.7 MHz to a frequency that can be tuned by active RC filters, the op-amps and resistors of which can be integrated. An i.f. of zero seems to be ideal because it eliminates spurious signals such as repeat spots and image response, but it would not allow the i.f. signal to be limited prior to demodulation, resulting in poor S/N ratio and no a.m. suppression. With an i.f. of 70 kHz, these problems are overcome and the image frequency occurs about halfway between the desired signal and the centre of the adjacent channel. However, the i.f. image signal must be suppressed and, in common with conventional f.m. radios, there is also a need to suppress interstation noise and noise when tuned to a weak signal. Spurious responses above and below the centre frequency of the desired station (side tunings), and harmonic distortion in the event of very inaccurate tuning must also be eliminated.

We have now developed a mono f.m. reception system which is suitable for almost total integration. It uses an active 70 kHz i.f. filter and a unique correlation muting circuit for suppressing spurious signals such as side responses caused by the flanks of the demodulator S-curve. With such a low

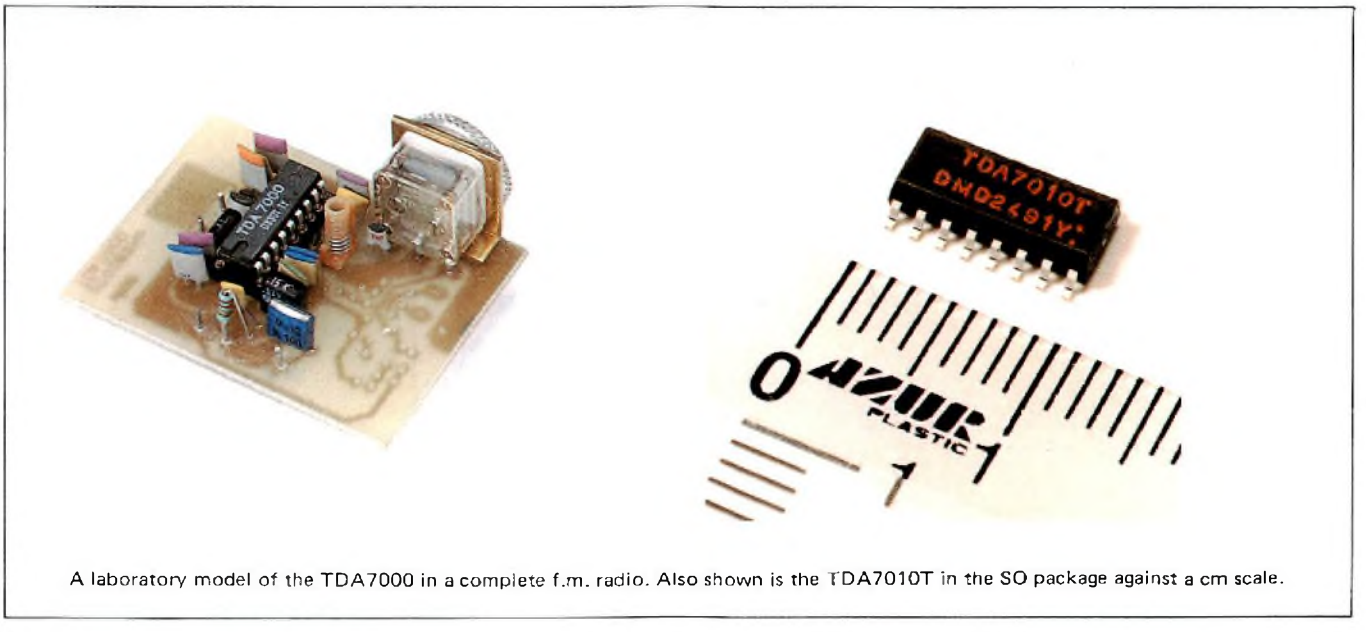

A laboratory model of the TDA7000 in a complete f.m. radio. Also shown is the TDA7010T in the SO package against a cm scale.

i.f., distortion would occur with the ±75 kHz i.f. swing due to received signals with maximum modulation. The maximum i.f. swing is therefore compressed to ±15 kHz by controlling the local-oscillator in a frequency locked loop (FLL). The combined action of the muting circuit and the FLL also suppresses image response.

The new circuit is the TDA7000 which integrates a mono f.m. radio all the way from the aerial input to the audio output. External to the IC are only one tunable LC circuit for the local-oscillator, a few inexpensive ceramic plate capacitors and one resistor. The TDA7000 dramatically reduces assembly and post-production alignment costs because only the oscillator circuit needs adjustment during manufacture to set the limits of the tuned frequency band. The complete f.m. radio can be made small enough to fit inside a calculator, cigarette lighter, key-ring fob or even a slim watch. The TDA7000 can also be used as a receiver in equipment such as cordless telephones, CB radios, radio-controlled models, paging systems, the sound channel of a tv set or other f.m. demodulating systems.

Using the TDA7000 results in significant improvements for all classes of f.m. radio. For simpler portables, the small size, lack of i.f. coils, easy assembly and low power consumption are not the only attractive features. The unique correlation muting system and the FLL make it very easy to tune, even when using a tiny tuning knob. For higher-performance portables and clock radios, variable-capacitance diode tuning and station presetting facilities are often required. These are easily provided with the TDA7000 because there are no variable tuned circuits in the r.f. signal

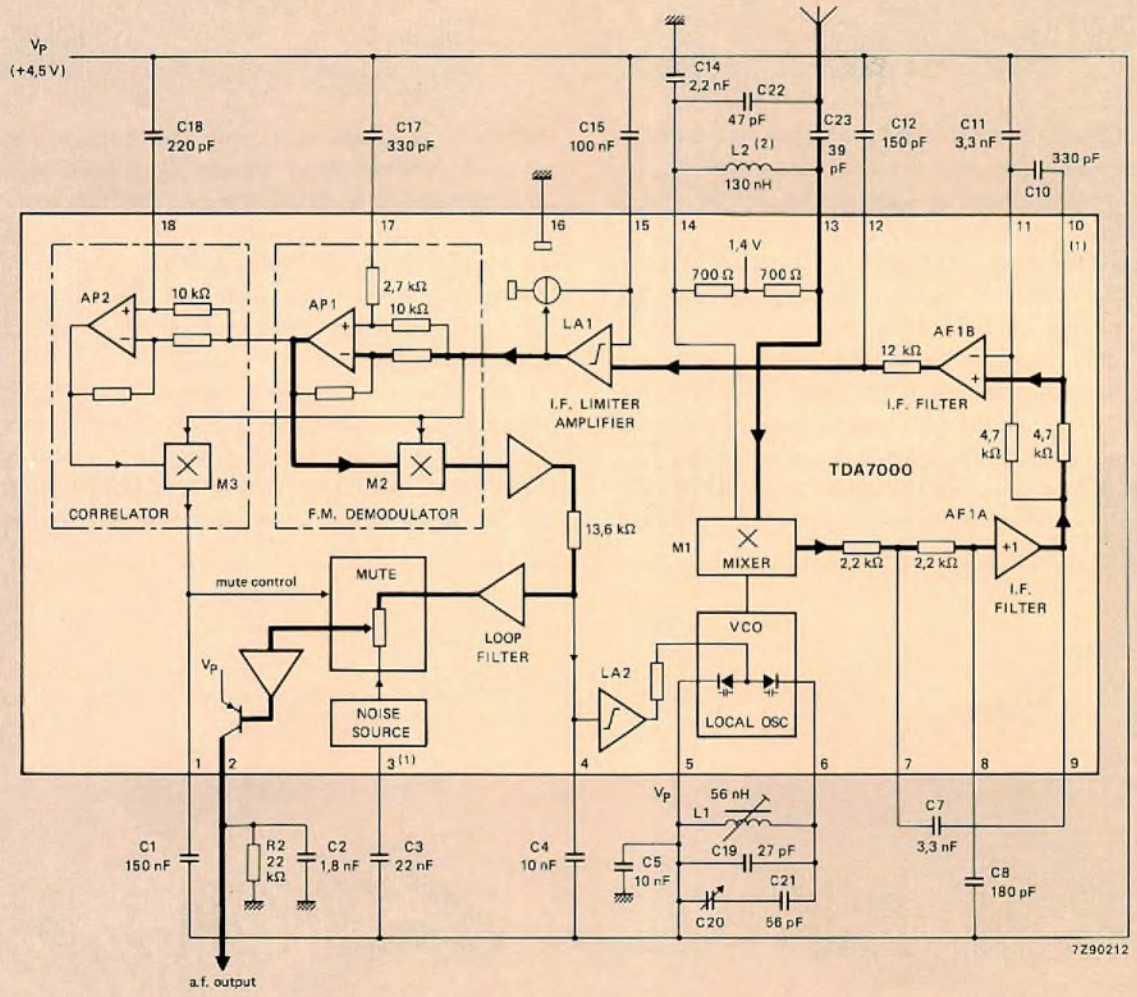

Fig.1 The TDA7000 as a variable capacitor tuned f.m. broadcast receiver

1) These pins are not used in the SO package version (TDA7010T)
AP = All-Pass filter.

2) L_2 is printed on the experimental PCB (Fig.12).
L_1 = Toko MC108 No.514 HNE 150013S13.
C_{20} = Toko No. 2A-15BT-R01.

path. Only the local-oscillator needs to be tuned, so tracking and distortion problems are eliminated.

The TDA7000 is available in either an 18-lead plastic DIL package (TDA7000), or in a 16-pin SO package (TDA7010T). Future developments will include reducing the present supply voltage (4.5 V typ.), and the introduction of f.m. stereo and a.m./f.m. versions.

BRIEF DATA

typical supply voltage	V_p	4.5 V
typical supply current	I_p	8 mA
r.f. input frequency range	f_{rf}	1.5 to 110 MHz
sensitivity for −3 dB limiting e.m.f. with $Z_s = 75\Omega$, mute disabled	$V_{rf\text{-}3\,dB}$	1.5 μV
maximum signal input for THD < 10%, Δf = ±75 kHz e.m.f. with $Z_s = 75\Omega$	V_{rf}	200 mV
audio output (r.m.s.) with $R_L = 22\,k\Omega$, Δf = ±22.5 kHz	V_o	75 mV

CIRCUIT DESCRIPTION

As shown in Fig.1, the TDA7000 consists of a local-oscillator and a mixer, a two-stage active i.f. filter followed by an i.f. limiter/amplifier, a quadrature f.m. demodulator, and an audio muting circuit controlled by an i.f. waveform correlator. The conversion gain of the mixer, together with the high gain of the i.f. limiter/amplifier, provides a.v.c. action and effective suppression of a.m. signals. The r.f. input to the TDA7000 for −3 dB limiting is 1.5 μV. In a conventional portable radio, limiting at such a low r.f. input level would cause instability because higher harmonics of the clipped i.f. signal would be radiated to the aerial. With the low i.f. used with the TDA7000, the radiation is negligible.

To prevent distortion with the low i.f. used with the TDA7000, it is necessary to restrict the i.f. deviation due to heavily modulated r.f. signals to ±15 kHz. This is achieved with a frequency-locked loop (FLL) in which the output from the f.m. demodulator shifts the local-oscillator frequency in inverse proportion to the i.f. deviation due to modulation.

Active i.f. filter

The first section of the i.f. filter (AF1A) is a second-order low-pass Sallen-Key circuit with its cut-off frequency determined by internal 2.2 kΩ resistors and external capacitors C_7 and C_8. The second section (AF1B) consists of a first-order bandpass filter with the lower limit of the passband determined by an internal 4.7 kΩ resistor and external capacitor C_{11}. The upper limit of the passband is determined by an internal 4.7 kΩ resistor and external capacitor C_{10}. The final section of the i.f. filter consists of a first-order low-pass network comprising an internal 12 kΩ resistor and external capacitor C_{12}. The overall i.f. filter therefore consists of a fourth-order low-pass section and a first-order high-pass section. Design equations for the filter are given in Fig.2. Figure 3 shows the measured response for the filter.

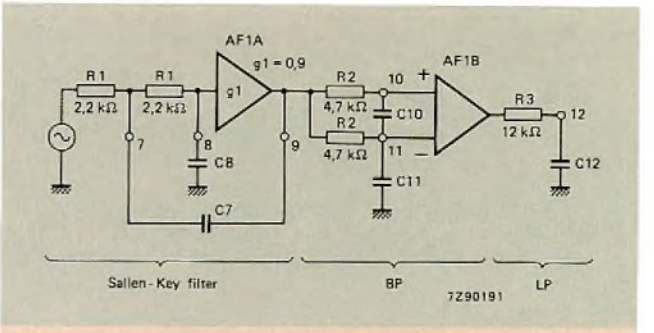

Sallen-Key circuit

$$A_{SK} = \frac{g}{1 + j\omega a - \omega^2 b} \qquad \text{with } a = 2R_1C_8,\ b = R_1^2C_7C_8$$

$$\text{With } f_0 = \frac{1}{2\pi R_1\sqrt{(C_7C_8)}} \text{ and } Q = \frac{\sqrt{b}}{a} = 0.5\sqrt{\frac{C_7}{C_8}}$$

$$A_{SK} = \frac{g}{1 + \left(j\,\frac{\omega}{\omega_o} \times \frac{1}{Q}\right) - \frac{\omega^2}{\omega_o^2}}$$

For C_7 = 3.3 nF, C_8 = 180 pF; Q = 2.1 and f_o = 94 kHz

Bandpass circuit

$$A_{BP} = \frac{1}{1 + j\omega C_{10}R_2} \times \frac{j\omega C_{11}R_2}{1 + j\omega C_{11}R_2 + \frac{j\omega C_{10}R_2}{1 + j\omega C_{10}R_2}}$$

$$\text{for } f_{LP} = \frac{1}{2\pi R_2 C_{10}} \text{ and } f_{HP} = \frac{1}{2\pi R_2 C_{11}}$$

$$A_{BP} = \frac{f_{LP}}{f_{HP}} \times \frac{1}{\left(1 + j\,\frac{f}{f_{HP}}\right)\left(1 - j\,\frac{f_{LP}}{f}\right) + 1}$$

For C_{10} = 330 pF, C_{11} = 3.3 nF; f_{LP} = 103 kHz, f_{HP} = 10.3 kHz

Low-pass circuit

$$A_{LP} = \frac{1}{1 + j\omega C_{12}R_3}$$

$$\text{for } f_{LP} = \frac{1}{2\pi C_{12}R_3}$$

$$A_{LP} = \frac{1}{1 + j\,\frac{\omega}{\omega_{LP}}}$$

For C_{12} = 150 pF; f_{LP} = 88.4 kHz.

Fig.2 I.F. filter of the TDA7000

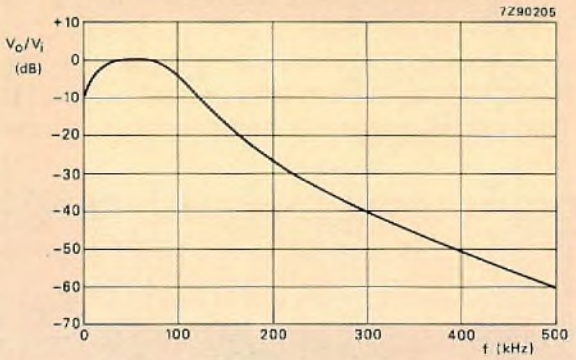

Fig.3 Measured response of the i.f. filter

F.M. demodulator

The quadrature f.m. demodulator M2 converts the i.f. variations due to modulation into an audio frequency voltage. It has a conversion gain of −3.6 V/MHz and requires phase quadrature inputs from the i.f. limiter/amplifier. As shown in Fig.4, the 90° phase shift is provided by an active all-pass filter which has about unity gain at all frequencies but can provide a variable phase shift, dependent on the value of external capacitor C_{17}.

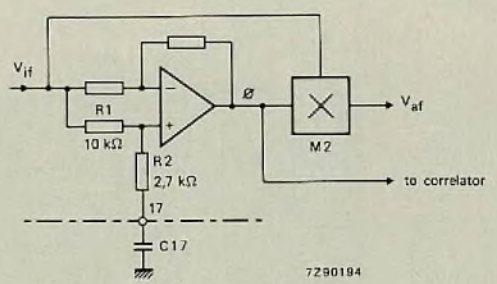

With $R_2 = 0$,

$\phi = -2 \tan^{-1} \omega R_1 C_{17}$

for $\phi = -90°$, $C_{17} = \frac{1}{\omega R_1}$, = 227 pF for f_{if} = 70 kHz.

To improve the performance of the all-pass filter with the amplitude limited i.f. waveform, R_2 has been added. Since this influences the phase angle, the value of C_{17} must be increased by 50% i.e. to 330 pF for f_{if} = 70 kHz.

Fig.4 F.M. demodulator phase shift circuit (all-pass filter)

I.F. swing compression with the FLL

With a nominal i.f. as low as 70 kHz, severe harmonic distortion of the audio output would occur with an i.f. deviation of ±75 kHz due to full modulation of a received f.m. broadcast signal. The FLL of the TDA7000 is therefore used to compress the i.f. swing by using the audio output from the f.m. demodulator to shift the local-oscillator frequency in opposition to the i.f. deviation. The principle is illustrated in Fig.5, which shows that an i.f. deviation of 75 kHz is compressed to about 15 kHz. The THD is thus limited to 0.7% with ±22.5 kHz modulation, and to 2.3% with ±75 kHz modulation.

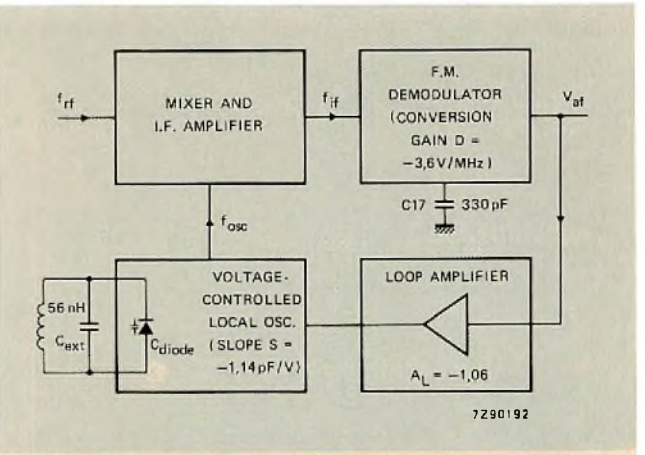

$C_o = C_{ext} + C_{stray} + C_{diode}$ with open loop = 49 pF at f_o = 96 MHz

feedback factor $\beta = \frac{A_L S f_o}{2C_o}$

open loop conversion gain = D = −3.6 V/MHz

closed loop conversion gain = $\frac{D}{1 + D\beta}$ = 0.68 V/MHz for f_o = 96 MHz

modulation compression factor $K = \frac{\text{open loop gain}}{\text{closed loop gain}} = \frac{3.6 \text{ V/MHz}}{0.684 \text{ V/MHz}} \approx 5$

$\Delta f_{osc} = \Delta f_{rf} \left(1 - \frac{1}{K}\right)$

$\Delta f_{if} = \frac{\Delta f_{rf}}{K}$

for Δf_{rf} = 75 kHz, Δf_{osc} = 60.74 kHz, $\Delta f_{if} \approx$ 15 kHz

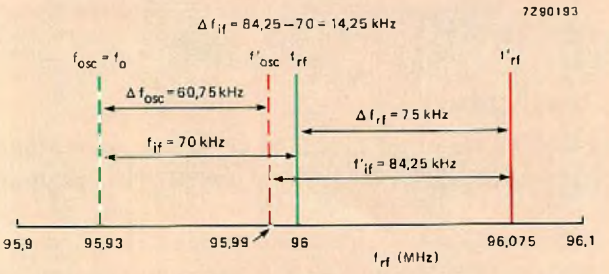

Fig.5 I.F. swing compression with the FLL

Correlation muting system with open FLL

A well-known difference between f.m. and a.m. is that, for f.m., each station is received in at least three tuning positions. Fig.6 shows the frequency spectrum of the output from the demodulator of a typical portable f.m. radio receiving an r.f. carrier frequency-modulated with a tone of constant frequency and amplitude. In addition to the audio response at the correct tuning point in the centre of Fig.6, there are two side responses due to the flanks of the demodulator S-curve. Because the flanks of the S-curve are non-linear the side responses have increased harmonic distortion. In Fig.6, the frequency and intensity of the side responses are functions of the signal strength, and they are separated from the correct tuning point by amplitude minima. However, in practice, the amplitude minima are not well defined because the modulation frequency and index are not constant and moreover, the side responses of adjacent channels often overlap.

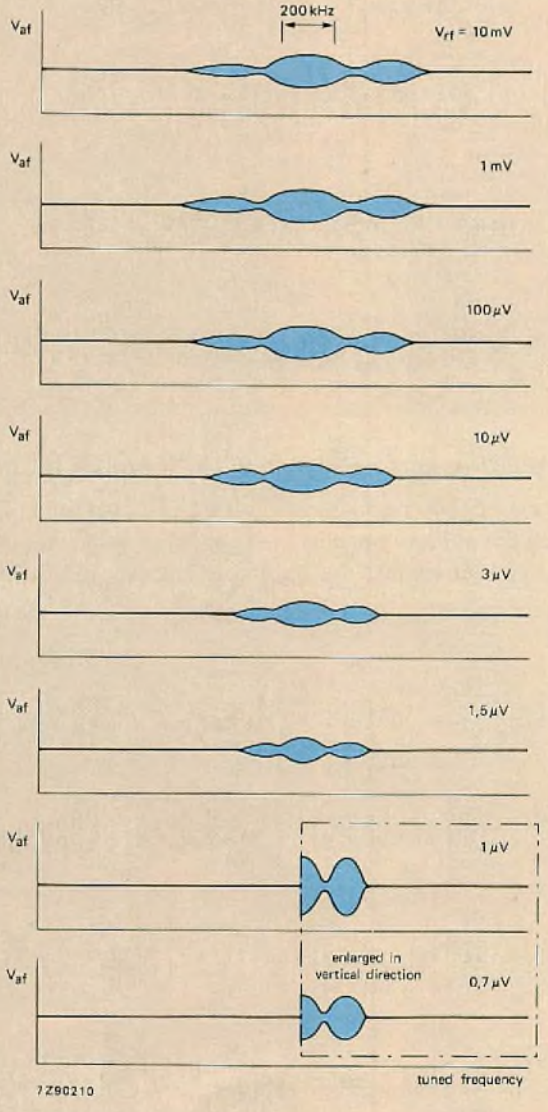

Fig.6 Audio signal of a typical portable radio as a function of tuned frequency with r.f. input as a parameter. The modulation frequency and amplitude are both constant

High performance f.m. radios incorporate squelch systems such as signal-strength-dependent muting and tuning-deviation-dependent muting (Ref.1) to suppress side responses. They also have a tuning meter to facilitate correct tuning. Although the TDA7000 is mainly intended for use in portables and clock radios, it incorporates a very effective new correlation muting system which suppresses interstation noise and spurious responses due to detuning to the flanks of the demodulator S-curve. The muting system is controlled by a circuit which determines the correlation between the waveform of the i.f. signal and an inverted version of it which is delayed (phase shifted) by half the period of the nominal i.f. (180°). A noise generator works in conjunction with the muting system to give an audible indication of incorrect tuning.

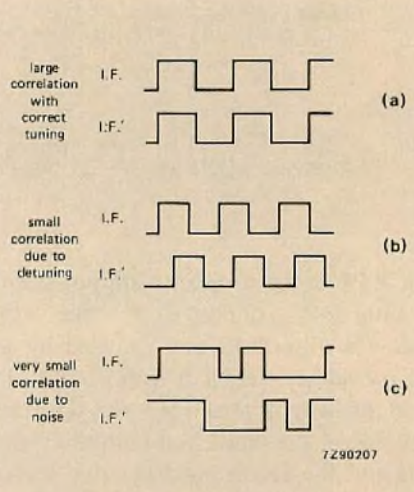

Fig.7 Function of the correlation muting system

Figure 7 illustrates the function of the muting system. Signal IF′ is derived by delaying the i.f. signal by half the period of the nominal i.f. and inverting it. With correct tuning as shown in Fig.7(a), the waveform of the two signals are identical resulting in large correlation. In this situation, the audio signal is not muted. With detuning as shown in Fig.7(b), signal IF′ is phase-shifted with respect to the i.f. signal. The correlation between the two waveforms is therefore small and the audio output is muted. Figure 7(c) shows that, because of the low Q of the i.f. filter, noise causes considerable fluctuations of the period of the i.f. signal waveform. There is then small correlation between the two waveforms and the audio is muted. The correlation muting system thus suppresses noise and side responses due

to detuning to the flanks of the demodulator S-curve. Since the mute threshold is much lower than that obtained with most other currently used muting systems, this muting system is ideal for portable radios which must often receive signals with a level only slightly above the input noise.

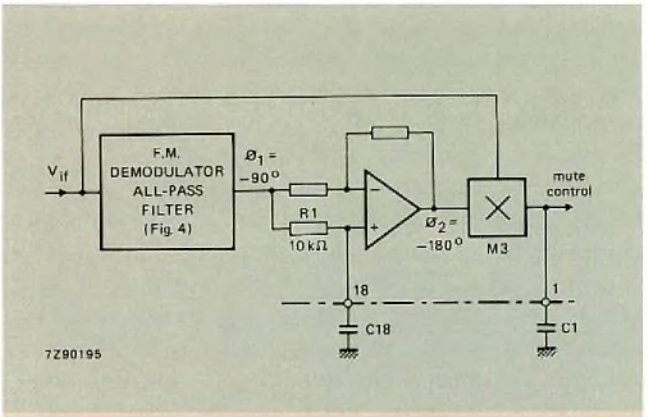

$$\phi_2 = -2 \tan^{-1} \omega R_1 C_{18}$$

$$\text{for } \phi_2 = -90° \; C_{18} = \frac{1}{\omega R_1}$$

for f_{if} = 70 kHz, C_{18} = 227 pF

Fig.8 Correlator of the TDA7000

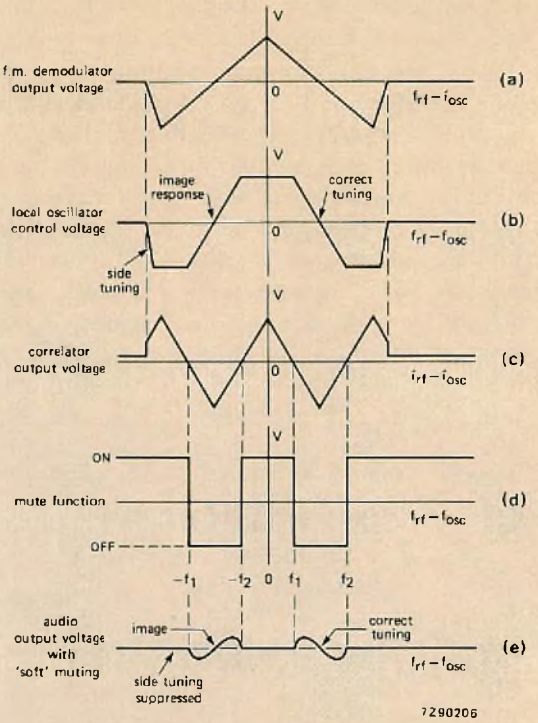

Fig.9 Operation of the correlation muting system with open-loop FLL

As shown in Fig.8, the correlation muting circuit consists of all-pass filter AP2 connected in series with f.m. demodulator all-pass filter AP1 and adjusted by an external capacitor to provide a total phase shift of 180°. The output from AP2 is applied to mixer M3 which determines the correlation between the undelayed limited i.f. signal at one of its inputs and the delayed and inverted version of it at its other input. The output from mixer M3 controls a muting circuit which feeds the demodulated audio signal to the output when the correlation is high, or feeds the output from a noise source to the output to give an audible indication of incorrect tuning when the correlation is low. The switching of the muting circuit is progressive (soft muting) to prevent the generation of annoying audio transients. The output from mixer M3 is available externally at pin 1 and can also be used to drive a detuning indicator.

Figure 9 shows that there are two regions where the demodulated audio signal is fed to the output because the muting is inactive. One region is centred on the correct tuning point f_L. The other is centred on the image frequency $-f_L$. The image response is therefore not suppressed by the muting system when the frequency-locked loop is open. When the loop is closed, the time-constant of the muting system, which is determined by external capacitor C_1, prevents the image response being passed to the audio output. This is described under the next heading.

Correlation muting system with closed FLL

The closed-loop response of the FLL is shown in Fig.10, in which the point of origin is the nominal i.f. ($f_{rf} - f_{osc} = f_L$). With correct tuning, the muting is inactive and the audio

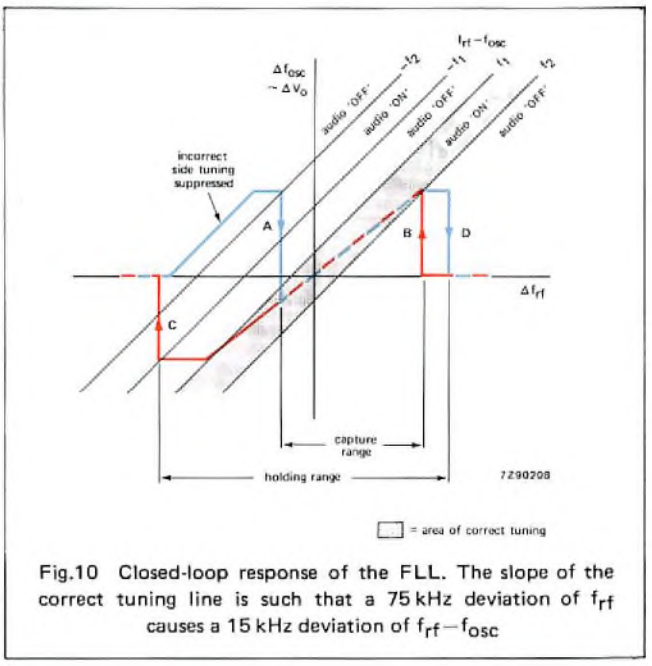

Fig.10 Closed-loop response of the FLL. The slope of the correct tuning line is such that a 75 kHz deviation of f_{rf} causes a 15 kHz deviation of $f_{rf}-f_{osc}$

signal is fed to the output. Spurious responses due to the flanks of the demodulator S-curve which occur outside the i.f. band $-f_2$ to f_2 are suppressed because the muting is active. Fast transients of the audio signal due to locking of the loop (A and B), and to loss of lock (C and D) are suppressed in two ways.

Lock and loss of lock transients B and D occur when the i.f. is greater than f_2 and are therefore suppressed because the muting is active. The situation is different during loss of lock transient C because the muting is only active for the last part of the transient. To completely suppress this transient, capacitor C_1 in Fig.1 holds the muting control line positive (muting active) during the short interval whilst the i.f. traverses from $-f_1$ to $-f_2$. The same applies for lock transient A during the short interval whilst the i.f. traverses from $-f_2$ to $-f_1$. Since the image response occurs halfway between $-f_1$ and $-f_2$, it is also suppressed.

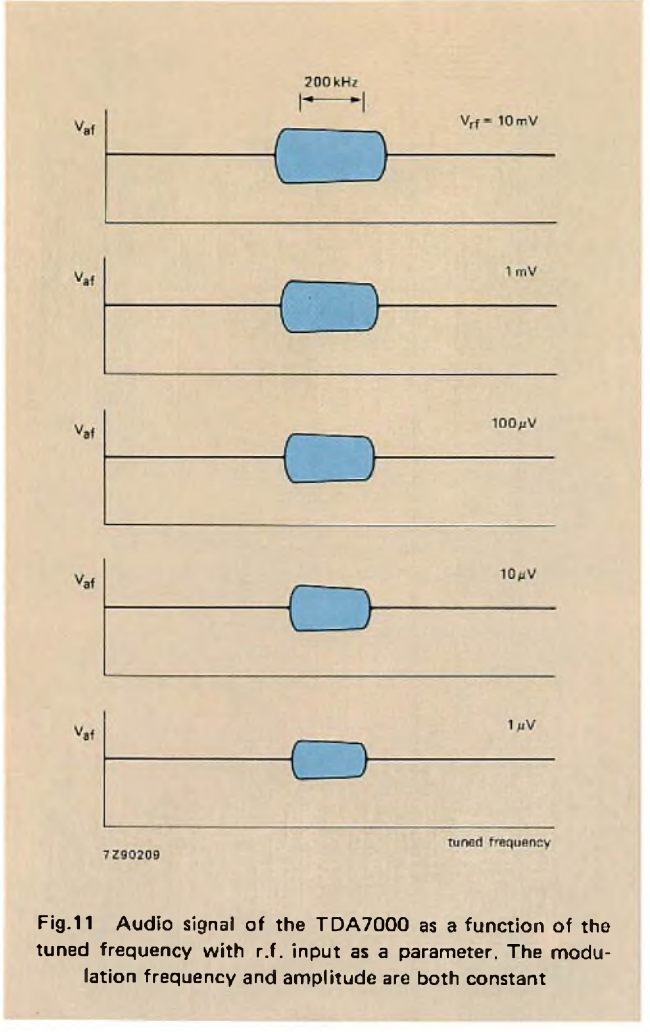

Fig.11 Audio signal of the TDA7000 as a function of the tuned frequency with r.f. input as a parameter. The modulation frequency and amplitude are both constant

Figure 11 shows the audio output from the TDA7000 radio as a function of tuned frequency with aerial signal level as a parameter. Compared with the similar diagram for a typical conventional portable radio (Fig.6), there are three important improvements:

- There are no side responses due to the flanks of the demodulator S-curve. This is due to the action of the correlation muting system (soft mute) which combines the function of a detuning-dependent muting system with that of a signal-strength-dependent muting system
- The correct tuning frequency band is wide, even with weak aerial signals. This is due to the a.f.c. action of the FLL which reduces a large variation of aerial input frequency (equivalent to detuning) to a small variation of the i.f. There is no audio distortion when the radio is slightly detuned
- Although the soft muting system remains operative with low-level aerial signals, there is no degradation of the audio signal under these conditions. This is due to the high gain of the i.f. limiter/amplifier which provides −3 dB limiting of the i.f. signal with an aerial input level of 1.5 µV. However, the soft muting action does reduce the audio output level with low level aerial signals.

RECEIVER CIRCUITS

Circuits with variable capacitor tuning

The circuit diagram of the complete mono f.m. radio shown in the frontispiece is given in Fig.1. An experimental printed-wiring board layout is given in Fig.12. Special attention has been paid to supply lines and the positioning of large-signal decoupling capacitors.

The functions of the peripheral components of Fig.1 not already described are as follows:

C_1:
Determines the time constant required to ensure muting of audio transients due to the operation of the FLL.

C_2:
Together with R_2 determines the time-constant for audio de-emphasis (e.g. $R_2C_2 = 40\,\mu s$).

C_3:
The output level from the noise generator during muting increases with increasing value of C_3. If silent mute is required, C_3 can be omitted.

C_4:
Capacitor for the FLL filter. It eliminates i.f. harmonics at the output of the f.m. demodulator. It also determines the time-constant for locking the FLL and influences the frequency response.

C_5:
Supply decoupling capacitor which must be connected as close as possible to pin 5 of the TDA7000.

C_7 to C_{12}, C_{17} and C_{18}:
Filter and demodulator capacitors. The values shown are for an i.f. of 70 kHz. For other intermediate frequencies, the values of these capacitors must be changed in inverse proportion to the i.f. change.

C_{14}:
Decouples the reverse r.f. input. It must be connected to the common return via a good quality short connection to ensure a low-impedance path. Inductive or capacitive coupling between C_{14} and the local-oscillator circuit or i.f. output components must be avoided.

C_{15}:
Decouples the d.c. feedback for i.f. limiter/amplifier LA1.

C_{19} and C_{21}:
Local-oscillator tuning capacitors. Their values depend on the required tuning range and on the value of tuning capacitor C_{20}.

C_{22}, C_{23}, L_1, L_2:
The values given are for an r.f. bandpass filter with Q = 4 for the European and U.S.A. domestic f.m. broadcast band (87.5 MHz to 108 MHz). For reception of the Japanese f.m. broadcast band (76 MHz to 91 MHz), L_1 must be increased to 78 nH and L_2 must be increased to 150 nH. If stopband attenuation for high level a.m. or tv signals is not required, L_2 and C_{22} can be omitted and C_{23} changed to 220 pF.

R_2:
The load for the audio output current source. It determines the audio output level, but its value must not exceed 22 kΩ for V_p = 4.5 V, or 47 kΩ for V_p = 9 V.

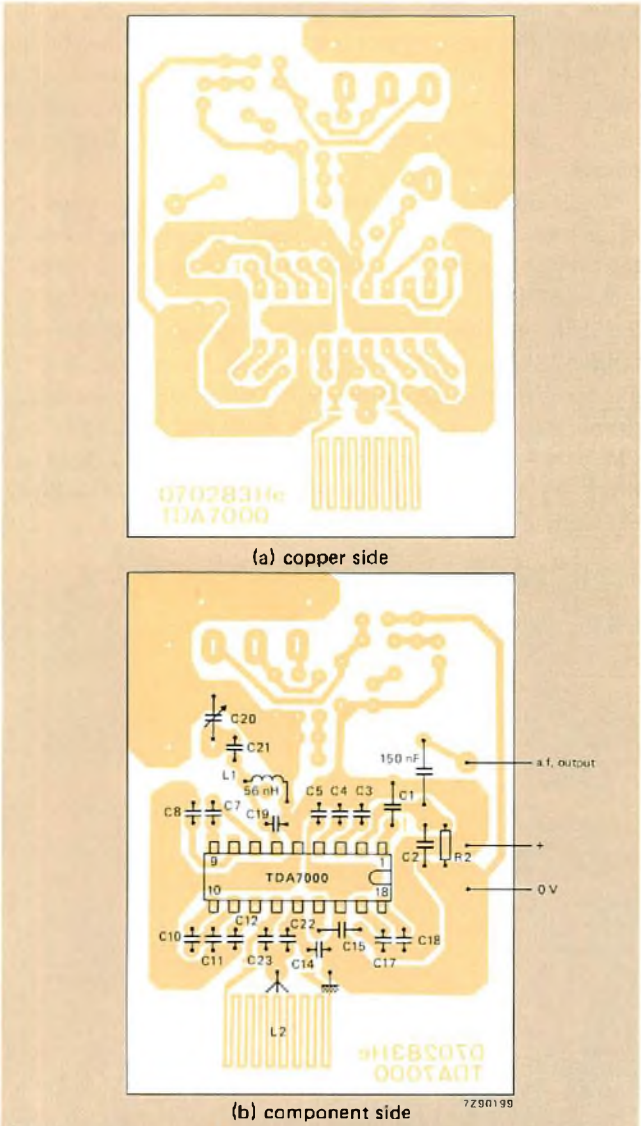

Fig.12 Experimental printed-wiring board for the circuit of Fig.1

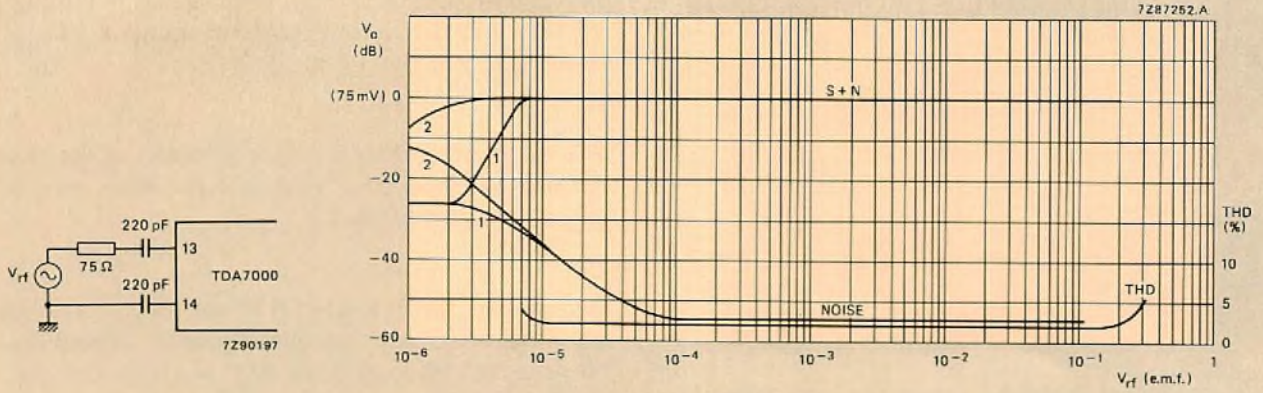

Fig.13 Audio output as a function of input e.m.f. The curves numbered 1 were measured with the muting system active. The curves numbered 2 were measured with the muting system disabled by injecting about 20 μA into pin 1 of the TDA7000. The input frequency was 96 MHz modulated with 1 kHz with a deviation of ±22.5 kHz for the output level curves, and ±75 kHz for the distortion curve

Performance of the circuit

unless otherwise specified, V_p = 4.5 V, T_{amb} = 25 °C, f_{rf} = 96 MHz, V_{rf} = 0.2 mV e.m.f. from a 75 Ω source, modulated with Δf = ±22.5 kHz, f_m = 1 kHz. Noise voltage measured unweighted over the bandwidth 300 Hz to 20 kHz

parameter	symbol	typ.	max.	unit
sensitivity				
(e.m.f. voltage)				
for −3 dB limiting:				
muting disabled	EMF	1.5	–	μV
for −3 dB muting	EMF	6	–	μV
for (S+N)/N = 26 dB	EMF	5.5	–	μV
signal handling (e.m.f. voltage)				
for THD < 10%; Δf = ±75 kHz	EMF	200	–	mV
signal-to-noise ratio (see Fig.13)	(S+N)/N	60	–	dB
total harmonic distortion (see Fig.13)				
at Δf = ±22.5 kHz	THD	0.7	–	%
at Δf = ±75 kHz	THD	2.3	–	%
a.m. suppression				
(ratio of the a.m. output signal				
referred to the f.m. output signal)				
f.m. signal: f_m = 1 kHz; Δf = ±75 kHz				
a.m. signal: f_m = 1 kHz; m = 80%	AMS	50	–	dB
ripple rejection (ΔV_p = 100 mV;				
f = 1 kHz)	RR	10	–	dB
oscillator voltage (r.m.s. value)				
at pin 6	$V_{6\text{-}5(rms)}$	250	–	mV
variation of oscillator frequency				
with supply voltage (ΔV_p = 1 V)	Δf_{osc}	60	–	kHz/V
selectivity	S_{+300}	45	–	dB
	S_{-300}	35	–	dB
a.f.c. range	Δf_{rf}	±300	–	kHz
audio bandwidth at ΔV_o = 3 dB				
measured with pre-emphasis (t = 50 μs)	B	10	–	kHz
a.f. output voltage (r.m.s. value)				
at R_L = 22 kΩ	$V_{o(rms)}$	75	–	mV
load resistance for audio output current source				
at V_p = 4.5 V	R_L	–	22	kΩ
at V_p = 9.0 V	R_L	–	47	kΩ

Circuit with variable-capacitance diode tuning

Since it is only necessary to tune the local-oscillator coil, it is very simple to modify the circuit of Fig.1 for variable-capacitance diode tuning. The modifications are shown in Fig.14. A circuit board layout for the modified receiver and a photograph of a complete laboratory model are shown in Fig.15.

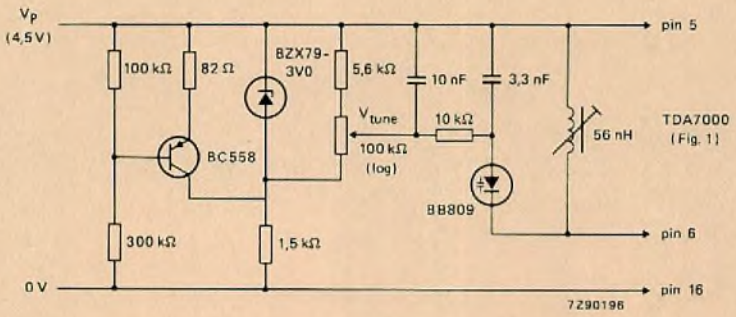

Fig.14 Variable-capacitance diode tuning for the local-oscillator. Additonal measures must be taken to ensure temperature stability

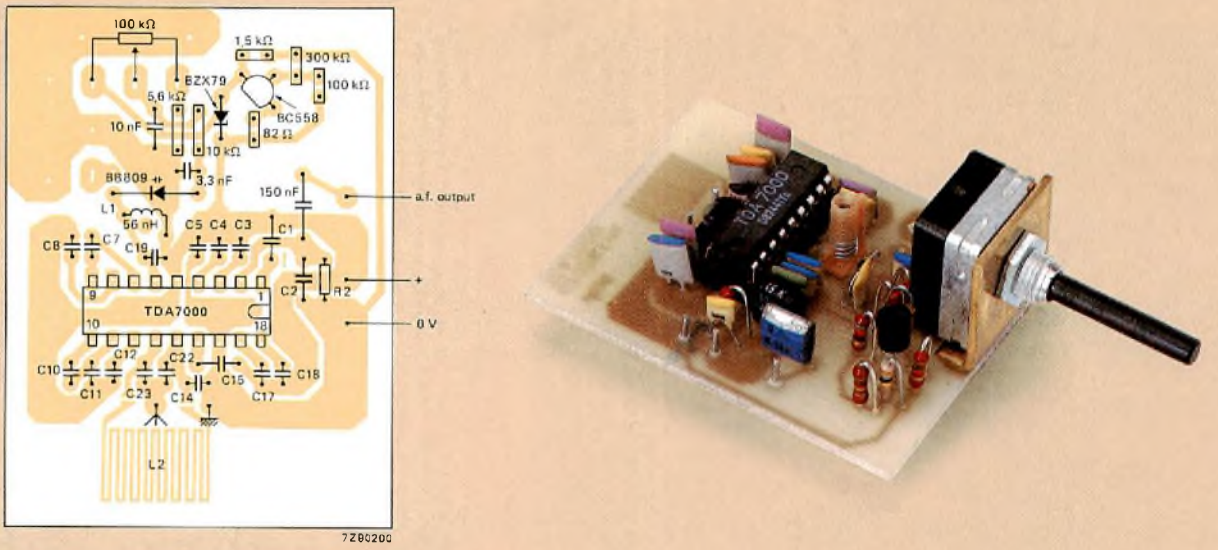

Fig.15 Circuit board layout and complete model of a TDA7000 radio with variable-capacitance diode tuning. This is the same pcb as shown in Fig.12

Narrow-band f.m. receiver

The TDA7000 can also be used for reception of narrow-band f.m. signals. In this case, the local-oscillator is crystal-controlled as shown in Fig.16 and there is therefore hardly any compression of the i.f. swing by the FLL. The deviation of the transmitted carrier frequency due to modulation must therefore be limited to prevent severe distortion of the demodulated audio signal.

The component values in Fig.16 result in an i.f. of 4.5 kHz and an i.f. bandwidth of 5 kHz (Fig.17). If the i.f. is multiplied by N, the values of capacitors C_{17} and C_{18} in the all-pass filters and the values of filter capacitors C_7, C_8, C_{10}, C_{11}, and C_{12} must be multiplied by 1/N. For improved i.f. selectivity to achieve greater adjacent channel attenuation, second-order networks can be used in place of C_{10} and C_{11}.

In this circuit the detuning noise generator is not used. Since the circuit is mainly for reception of audio signals, the audio output must be passed through a low-pass Chebyshev filter to suppress i.f. harmonics.

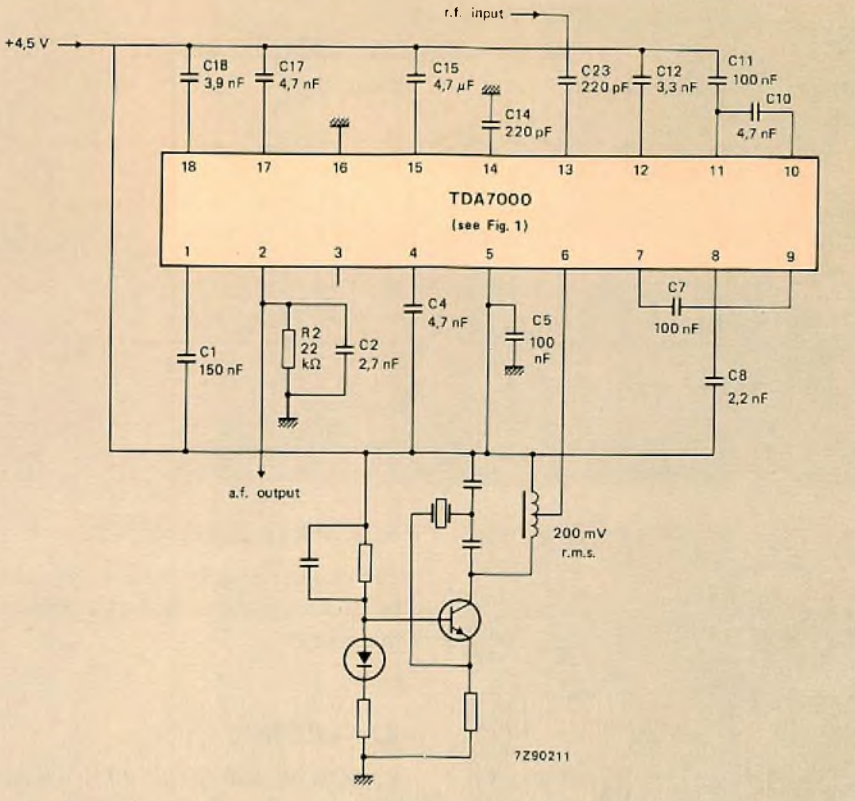

Fig.16 A narrow-band f.m. receiver with a crystal-controlled local-oscillator

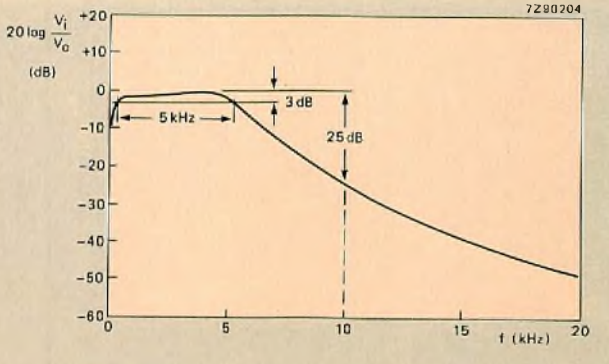

Fig.17 I.F. selectivity for the narrow-band f.m. receiver

AUDIO AMPLIFIER AND DETUNING INDICATOR CIRCUITS

Audio output stages suitable for use with the TDA7000 are shown in Fig.18 and 19. Figure 20 shows how the muting signal can be used to operate a LED to give an indication of detuning.

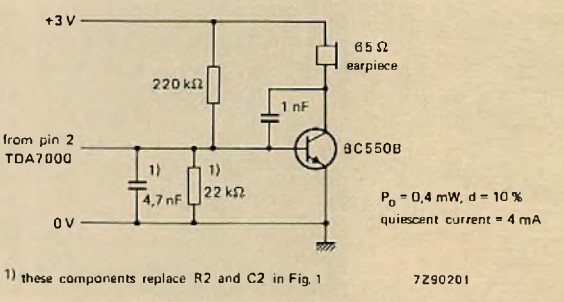

Fig.18 A 0.4 mW transistor audio output stage without volume control for driving an earpiece

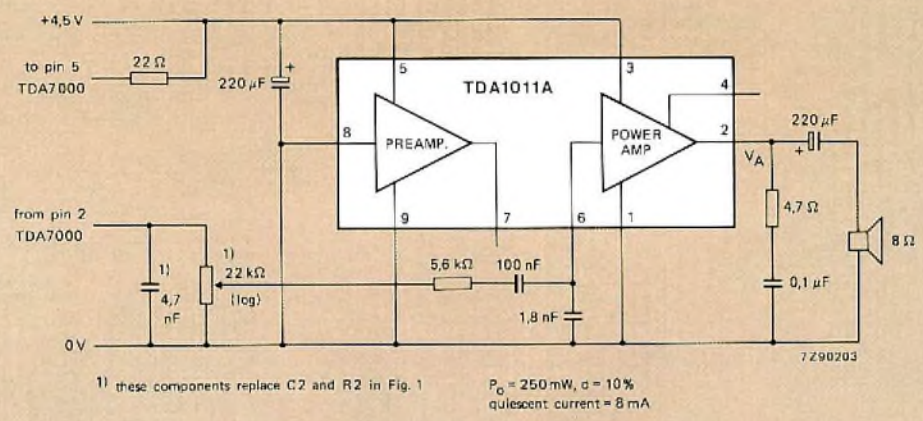

Fig.19 An integrated 250 mW audio output stage

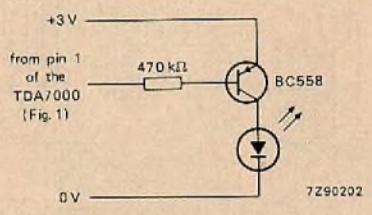

Fig.20 A detuning indicator driven by the mute signal from the TDA7000

ACKNOWLEDGEMENTS

The authors wish to acknowledge the information provided by D. Kasperkovitz and H. v. Rumpt for incorporation in this article.

REFERENCE

KANOW, W. and SIEWERT, I., 'Integrated circuits for hi-fi radios and tuners', Electronic Components and Applications, Vol. 4, No. 1, November 1981, pp. 11 to 27.

The TDA7000 allows f.m. radios to be made small enough to fit inside a pencil, a cigarette lighter, or a wristwatch

Progress in SMPS magnetic component optimisation

L. P. M. BRACKE

The last ten years have seen considerable progress in the development of the switched-mode power supply. Both design methods and associated hardware have been refined by experience and intensive development. These improvements, especially in the understanding of the influence of magnetic material and winding-conductor properties on SMPS operation, are reflected in the more straightforward and complete design routines now available. The better understanding that made for the improved design routines has also resulted in improved core designs: the ETD range of ferrite cores. Furthermore, lessons learned from experience in wound-component production have been applied to the design of the associated hardware, especially the coil former. The improved core and coil former, together with specially-developed assembly hardware, form the ETD system.

IMPROVED DESIGN ROUTINES

References 1 to 4 form a series of publications that presents complete design routines for the magnetic components of all common versions of SMPS. Part 1 of the Series (Ref.1) covers most aspects of SMPS design, with emphasis on the interaction between the electronic and magnetic aspects. The basic electrical relationships are given for forward, push-pull and flyback converters. Practical formulae are given for inductance and effective-current values. Auxiliary outputs and other special features are included in the coverage, as are related control aspects. All treatments are related to the magnetic design.

The data derived from Ref.1 are used in Part 2 of the Series (Ref.2) to select a suitable ferrite core for the transformer. Here, the magnetic and thermal properties of ferrite cores are considered as they affect their suitability for a given application. Initial selection of a suitable core is by means of charts showing the limits of performance to be expected at various frequencies. The optimum working conditions for cores in various transformer types are discussed, and a further chart enables this optimum to be determined. Wound transformer thermal characteristics are discussed, and formulae given for the losses in the core itself. Together with expressions for the number of turns required, Ref.2 allows the design of an SMPS transformer to progress from the electrical requirements set forth in Ref.1 to the mechanical design of the windings themselves discussed in Ref.3.

SELECTING THE CORRECT CORE

Most SMPS requirements can be satisfied by the range of cores currently available (Ref.5). The preferred grade of material for such high-frequency power applications is Ferroxcube 3C8.

Core selection charts

Due to the wide variation in application conditions, the selection charts have been designed to indicate the range of operation of the cores. This is done by using areas of throughput power as a function of frequency as shown in Fig.1. These are effectively areas of good design, since both boundaries represent the performance of a well-designed transformer.

The upper boundary of each area corresponds to a transformer design operating at optimum flux density sweep, with maximum use of the winding window, and Litz-wire windings, for minimum a.c. resistance. The lower boundary corresponds to a transformer design that also operates at optimum flux density, but has optimised solid-wire windings

incorporating 8 mm creepage distance for IEC 435 mains isolation, and with a demagnetising winding occupying one third of the winding space.

Selection charts are given for push-pull, forward and flyback converter SMPS. However, the flyback converter charts are mainly intended as a cross-check on the design obtained by the method given in Ref.4 for chokes.

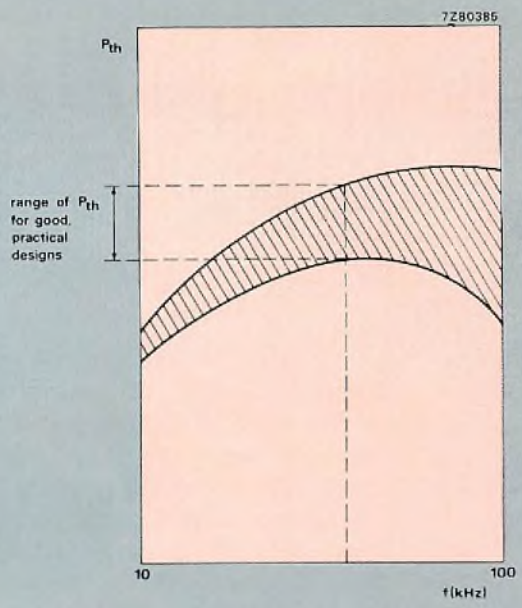

Fig.1 In the core selection charts given in Part 2 of the SMPS transformer design series (Ref.2), the power-handling capability of each core is plotted as a shaded area extending from 10 kHz to 100 kHz. The vertical boundaries of this area are the upper and lower limits of throughput power capacity achievable by good design but depending on conductor type and insulation requirements

Operating conditions

Converter type has the largest influence on throughput power obtainable, but other factors also influence performance, principally

- flux-density sweep
- winding configuration (simple or split, for example) and
- the presence of sensor or demagnetising windings
- the type of conductor used in the windings
- the number of output windings required
- mains insulation requirements.

Generally, the selection charts assume worst-case conditions. Operation at ambient temperatures lower than the 60 °C assumed, the use of feed-forward to ease the restriction on peak flux density (1/1.72 of saturation to allow for transient conditions), or heatsinking or potting to reduce thermal resistance, will all increase transformer power capacity.

Flyback transformers and chokes

Flyback converter transformers and output chokes are magnetically much the same: the main design requirement is stored energy, $\frac{1}{2}I^2L$. This is the basis of a separate design routine that includes winding design (Ref.4). This routine, using specially-developed design charts, leads directly to spacer thickness and number of turns.

OPERATING FLUX DENSITY

For chokes and flyback-converter transformers (which operate as chokes), stored energy is the basis of the design (subject to the core not being driven into saturation). With forward and push-pull converter transformers, the operating flux density (both a.c. and d.c. components) is set at the beginning of the design process.

Forward and push-pull converters

The operating flux density in forward and push-pull converter transformers strongly influences the overall volume of the transformer. Thus, it is set at the beginning of the design process to as high a level as practicable. For forward converter transformers, this level is determined by transient protection requirements or permissible core loss only. With push-pull converters, however, considerations of symmetry may dominate the choice.

Both forward and push-pull converter transformers must be designed to accommodate rapid changes of load. This is done by introducing a transient factor, usual symbol α, related to the range of input voltage for which the power supply is designed. A common value of α is 1.72. This is suitable for mains-fed supplies (215 V to 370 V or 200 V to 340 V), telephone supplies (40 V to 70 V), and mobile supplies (9 V to 15.5 V).

Considerations of symmetry usually result in the value of α being multiplied by a further factor ϵ for push-pull converter transformers. Asymmetry leads to core saturation, which in turn results in destruction of power switches. Principal causes of asymmetry are unbalanced flux linkage in windings (Ref.3) and unequal conduction times in switches. Where care has been taken to achieve balanced transformer windings, and protection circuitry is incorporated to ensure equal conduction times, the value of ϵ may be 1.15; that is, α is increased from 1.72 to 2 for a typical core. Where unbalance is accepted, however, the value of ϵ should be 2. (A list of the symbols used in this article, together with their definitions, is given as Table 1).

The use of feedforward (Ref.1) can considerably reduce the value of α required but at the expense of reduced transient response.

In forward-converter transformers core remanence should also be taken into consideration. However, the introduction of a small airgap in the core, and the use of a slow-rise capacitor (Ref.1) allows the whole first quadrant of the core hysteresis loop to be used.

TABLE 1
List of symbols

symbol	unit	definition
B_{ac}	T	flux-density sweep; half the peak-to-peak flux density excursion
B_{CF}	mm	coil former breadth
f	Hz	operating frequency
f_1	Hz	the frequency at which the number of turns on the lowest-voltage transformer winding becomes unity
f_L	Hz	the lowest frequency at which the coil former height is sufficient to accommodate ideal (minimum-loss) windings
f_T	Hz	the frequency above which no useful increase in the throughput-power capacity of a transformer can be obtained
H_{CF}	mm	coil former height
L	H	choke inductance
ℓ_{av}	mm	average turn length
P_c	W	total transformer core loss
$R_{th\,c}$	K/W	transformer or choke thermal resistance with winding creepage distance incorporated
$R_{th\,n}$	K/W	transformer or choke thermal resistance for a winding without creepage distance
V_e	m^3	effective volume of a core
α	–	ratio of core saturation flux to working flux allowed: for transient response without saturation
ΔT	K	temperature rise above ambient
ϵ	–	unbalance factor

subscripts

e	effective value
cp	pertains to centre pole

TABLE 2
Maximum values of flux-density sweep for various converter types and control circuits

boundary conditions	flux-density sweep $B_{ac\,cp}$ (T)	
	forward	push-pull
maximum sweep for FXC 3C8 (100 °C)	0.16	0.32
at transient factor α	$\frac{0.32}{2\alpha}$	$\frac{0.32}{\alpha}$
with unbalance factor ϵ*	–	$\frac{0.32}{\epsilon\alpha}$
with x% feedforward	$\frac{0.32}{2\,(1 + x/100)}$	$\frac{0.32}{(1 + x/100)}$
with unbalance factor ϵ and x% feedforward	–	$\frac{0.32}{\epsilon\,(1 + x/100)}$

* ϵ is the ratio of peak flux density in a balanced converter to the peak flux density in an unbalanced converter.

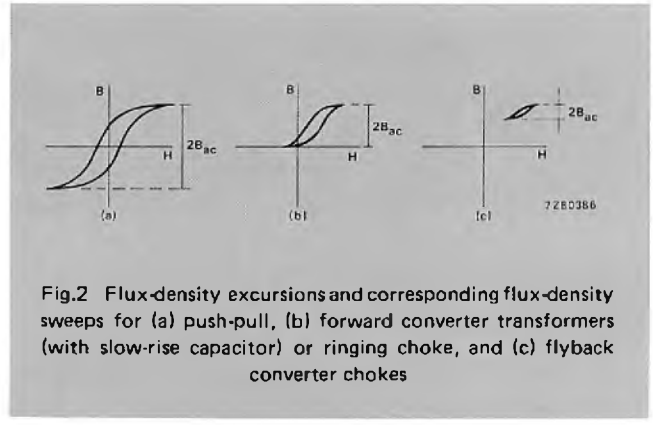

Fig.2 Flux-density excursions and corresponding flux-density sweeps for (a) push-pull, (b) forward converter transformers (with slow-rise capacitor) or ringing choke, and (c) flyback converter chokes

Figure 2 shows the maximum transformer flux-density sweeps for various converter types, and Table 2 gives the value of transient factors α and ϵ under various conditions.

Optimum flux-density sweeps

Manipulation of the expression (Ref.6) for the throughput power of an SMPS transformer shows that power reaches a maximum at a combination of operating frequency and flux density such that core loss is 44% of total loss. That is, when

$$0.44\ \frac{\Delta T}{R_{th}} = 16.7\ f^{1.3}\ B_{ac\,em}^{2.5}\ V_e$$

Here, the right-hand part of the expression is the typical hysteresis loss of Ferroxcube 3C8 ferrite. Since eddy-current loss is neglected, this expression applies only up to about 100 kHz.

Using this expression, curves of $B_{ac\,em}$, the peak flux-density sweep, have been derived for all Philips' SMPS transformer cores (See Fig.3).

THERMAL RESISTANCE AND TEMPERATURE RISE

The maximum permissible dissipation of a transformer or choke is set by its maximum operating temperature; ambient temperature and thermal resistance depend on core size, mounting method and attitude, the type of conductor in the winding and the amount of insulation incorporated. Due to the insulating effect of the interleaving where 8 mm creepage distance is allowed for in the windings, two values are quoted for thermal resistance in Ref.2: with and without creepage allowance.

Measurement methods are discussed in Ref.2 and 7. Results given in Ref.7 confirm that transformer temperature rise can be accurately calculated from the product of total transformer dissipation and thermal resistance for any ratio of core to winding loss.

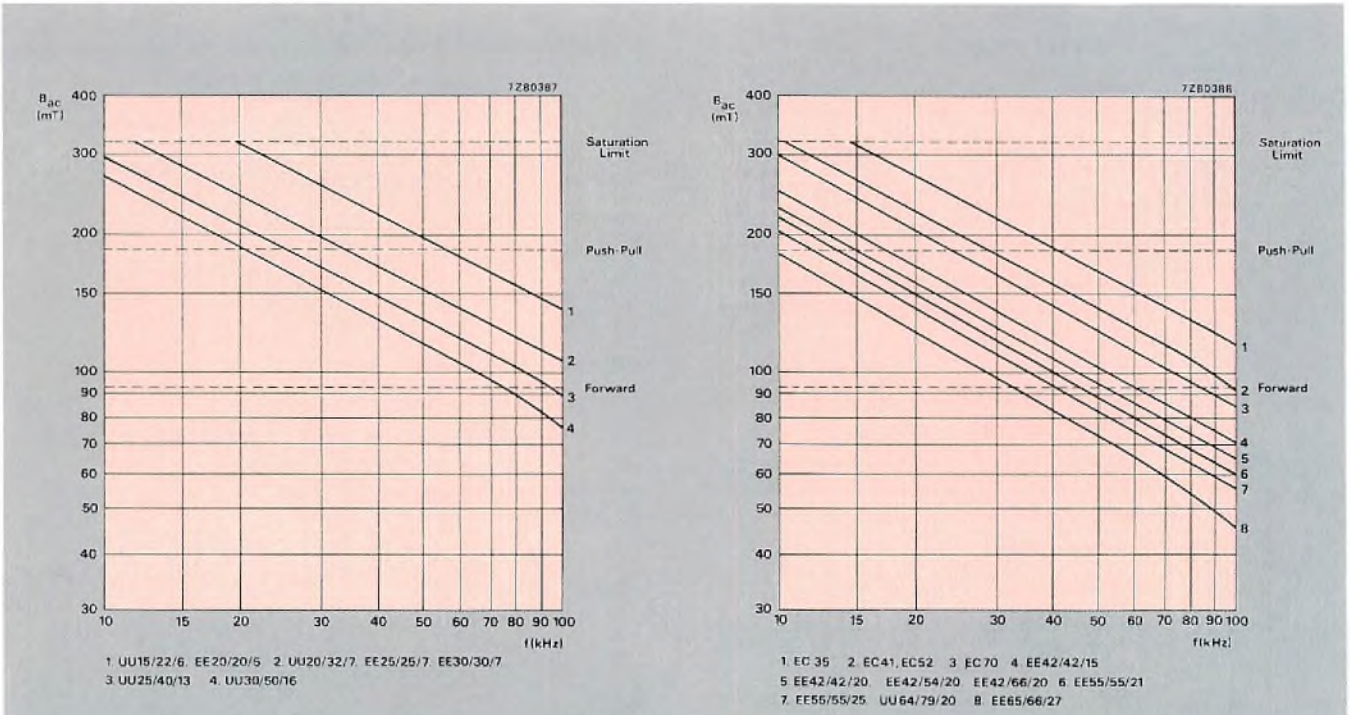

Fig.3 Optimum, peak, centre-pole flux-density sweeps $B_{ac\,cp}$ for a variety of cores for SMPS applications. Horizontal lines indicate the limits for various converter types ($\alpha = 1.72$). The curves were calculated for a peak temperature rise of 40 K

THE EFFECT OF OPERATING FREQUENCY

Winding properties

Depending on frequency, the windings of an SMPS transformer fall into one of three categories. At low frequencies, the available winding-window height will be insufficient to accommodate minimum-loss (ideal) windings. At some higher frequency, f_L, the height of minimum-loss windings becomes less than that of the winding window. Finally, at some higher frequency, f_1, the number of turns required for the lowest-voltage winding becomes unity.

It is shown in Ref.8 that, where the winding height is insufficient for minimum-loss windings, winding loss is inversely proportional to the squares of both flux-density sweep and operating frequency. At frequencies above f_L winding loss becomes inversely proportional to operating frequency.

Flux density sweep

From the considerations given earlier, it is apparent that at lower frequencies, operating flux density is limited by core saturation rather than loss. Above some frequency f_T, the optimum operating flux density (for maximum power) becomes less than the saturation-related maximum, and the flux-density sweep is limited by the requirement that (for Ferroxcube 3C8) core loss $P_c = 0.44\,P_{tot}$, where P_{tot} is the total permissible dissipation.

Throughput power

In Ref.8, these various effects of operating frequency are combined to explain the observed variation of SMPS transformer throughput power with operating frequency for Ferroxcube 3C8 cores. Figure 4(a) shows the division between core and winding loss for an SMPS transformer as a function of operating frequency. Frequencies f_L, f_T and f_1, are marked. (Note that f_L may, in fact, be higher than f_T for some cores. This does not alter the main argument.) In Region I, operating flux density is limited by saturation considerations only, so that throughput power is roughly proportional to frequency. Operation remains saturation limited into Region II, but here power increases roughly as the root of the frequency. (This relationship is complicated by the fact that average turn length decreases as ideal-winding height decreases.) Region III begins at f_T, where core operating flux density becomes limited by core loss to the optimum value for that frequency. The shape of the throughput power curve in the region depends on core material characteristics: the Steinmetz coefficient and its associated flux-density and frequency exponents. For Ferroxcube 3C8, flux density is inversely proportional to the root of frequency. Then, winding resistance decreases slightly with frequency so that, since winding loss is constant, throughput power is also about constant.

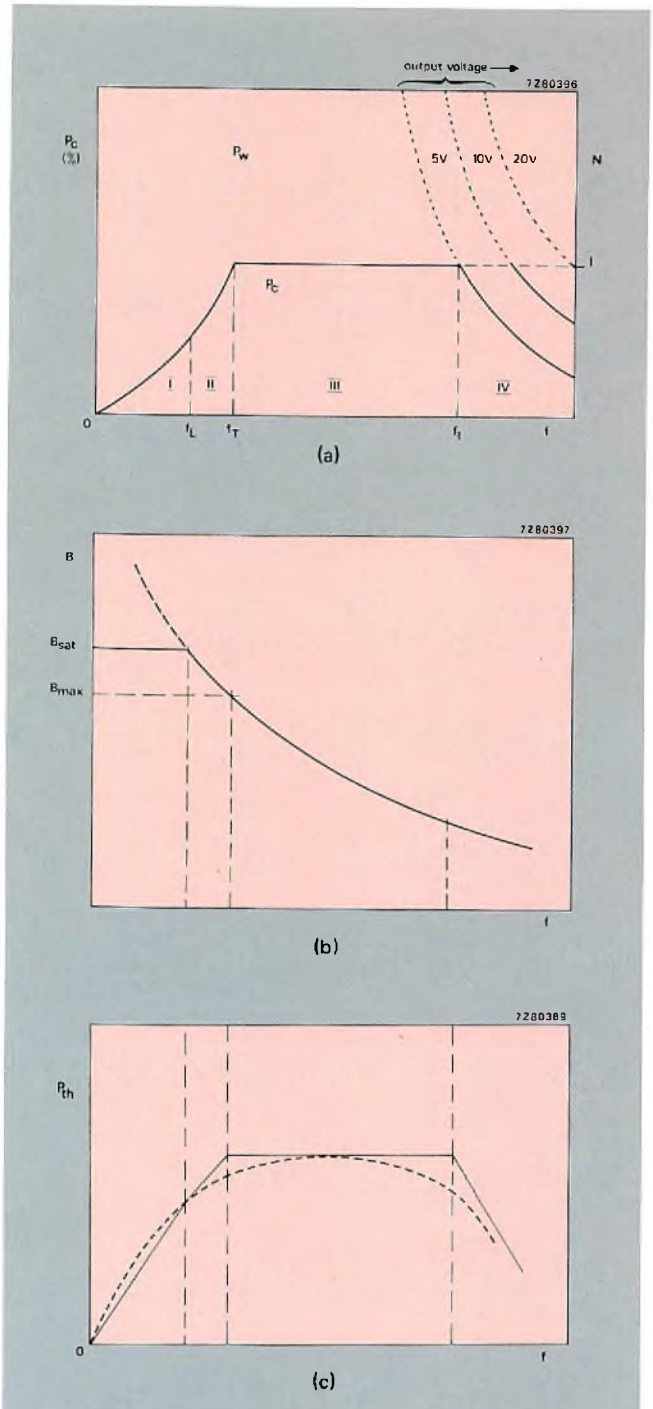

Fig.4 (a) Division of transformer loss between core loss and winding loss as a function of frequency, showing the various boundary frequencies. (b) Relation between flux density and frequency for maximum throughput power. (c) The corresponding throughput power characteristic

Region IV begins where frequency increases to the point where the number of turns required on the lowest-voltage winding falls to unity. (Contours of number of turns N as a function of frequency for various voltages are indicated in Fig.4(a)). When this happens, flux density must then decrease with frequency. The rate of this decrease is greater than that required for optimum core loss, so that throughput power decreases. The effect is accentuated by the increasing contribution of eddy-current losses at high frequencies.

In practice, other factors, such as eddy-currents, parasitic capacitance and rounding of numbers of turns, cause the transitions from one Region to another to become blurred so that, as Fig.4(c) shows, the thoughput power characteristic is more rounded. Calculated values for real cores, Fig.5, shows that the general characteristics remain, however: there is always a frequency, close to the core transition frequency, above which no useful increase in throughput power can be obtained.

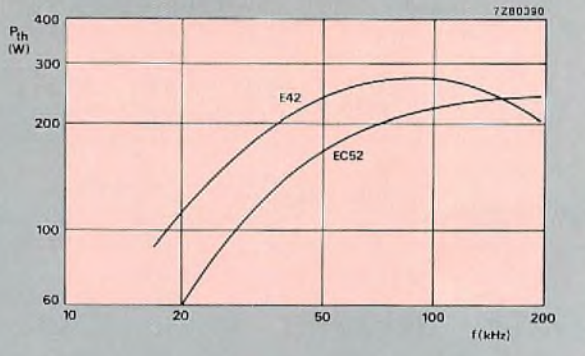

Fig.5 Calculated throughput powers (5 V forward converters) with frequency for EC52 and E42/21/20 core show the same general characteristics: there is a frequency (from Fig.3) above which no useful increase in throughput power can be obtained. For the EC52 core this is 100 kHz, for the E42 core it is 52 kHz

EFFECT OF CORE DESIGN

The more complete understanding of the factors that influence throughput power obtainable has made it possible to examine established core designs with a view to improving the designs available. Electrical, magnetic and mechanical considerations can now be combined so that the core can be made as effective as possible.

Existing core designs

Analysis of existing core designs (E, EC, PM, PQ and RM cores, Ref.8) shows that performance agrees well with values of f_T. The performance of the smaller cores is found to be relatively poor at 50 kHz due to lack of sufficient winding-window height for ideal windings.

The effectiveness of the use of core materials is another important consideration, since it directly affects the weight of an SMPS. Constant cross-section E cores generally have the best power-to-weight ratios.

SWITCHED-MODE POWER SUPPLIES

The essential difference between switched-mode and conventional (mains) power supplies is operating frequency. Whereas conventional power supplies operate at mains frequencies, 50 Hz or 60 Hz, switched-mode power supplies (SMPS) operate at frequencies of the order of 50 kHz. The complications associated with operation at these high frequencies are more than compensated for by the savings in weight and volume, especially of transformers and smoothing components.

Voltage conversion and control in SMPS is achieved by chopping the incoming supply voltage with a high-speed switch such as a transistor. The chopped voltage is applied to a transformer which performs voltage conversion and provides isolation. This transformer is generally wound on a ferrite core, and is much smaller and lighter than a 50 Hz unit of comparable power capacity. Fine control of output voltage is obtained by varying the duty cycle of the switch.

Most SMPS converters require a d.c. input and provide a d.c. output. For operation from the mains, therefore, a rectifier and smoothing circuit generally precedes the converter itself, Fig.A.

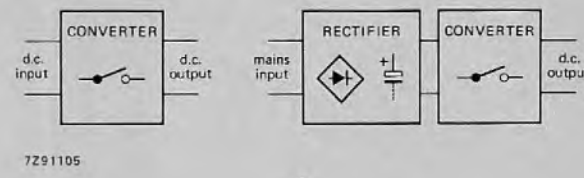

A

SMPS converters

There are three basic SMPS converter arrangements; they and their variants are discussed in detail in Ref.1.

In the forward converter, Fig.B, power is transferred directly to the load while the switch is closed; the energy stored in the inductor is transferred to the load while the switch is open. The switch may be transformer coupled to the inductor for input/output isolation.

In the flyback converter, Fig.C, power is stored in the inductor while the switch is closed and transferred to the load while the switch is open. The functions of transformer and inductor may be combined where voltage transformation is required.

The push-pull converter is, effectively, a forward converter in which the output choke is driven by any push-pull arrangement of power transistors, including a full bridge, Fig.D. Operation after the transformer is similar to that of a forward converter, but with twice the effective switching frequency.

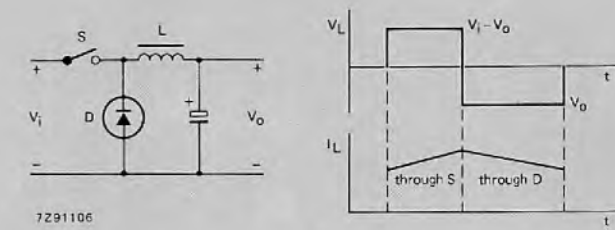

B

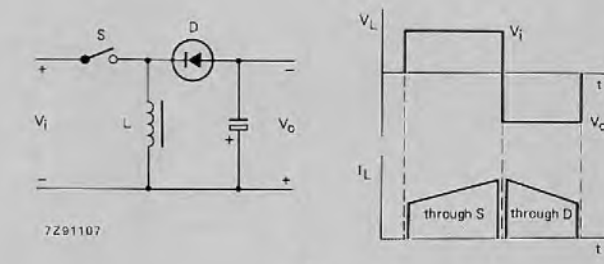

C

Transformer and choke requirements

There are two main boundary conditions for the power transformer: it must not saturate (otherwise the power transistors will be damaged) and it must not overheat. In addition to these boundary conditions, the output choke should be capable of storing sufficient energy to deliver one output cycle so that ripple will be low and regulation good.

Saturation is prevented by designing for worst probable combinations of load change and input voltage fluctuation. In forward converters, provision must be made for removing energy stored in the transformer at the end of the ON period of the switch. In push-pull converters, the degree of symmetry achievable in both power switches and transformer windings determines the unbalance allowance.

Overheating of the transformer and choke is prevented by calculation of total power dissipation: core hysteresis and eddy current losses, and winding losses.

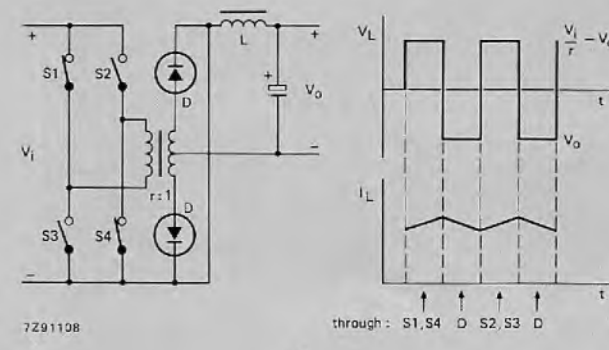

D

Mechanical design is of great importance since this influences manufacturing cost and transformer production cost. The core should be cheap to manufacture. Enclosed cores, such as pot cores and their variants (RM, PQ, PM cores) are more expensive to make than E cores for a given power capacity. However, round centre legs make for easier winding, with less leakage inductance – especially for strip. For all but the smallest transformers, E cores result in more compact design than U cores. Finally, due to their symmetry, E cores require some 20% less core material for a given power capacity than U cores, with a consequent reduction in eddy-current losses. This last point is of especial importance at higher operating frequencies.

Core design requirements

From this theoretical and practical background the requirements for a new core design are clear. The range of cores should be optimised for frequencies appropriate to their power handling capacity: 50 kHz for 300 W, 100 kHz for 100 W, for example. This requires proper choice of f_L and f_T. Optimisation should be aimed at forward-converter applications (the cores will then also be suitable for unbalanced push-pull converters).

The design of the associated coil formers is also critically important. They should be suitable for automatic handling. A large number of pins is required, both for flexibility of layout and to accommodate multiple secondaries.

The core and wound coil former should be quick and easy to assemble. The combination should be designed for horizontal mounting on p.c. boards to minimise height and make termination of strip windings easier.

THE ETD SYSTEM

The cores

These criteria have been adopted in the design of the ETD cores (Ref.8). They are constant cross-section E cores in Ferroxcube 3C8 ferrite with round centre legs, photo and Fig.6, and are designed for

- minimum throughput powers in the range 100 W to 300 W
- economical manufacture
- minimum weight of ferrite
- operating frequencies in the range 50 kHz to 150 kHz
- high throughput power density
- mains isolation
- minimum transformer volume and p.c. board areas.

Magnetic properties are given in Table 3.

The ETD cores are compared with existing core designs for power per unit weight in Fig.7. Throughput power areas as a function of frequency for ETD cores are given in Fig.8, and the optimum flux density sweep in Fig.9.

TABLE 3
Magnetic dimensions of ETD system cores

core type	$A_{cp\ min}$ (mm^2)	A_e (mm^2)	V_e (mm^3)	ℓ_e (mm)
ETD 34	87	97.1	7 640	78.6
ETD 39	117	125	11 500	92.2
ETD 44	167	173	17 800	103
ETD 49	204	211	24 000	114

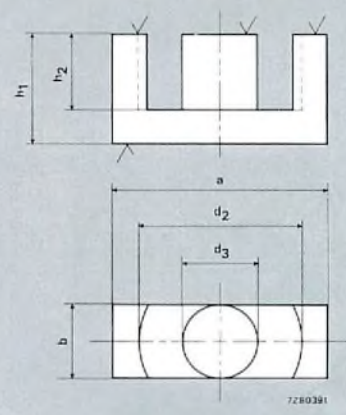

core type	mid-limit dimensions (mm)						mass (g) (core half)
	a	d_2	d_3	h_1	h_2	b	
ETD 34	34.2	26.3	10.8	17.3	12.1	10.8	20
ETD 39	39.1	30.1	12.5	19.8	14.6	12.5	30
ETD 44	44.0	33.3	14.9	22.3	16.5	14.9	47
ETD 49	48.7	37.0	16.4	24.7	18.1	16.4	62

Fig.6 Outline drawing and dimensions of the new ETD core range

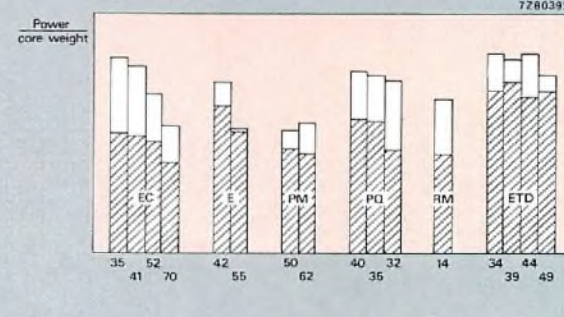

Fig.7 The throughput power per unit weight of core material for ETD cores compared with that of other popular core types at two operating frequencies: 50 kHz (shaded areas) and 100 kHz (open areas). Forward-converter operation is assumed

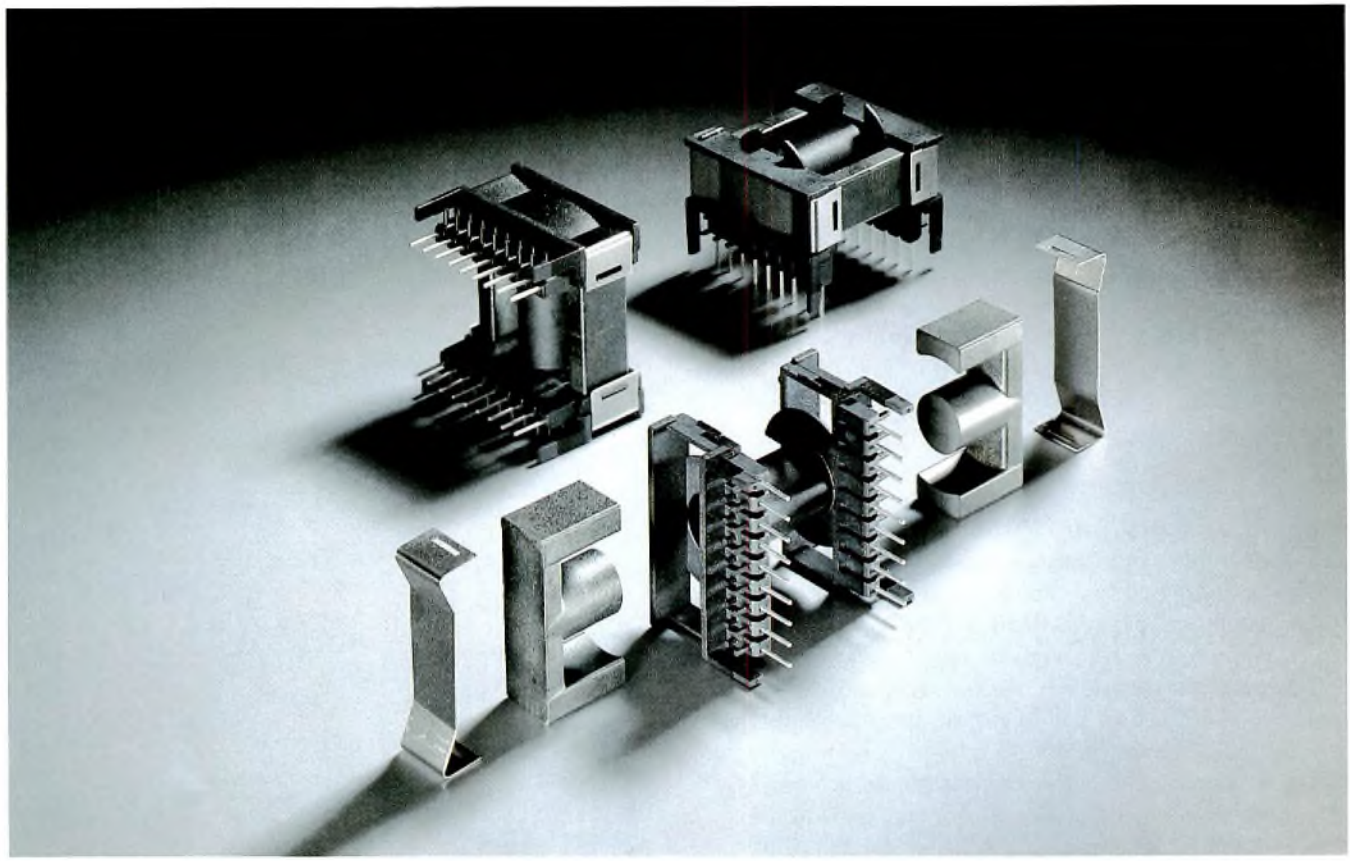

These ETD system components provide OEMs with the most efficient and economical route to SMPS transformers

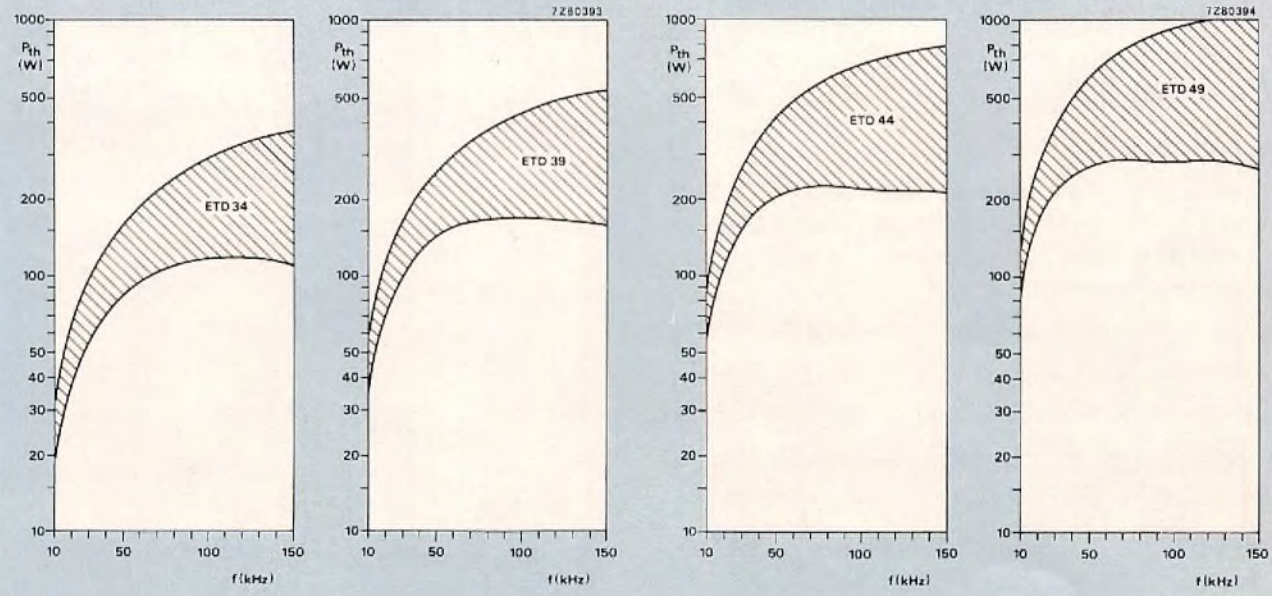

Fig.8 Throughput power as a function of frequency for ETD cores in forward-converter transformers

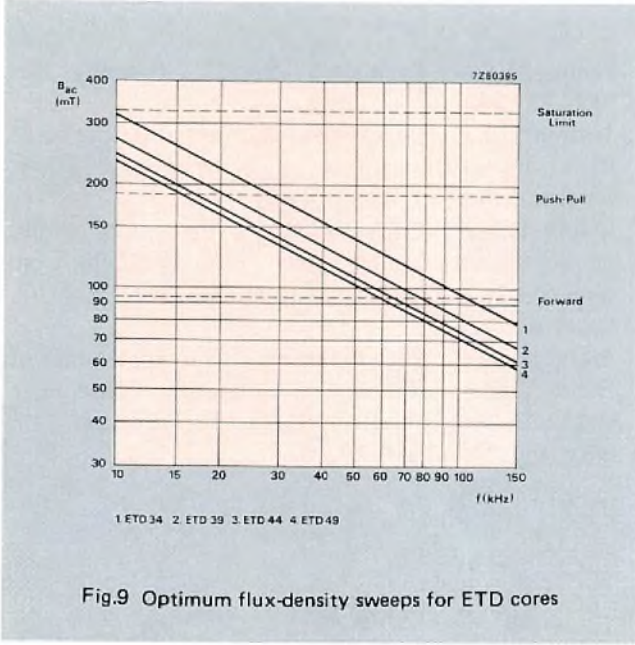

Fig.9 Optimum flux-density sweeps for ETD cores

The coil former and assembly hardware

Simple, rapid winding and assembly of ETD-system based transformers and chokes is made possible by the coil former of Fig.10, together with the associated snap-on stainless-steel assembly clips.

Principal features of the design are indicated in Fig.10:

- the length and number of slots gives a wide choice of lead-out position
- there is at least 8 mm creepage distance from the pins to the ferrite core
- the pegs between the slots allow wire to be run from any one slot or pin to any other
- the four support legs provide 8 mm creepage distance between the windings and the p.c. board
- the hood over the pins provides 8 mm creepage distance between leadouts and assembly clips
- a separate earthing clip for the core is to be available.

The coil former itself is moulded in polybutylene terephthalate, a high-grade, flame retardant (UL 94-VO), thermoplastic. Windings dimensions are given in Table 4.

TABLE 4
Winding dimensions of ETD-system coil formers

type	B_{CF} (mm)	H_{CF} (mm)	ℓ_{av} (mm)
ETD 34	20.9	5.9	61
ETD 39	25.7	6.9	69
ETD 44	29.5	7.3	78
ETD 49	32.7	8.4	86

ETD system components provide OEMs with the most efficient electrical, magnetic and mechanical route to full, economical, automated production of SMPS transformers.

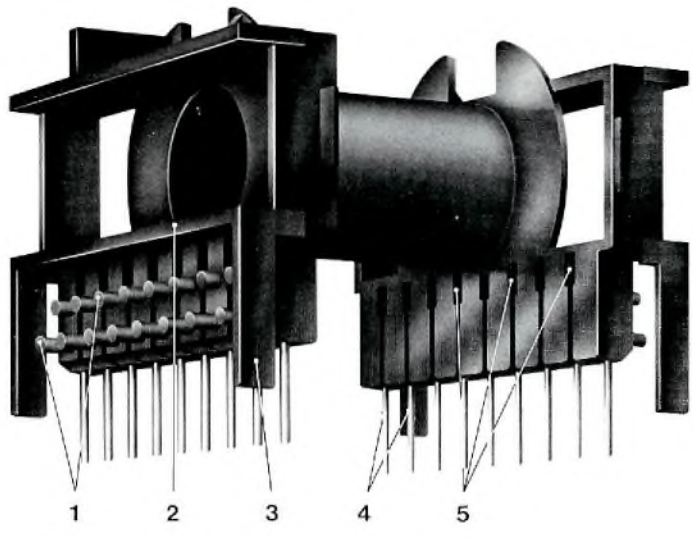

1 – pegs allow wires to be taken from most appropriate slot to chosen pin
2 – these plates give 8 mm creepage distance between wires and assembly clips
3 – legs give 8 mm creepage distance from windings and p.c. board.
4 – 8 mm creepage from pins to core
5 – multiple slots for maximum freedom of lead-out position

Fig.10 Coil former design for the ETD system, intended for automatic winding

REFERENCES

1. Bracke, L. P. M. and Geerlings, F. C. 1982. High-frequency ferrite power transformer and choke design. Part 1: Switched-mode power supply magnetic component requirements. Philips' ordering code: 9398 923 20011.
2. Bracke, L. P. M. 1982. High-frequency ferrite power transformer and choke design. Part 2: Switched-mode power supply magnetic considerations and core selection. Philips' ordering code: 9398 923 30011.
3. Jongsma J. 1982. High-frequency ferrite power transformer and choke design. Part 3: Transformer winding design. Philips' ordering code: 9398 923 40011.
4. Bracke, L. P. M. and Jongsma, J. 1982. High-frequency ferrite power transformer and choke design. Part 4: Improved method of power-choke design. Philips' ordering code 9398 923 50011.
5. Philips' Data Handbook, Vol. C5. Ordering code 9398 923 50011.
6. Jansson, L. E. 1976. Power capacity of ferrite-cored transformers and chokes in switched-mode power supplies. E.A.B. 34, 20-47 (No. 1).
7. Bracke, L. P. M. 1982. Optimizing the power density of ferrite-cored transformers. Proc. PCI/Motorcon, Geneva. Intertech Communications, Inc., Oxnard, California.
8. Bracke, L. P. M. 1982. Optimizing the configuration of ferrite-cored transformers for advanced switched-mode magnetics, Proc. Powercon 9, Washington. Power Concepts, Inc., Ventura, California.

Data converters for robotics

STEPHAN OHR*

The high level of interest in robotics technology is due to the increased industrial manufacturing productivity it promises. Despite popular fancy, the vast majority of commercial robots are not the least bit anthropomorphic. No matter how sophisticated, these machines are primarily intended as intelligent aids to productivity. They simplify many repetitive operations, such as component inspection, bin sorting, and assembly, by putting them under microprocessor control.

The designer of a robot control system has some tough and challenging choices to make. He must determine what he wants the system to do, what component parts it should include, and how to build it within certain cost constraints.

With regard to data converters in particular, a $20 device is not likely to significantly affect the price of a robot assembly costing from $10 000 to $50 000. The same data converter, however, will have a more substantial impact in a machine tool selling in the $500 to $1000 range.

In this article, we intend to look at some of the typical functions performed by industrial robots and examine some of the most obvious systems and components used for accomplishing these tasks. And for those areas which may be cost sensitive, we will propose some potentially useful alternatives.

THE BASIC CONTROL LOOP

Robots are typically required to perform two types of tasks: those involving some sort of sensing, and those involving some sort of locomotion. It doesn't matter whether the robot arm holds a drill, an arc welder, or a spray painter. The basic two-step operation is the same: the robot must sense, or 'see', the object or location it needs to work on, and then it must move to that object or location. There is, naturally, a feedback loop, in which the robot asks itself, 'How close am I?', but this will always be some variation on sensing/seeing. The corrective action, of course, will be some variation on locomotion.

The design engineer can use various approaches to developing the systems that accomplish the two main tasks. For sensing systems, the approaches would include non-contact visual systems, such as camera-based intelligent inspectors or laser-based optical scanners; contact systems, such as pressure or temperature sensors; and those in between, such as infrared scanners. For locomotion systems, the approaches would include those systems that involve some sort of rotational movement, such as elbow and wrist joint controllers, and those that involve linear positioning, such as microprocessor-controlled lathes or drill presses.

This is a logical point at which to review the basic functions of robotics system design. The basic control model is the same – almost regardless of the sophistication of the machine. Whether we focus on the dazzling strength and flexibility of Cincinnati Milacron's T-3 (Fig.1), or on the routine, but still sophisticated, operations of a Rowe International dollar bill changer, the system model is consistent.

Invariably, for the sense/seeing function, sensors/transducers produce an analog voltage as the first input. This voltage is typically conditioned or amplified, and fed to an analog-to-digital converter. The digital code produced is then given to a microprocessor which compares that code with the code information in its memory instruction set and look-up table. In the control loop, or locomotive task, the microprocessor feeds an instruction code to a digital-to-analog converter which translates the digital code back into an analog voltage. This voltage, in turn, can be used to dictate a variety of industrial operations, from motor speed to arc welding temperature to linear position.

* Formerly with Signetics Corporation.

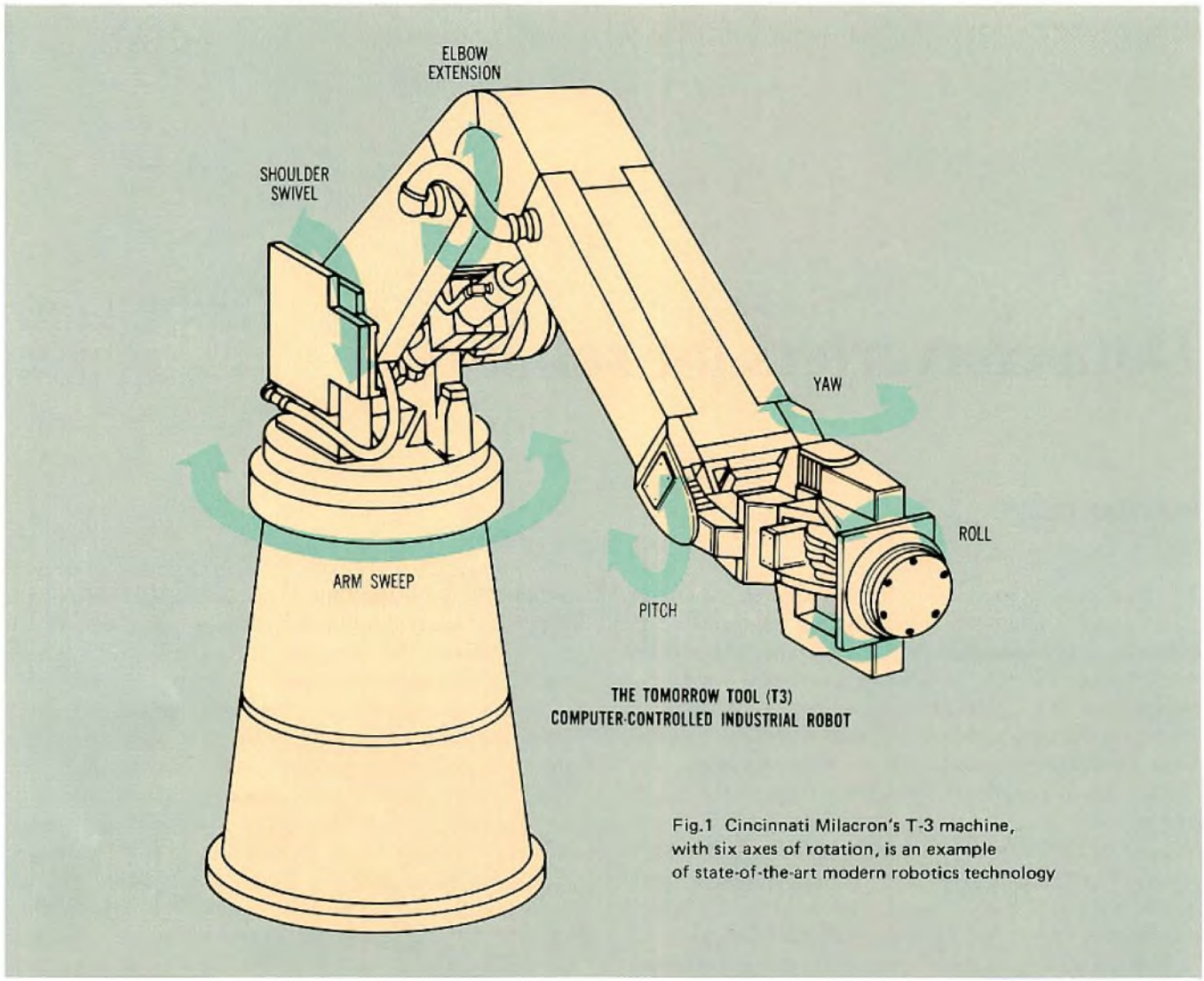

Fig.1 Cincinnati Milacron's T-3 machine, with six axes of rotation, is an example of state-of-the-art modern robotics technology

The feedback loop will typically be the same sensor-amplifier converter loop on a new 'read data' cycle of the controlling microprocessor. The typical system configuration is shown in Fig.2. While a typical control system may also use multiplexers, voltage references, and isolation or instrumentation amplifiers, in addition to a goodly number of buffer and/or storage registers between the converter and the microprocessor, all systems will involve some variation of this basic architecture.

The elements of the system, consequently, should be selected according to the complexity of the task that needs to be performed – but also with an eye to costs. The microprocessor element will be picked according to the amount of computing power required for the particular task, as well as speed and costs. On the analog front and tail of the system, the major choices revolve around bit resolution, speed, and again, component costs.

The selection of a data converter should, of course, be based on similar criteria. On one side of the interface, it is important to match the bit resolution and speed of the data converter with the capacity of the processor. On the other side of the interface, the converter will determine the precision with which the analog signal will get divided up.

If it weren't for the high costs of 16-bit converter modules (upwards of $1000), industrial controls would undoubtedly be using this as the standard. A 16-bit converter module, used for linear position finding, for example, will find a spot within 50 μm over a range of 3 metres. While 25 μm is closer to the resolution required in many precision machine-tool applications (such as turning or boring equipment), a higher bit resolution will increase the cost and complicate the task of software programming.

From an engineering point of view, it may be more sensible to first limit the range of the position finder in order to locate each 25 μm spot without making undue demands on converter bit resolution. One suggestion would be to make an 8-bit slice into the 3 metres travel, which would provide segments as small as 12 mm, and then make another 10-bit slice to yield better than 25 μm resolution. The components cost, by this route, is considerably less than $1000.

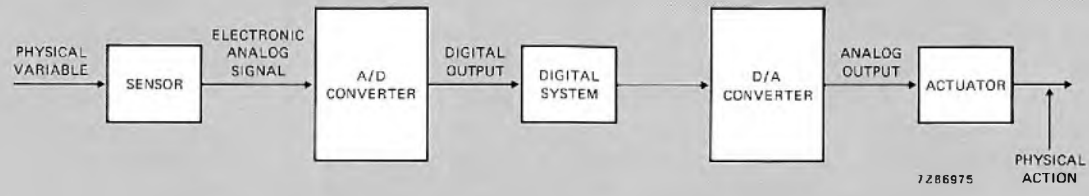

Fig.2 A simplified robotics control system

Among industrial controls manufacturers, 12-bits is at the moment the most popular number.

If you look closely at robotics applications, you will find situations in which speed rather than bit resolution is the criterion for data converter selection. You will also find situations in which cost factors far outweigh both speed and bit resolution.

ROBOT VISION SYSTEMS

Camera-based robot vision systems are one application area in which speed seems to take priority over bit resolution. This is especially true in those situations in which the robot intelligence must recognise patterns or objects on a changing field. A typical example is an operation requiring the robot to sort and bin parts from a fast moving conveyor belt.

Perhaps typical of the new generation of robot vision systems is the VS-110 from Machine Intelligence (Fig.3). Designed for high-speed object/pattern recognition among objects on a moving conveyor belt, this intelligent machinery can recognise up to 900 separately indexed parts per minute. The front end, the 'eyes' or seeing/sensing element of this system, is a CCD camera. The intelligence is supplied by an LSI-11 (Digital Equipment Corp.) with 256 Kbytes of memory. The interface between the CCD camera elements is accomplished by a video-speed 8-bit converter, a device with a 20 ns conversion time.

The camera field is divided into a 256 x 256 grid, or 65 536 pixels (see Fig.3). The voltage produced by the camera at each pixel is digitised almost instantaneously by an 8-bit converter. The 8-bit code generated will be a representation of the grey scale value of that pixel. An 8-bit converter will resolve 256 grey scale values.

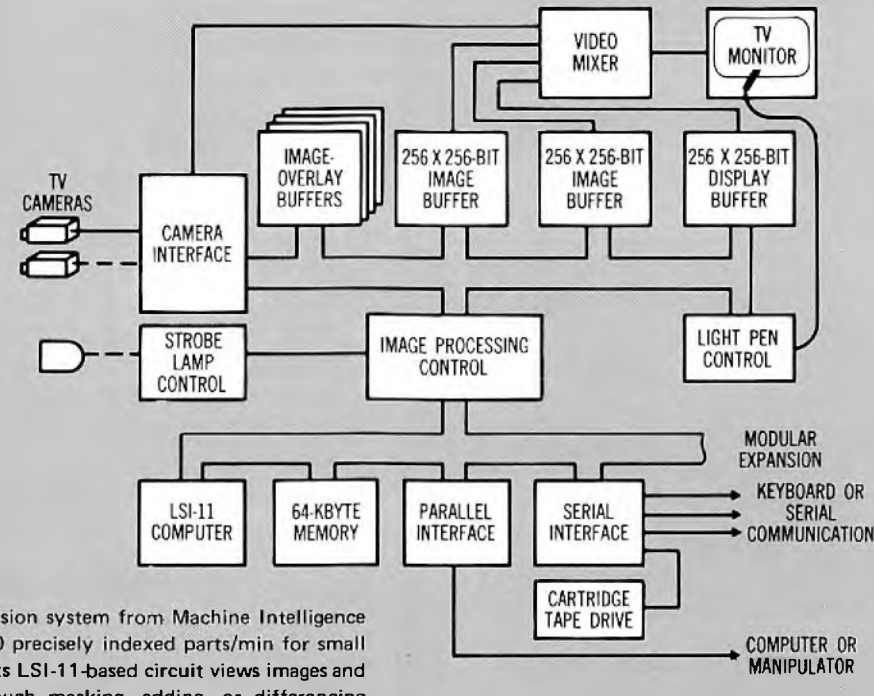

Fig.3 The VS-110 vision system from Machine Intelligence can inspect up to 900 precisely indexed parts/min for small dimensional defects. Its LSI-11-based circuit views images and transforms them through masking, adding, or differencing operations.

In the operation of the VS-110, the digitised information generated by the A/D converter is fed to the LSI-11 and compared with the digitised images already placed in the computer's memory bank and instruction set.

An illustration should clarify this operation. Assume the vision system must recognise an object like a screw/nut assembly among a whole field of metallic objects on a sorting table. The screw/nut assembly, as a general rule, will be recognised by its outline, and the light intensity at and around its pixels will help the processor distinguish it from its background of similarly-colored neighbors (see Fig.4).

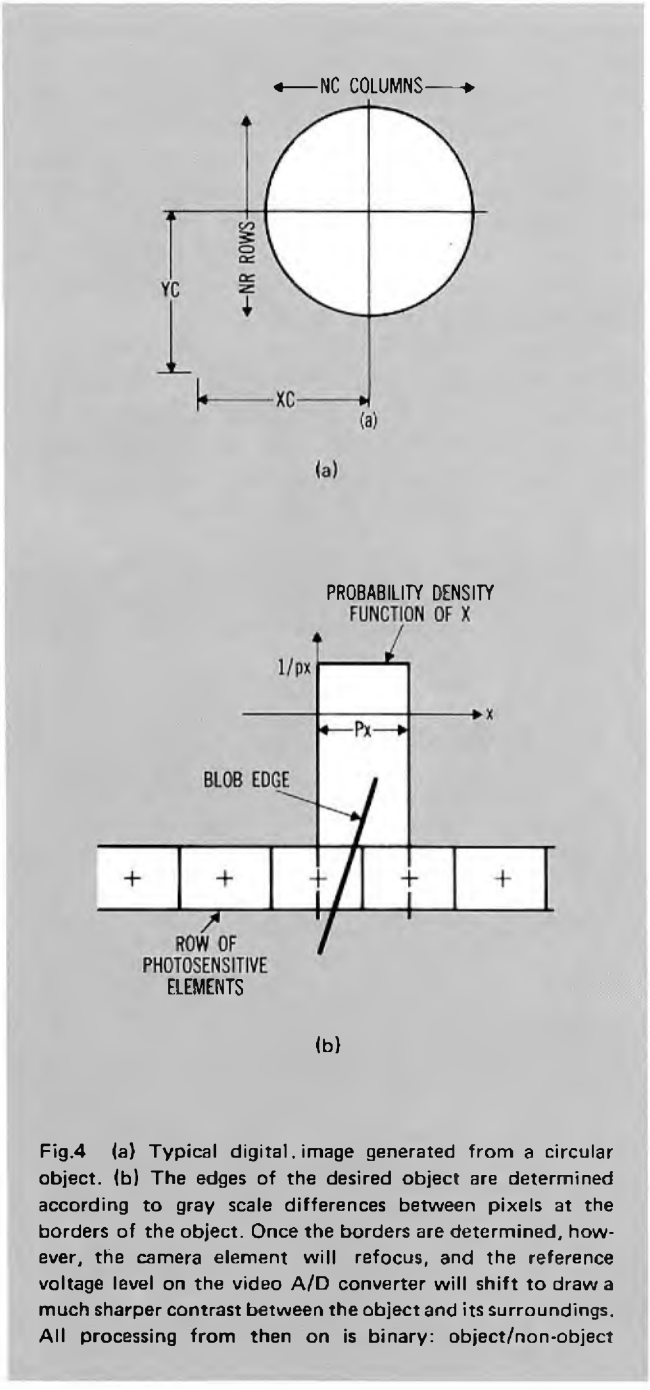

Fig.4 (a) Typical digital image generated from a circular object. (b) The edges of the desired object are determined according to gray scale differences between pixels at the borders of the object. Once the borders are determined, however, the camera element will refocus, and the reference voltage level on the video A/D converter will shift to draw a much sharper contrast between the object and its surroundings. All processing from then on is binary: object/non-object

But to make certain, the vision system may make a second pass at the object: the camera will refocus and the voltage reference level on the A/D converter will shift in order to help the converter and the processor make a gross black and white distinction between the object and its neighbours. In other words, once the objects has been located in its field, the processor will no longer require grey scale information and will work entirely in binary.

In the VS-110, an industry-standard DAC-08 controls the reference voltage level on the 8-bit A/D converter. The use of a multiplying D/A converter like a DAC-08 would most typically require the addition of an outboard data latch, voltage reference, and high-speed op amp, all of which can be conveniently integrated on one chip, such as Signetics' NE5018, a microprocessor-compatible voltage output D/A converter.

In certain applications, it may be possible to reduce some of the bit resolution requirements of the video-speed converter, and thereby some of the cost. If the vision system were dedicated, for example, to distinguishing light objects on a dark background, such as light-colored scratches on a dark paint job, a 6-bit device could be substituted for the 8-bit converter. In some cases even a 4-bit device might do.

LOWER-COST ALTERNATIVES

While the cost of video-speed A/D converters is small compared with the price of a complete LSI-11 computer, it is still a considerable expense, and one that can be significantly reduced by lowering the speed requirements of the vision system. Sophisticated systems, like the VS-110 or General Electric's Optomation II, are designed to recognise up to 900 parts/min on a fast moving conveyor belt. If these objects were on a stationary field, and if there were a smaller number of them, it would naturally be possible to use an optical scanning system and A/D converter components which operate at less than video speeds. If we rationalise the requirement for speed (in fact, a hard thing to do, since the robot's speed and productivity are typically associated), we can substantially reduce the cost of automated visual inspections.

In many cases, a sensing system can use a laser or infrared light source to scan a visual field, and identify objects or patterns according to the way the light reflects onto a series of photodetectors. In some systems, a visual image or pattern can be generated by the ON/OFF sequencing of a photodiode array. In other systems, a single photodetector will register variations in light intensity. The resulting analog voltages can then be digitised and fed to a microprocessor to evaluate and identify patterns.

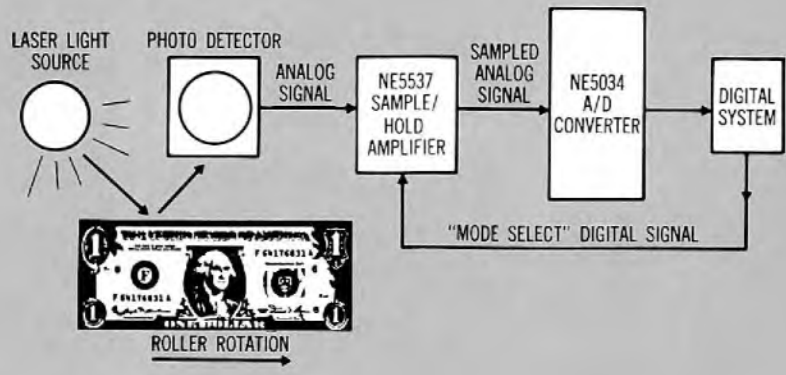

Fig.5 Simplified optical scanning system for dollar bill changers

Dollar bill changers are far more commonplace than industrial robots, yet their function as intelligent visual inspection systems is pretty much the same. A dollar bill is flattened onto the surface of a wide-diameter roller, and as the roller turns, the dollar bill is pulled across the beam of a laser or infrared light source (see Fig.5). The dollar bill will cross the path of the light source at a rate approximating 15 to 30 cm/s. While this rate is very similar to that of an industrial conveyor, it does not take a video-speed converter to distinguish a counterfeit or detective dollar from the good bills inserted in the machine.

In mechanical terms, 15 cm/s may seem fast, but in electronic terms it is enough time for even some of the moderately priced A/D converters to respond. Coupled with an NE5537 sample/hold amplifier on the analog front end, it is entirely possible to use something like Signetics' NE-5034, which converts 8 bits in less than 17 μs. If a high-slew op amp and an 8048 low-cost microprocessor are added, the system will provide enough speed and resolution for the bill changer to recognise foreign currency as well as American dollars. While this type of system is not as versatile as a camera-based system with videospeed converters, it costs considerably less, and – as illustrated with the dollar bill changers – still makes a very effective visual inspection system for robotics applications.

CONTROLLING ROTATIONAL MOVEMENT

While the technology for robotics visual systems is just beginning to develop, the technology for controlling the robot's rotational movements – elbow joints and wrists – is coming into a recognisable maturity. One way of classifying and rating industrial robots, in fact, is by their rotational flexibility. For example, a six-axis machine is more flexible than a four-axis machine; a four-axis machine, more flexible than a three-axis machine, etc. Because rotational flexibility is a strong robot arm selling point, precise control of elbow and wrist joint rotation is a primary concern among robot designers.

At present, there seem to be three main techniques for controlling robot arm rotation. The most popular technique uses an optical-digital encoder in the front end of the control loop, with a D/A converter and pulse-width modulator (PWM) controlling a brushless d.c. motor on the tail end of the loop. A technique used for some of the high-end machines involves high-resolution synchro-to-digital and digital-to-synchro converters. In some of the lower-cost ($10000 or below) machines, a potentiometer within an elbow or wrist joint produces changes in voltage with changes in rotational position. The resulting voltages are, in turn, fed to a processor by a high-resolution A/D converter.

While the 68000 16-bit microprocessor is mentioned more and more frequently in connection with robot controllers, many systems use a distributed intelligence in which the entire arm is under the control of a 16-bit device, and the individual joints are under control of an 8-bit microprocessor. Among those robots using potentiometer control, 12-bits is still the A/D converter standard. Those robot joints relying on synchro-to-digital conversion, on the other hand, often work with 14- and 16-bit resolutions.

Of the available converter elements for rotational position sensing, synchro/resolver and hybrid electronic combinations are most immune to the effects of temperature, humidity, vibration, shock, and power supply variations. Synchro rotational sensors are essentially motor windings – both stator and rotor coils – which measure the phase angle differences between the a.c. voltage reference input (applied to the stator winding) and the a.c. voltage output (both sine and cosine waves at rotor windings). The difference in phase angle will be a function of the rotational position of the rotor shaft (see Fig.6).

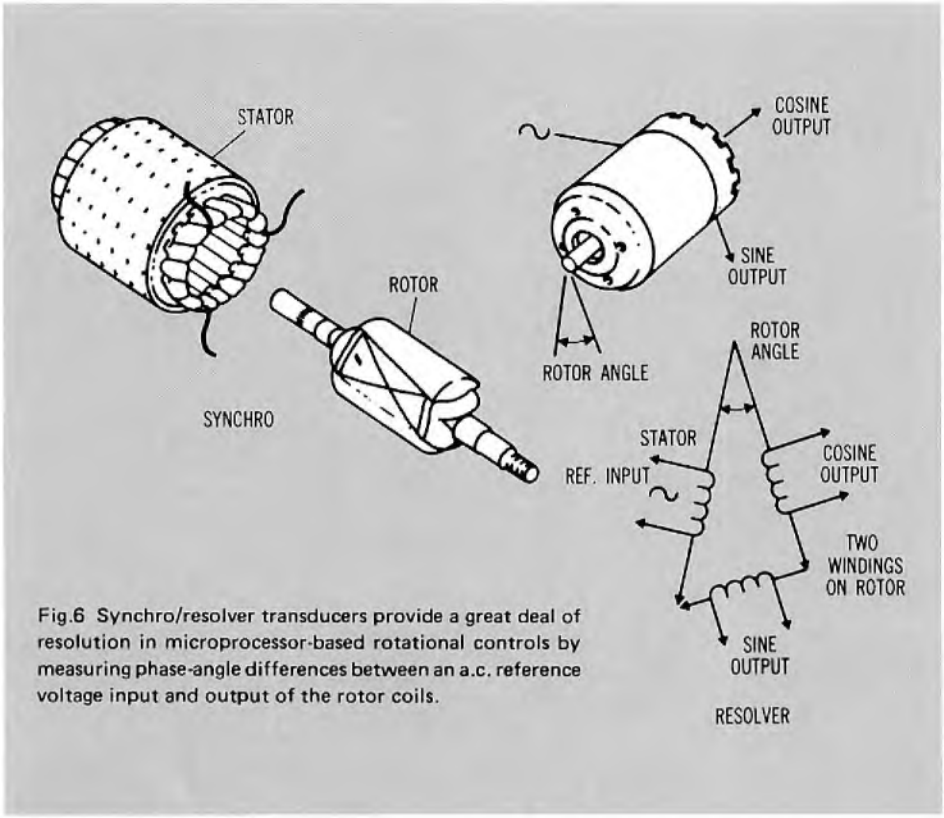

Fig.6 Synchro/resolver transducers provide a great deal of resolution in microprocessor-based rotational controls by measuring phase-angle differences between an a.c. reference voltage input and output of the rotor coils.

Bit resolution in terms of angular rotation

bits		degrees
MSB	1	180
	2	90
	3	45
	4	22.5
	5	11.25
	6	5.625
	7	2.813
	8	1.406
	9	0.7031
	10	0.3516
	11	0.1758
	12	0.08799
	13	0.04395
LSB	14	0.02197

By themselves, synchro/resolvers can provide resolution down to several arc-seconds, and because their voltage amplitude levels are fixed, they can be readily interfaced without amplification circuitry to converters or counters which generate the high-resolution microprocessor codes. Rather than the large resistor ladders used in conventional D/A and A/D converters, synchro-to-digital converters are essentially logic gates and counting mechanisms. Each a.c. signal can be gated (switched on) precisely at the zero crossing to generate a series of pulses. A counter-timer unit can easily digitise the rotor phase angle by indexing the timing interval between gated pulses. A shift register, in turn, can be used to provide binary notation.

Resolution from hybrid or modular synchro-to-digital converters is of the order of 14-bits (see table above). ILC Data Device is one of the leaders in this technology.

POPULAR ROTATIONAL CONTROL

The most widely used rotational control elements are the optical digital shaft encoders. These devices are popular because they provide a very high degree of resolution, with a minimum of interface components. A simplified disc/encoding scheme is shown in Fig.7. The sample disc shown, in combination with the optical sensors, will produce a 4-bit digital code. All 16 code combinations, in fact, are printed right on the disc, and each code combination corresponds to a different rotational position. Encoders with more than 16-bits resolution can be obtained. The only limitation is the number of digital code combinations which can be sensibly imprinted on the disc.

It is the control loop of this system, however, which will typically require data converter components. To find a specific rotational position, the joint-control processor will issue an instruction code to a D/A converter whose analog voltage output regulates the duty cycle of a pulse-width modulator. The PWM, in turn, controls the driving circuitry for a brushless d.c. motor.

A complete sample circuit of this type is shown in Fig.8. Because it includes a data latch, voltage reference, and op amp all on one chip, the NE5018 18-bit D/A converter shown simplifies the job of changing a processor code into the voltage needed to regulate the NE5560 PWM. In the circuit shown, a 50% PWM duty cycle (equivalent to a 3.5 V reference level on pin 5 of the 5560) will lock the motor in a stationary position. As the duty cycle of the PWM drops to 22% (a 2.4 V level on pin 5), the motor will reach maximum clockwise speed. Similarly, if the duty cycle comes up to 80% (4.65 V), the motor will reach maximum counterclockwise speed.

The precision of this particular loop will be in the precision of the digital-encoding feedback loop, rather than in the resolution or accuracy of the D/A converter. Since the basic functions of this control loop's operation are 'on-clockwise', 'stop', 'on-counterclockwise', and 'stop', the entire locomotion system can be controlled with the equivalent of a 4-bit code and very simple microprocessor software routines.

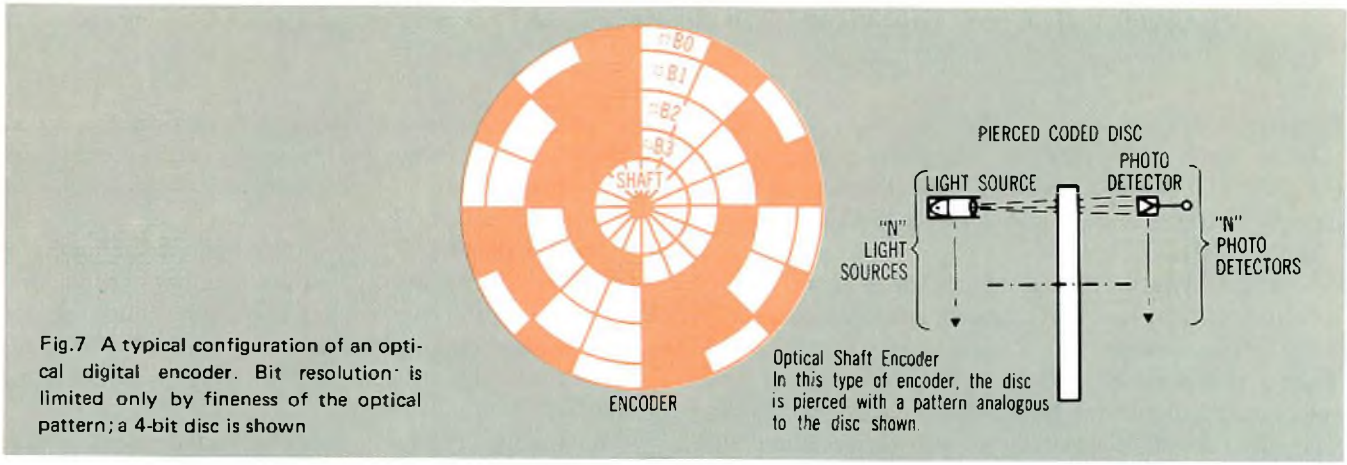

Fig.7 A typical configuration of an optical digital encoder. Bit resolution is limited only by fineness of the optical pattern; a 4-bit disc is shown

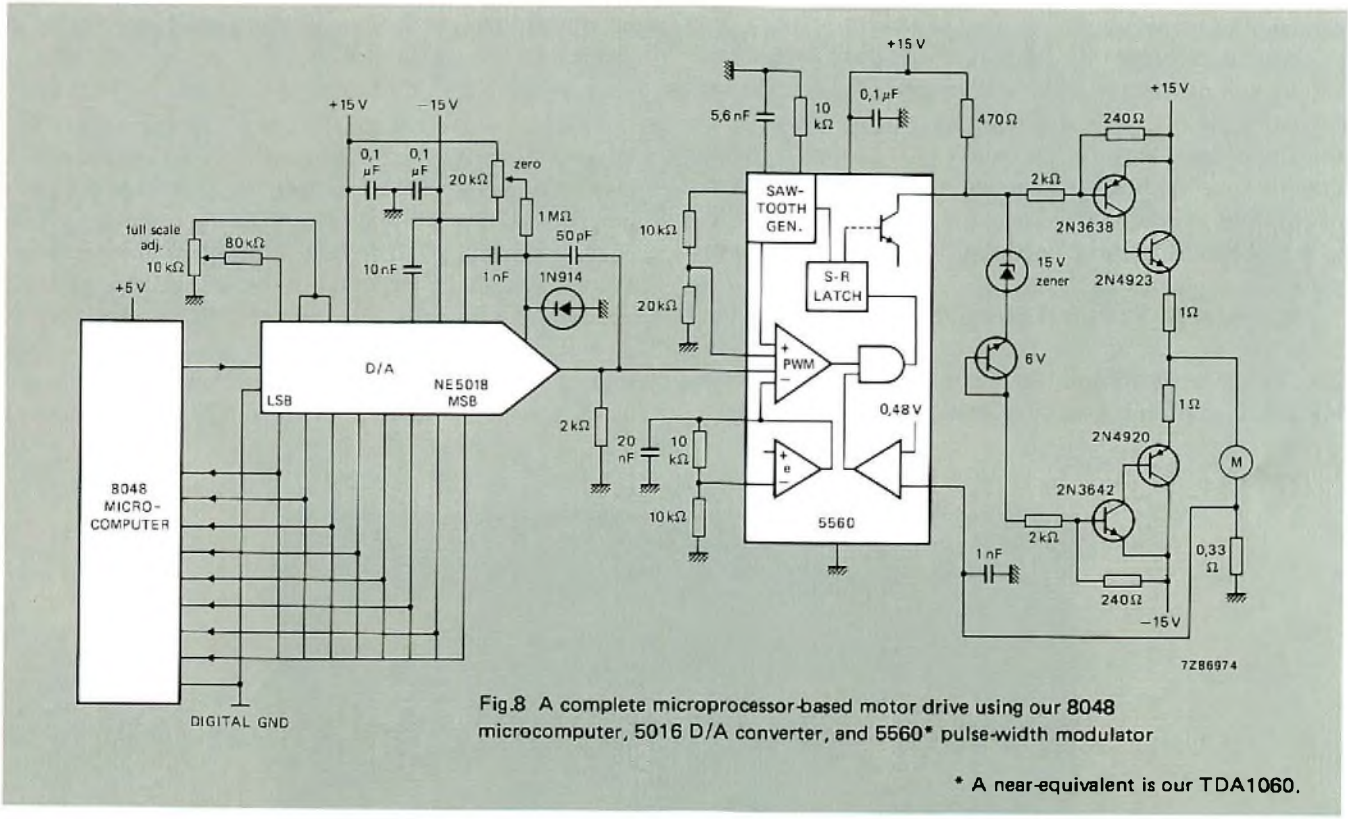

Fig.8 A complete microprocessor-based motor drive using our 8048 microcomputer, 5016 D/A converter, and 5560* pulse-width modulator

* A near-equivalent is our TDA1060.

FUTURE DIRECTIONS

Because of the need for increased industrial productivity, it is likely that industry will evolve a much larger variety of robot machine types. For most industrial customers, a robot assembly arm is a large capital equipment investment. Design engineers will have to evolve lower-cost alternatives to the $50 000 machines. There will undoubtedly be a proliferation of microprocessor-based 'productivity aids'. While not on the scale of fully-programmed robot assemblers, these inspection/sorting devices and simplified robot arm assemblies will typically function like a much needed 'third hand' in the industrial environment – never fully replacing the worker, but inevitably increasing his output.

ACKNOWLEDGEMENT

This article is based on one that was published in Electronic Products, 7 September 1982, copyright Hearst Business Communications, Inc.; permission to reprint is gratefully acknowledged.

REFERENCE

J. G. van den Hanenberg and J. Vredenbregt 'An experimental assembly robot', Philips Technical Review, Vol. 40, 1982, No. 2/3.

MEA8000 VOICE SYNTHESISER TO BE DEMONSTRATED AT PHONETICS CONGRESS

Philips will demonstrate the MEA8000 voice synthesiser (EC&A, Vol.4 No.2) and its simplified editing system (EC&A, Vol.4 No.4) at the tenth International Congress of Phonetic Sciences to be held August 1st to August 6th this year at Utrecht.

The simplicity of the techniques involved will be demonstrated live by means of a modem link to the company's VAX 11/70 computer at its Eindhoven headquarters. Visitors to the exhibition stand will be able to have their voices recorded onto the Philips Chatterbox II unit, which will then decode the analogue voice information and digitise it for transmission over a telephone line to the central VAX computer.

Once the decoded voice data has been down-loaded, an editing console on the stand will be used to access the information and display the resultant pitch, volume and formant codes. Using Philips' own VAX 11 software, these may then be modified as required, either to improve the match between the digital code and the voice print or to make subtle changes in inflection or pitch to meet a user's particular requirements.

Once satisfied with the results of the editing process, the operator can call up the codes to directly program an EPROM on a demonstration board that also contains an MEA8000, controlling circuitry, and an output loudspeaker to replay the synthesised speech. In this way visitors will be able to judge for themselves the quality results possible with the formant version of Linear Predictive Coding used in the MEA8000.

Despite all the publicity that has surrounded voice synthesizers, few commercial applications have so far been realised, in part due to misconceptions about supposed complications of implementing such devices. With the demonstration at Utrecht, Philips hopes to dispel these misconceptions.

In Europe, Philips currently operates speech editing centres at Eindhoven, Mitcham, Hamburg and Paris; and in the United States at Sunnyvale (Signetics). Users wishing to conduct their own synthesizer programming can also purchase a complete stand-alone coding and editing suite.

Product support extends from supplying the basic MEA8000 on its own, through complete coding and editing of a customer's own transcripts and supplying the ready programmed PROMs and MEA8000, to complete printed circuits (including MEA8000, MAB8048 microprocessor and PROMs) in quantities up to several hundred, as well as sub-assembly modules with complete I/O facilities. In this way the company believes it can guide potential users through the formative and educational stages of implementing voice synthesizer devices in a host of applications.

VACUUM PHOTO-TRIODES FOR HIGH-ENERGY PHYSICS

A new series of 3-inch vacuum photo-triodes from Philips operates in magnetic fields as high as one tesla. These 1500XP series triodes can therefore be used in modern solenoid-enclosed particle detection systems in high-energy physics experiments, where the fields generated are tens of thousands of times stronger than the earth's.

The low light levels which are produced by nuclear particles interacting with, for example, lead glass can be detected by these tubes. A triode gain of more than 10 lifts the signals out of the noise of the following preamplifier, and enables pulse height resolutions to be obtained which rival those of traditional photomultipliers.

The tubes have a high-sensitivity bialkaline photocathode and a unique mechanical design, which enables them to work in magnetic fields at angles up to 70° to their axis.

Abstracts

CMOS gate arrays – the fast way to semi-custom logic

This article describes a new range of silicon-gate CMOS gate arrays. The range is backed by a comprehensive CAD package which allows logic system designers to retain control of the IC design. Details of the internal structure of the arrays are given together with a description of the CAD package and performance data.

Data communications

As the number of computers in use and the speed and volume of their output have increased, so has the need to transmit their output to more places and over longer distances. Inherent to the data communication process are various elements, devices, techniques and systems, as well as standards and procedures. Understanding of these can help users of computer services to take advantage of the communications systems that are now available.

The magnetoresistive sensor – a sensitive device for detecting magnetic-field variations

The magnetoresistive sensor (MRS) is a recent development for measuring magnetic-field variations, and provides an attractive alternative to more conventional Hall-effect sensors. The device comprises four permalloy strips arranged to form a Wheatstone bridge – the output of which provides a measure of the prevailing magnetic field. Since even quite small movements of actuating components in machinery can create measurable changes in magnetic field, the MRS can act as a sensitive position sensor in instrumentation and control equipment, and in electronic ignition systems.

Circulators and isolators for reducing transmitter intermodulation

Circulators and isolators are highly effective in reducing intermodulation between transmitters operating on closely spaced frequencies. They are particularly useful when the intermodulation products fall in parts of the frequency spectrum removed by kilohertz rather than megahertz from the wanted frequencies. This article describes circular/isolator operation, discusses their use in transmitting systems and gives some operating recommendations.

A complete f.m. radio on a chip

This article describes a new superheterodyne f.m. reception system which is almost totally integrated and requires only one external coil and a few inexpensive ceramic capacitors. In-depth design information is given and several complete radios are presented together with a selection of suitable audio amplifiers.

Progress in SMPS magnetic components optimisation

The design of transformers and chokes for switched-mode power supplies is now well understood. Published design routines make for predictable performance and straightforward design optimisation. The understanding gained from the preparation of these routines has been applied to the design of the ferrite cores themselves. The result is a new range of hardware – cores, coil formers and mounting accessories – the ETD system.

Data converters for robotics

To the extent that they combine the functions of sensing, digital data processing, and locomotion, most industrial robots share fundamentally similar architecture. The important differences that affect cost are speed, resolution, and versatility. Correctly specifying the sensing and locomotion functions in relation to the robot's intended task has a decisive influence on the choice of A/D and D/A converters and on the ultimate cost/performance ratio.

CMOS Gate Arrays – Der schnelle Weg zu digitalen Kundenschaltungen

Der Aufsatz beschreibt eine neue Reihe CMOS Gate Arrays in Silizium-Gate-Technologie. Ein umfangreiches CAD-Paket unterstützt diese Reihe und erlaubt dem Systemingenieur die Kontrolle des IC-Design. Einzelheiten der inneren Struktur der Arrays werden diskutiert, zusammen mit einer Beschreibung der CAD-Programme und der Eigenschaften.

Datenübertragung

Mit dem Wachstum der Anzahl eingesetzter Computer nahmen auch Geschwindigkeit und Umfang ihrer Ausgabedaten erheblich zu. Entsprechend wuchs auch die Notwendigkeit, die Ausgabedaten an mehr Plätze sowie über grössere Entfernungen zu übertragen. Dieser Datenübertragungsprozess wird mit verschiedenen, speziell dafür ausgelegten Komponenten, Geräten, Technologien, aber auch Normen und Vereinbahrungen realisiert. Das Verständniss dieser Grundlagen kann dem Kunden von Computerdiensten dabei helfen, die Möglichkeiten, die Übertragungssysteme heute bieten, zu seinen Vorteil zu nutzen.

Der magnetoresistive Sensor – ein empfindliches Bauelement für Messung von Magnetfeldern

Der magnetoresistive Sensor (MRA) ist eine Neuentwicklung für Messung von Magnetfeldern, die eine interessante Alternative zu den konventionellen Hall-Elementen darstellt. Der Sensor enthält vier Permalloy-Streifen, die so angeordnet sind, dass die eine Wheatstone-Brücke bilden. Das Ausgangssignal dieser Brücke ist ein Mass für das herrschende Magnetfeld. Da auch sehr kleine Bewegungen von Maschinenbauteilen messbare Änderungen des Magnetfeldes hervorrufen können, lässt sich der magnetoresistive Sensor als empfindlicher Positionsfühler in Instrumenten, Steuergeräten und elektronischen Zündsystemen verwenden.

Zirkulatoren und Einwegleitungen zur Verminderung von Intermodulation bei Sendern.

Mit Hilfe von Zirkulatoren und Einwegleitungen lässt sich ausserordentlich wirksam die Intermodulation zwischen Sendern mit eng benachbarten Frequenzen reduzieren. Zirkulatoren und Einwegleitungen erweisen sich in höherem Masse nützlich, wenn die Intermodulationsprodukte in einem Frequenzbereich, der nur einige kHz entfernt ist, anfallen, als wenn sie um MHz von den Betriebsfrequenzen entfernt liegen würden. Der Artikel beschreibt den Betrieb von Zirkulatoren und Einwegleitungen, diskutiert ihre Anwendung in Sendesystemen und gibt einige Betriebsempfehlungen.

Ein vollständiges FM-Radio auf einem Chip

In diesem Artikel wird ein FM-Überlagerungsempfänger beschrieben, der nach einem neuartigen Prinzip arbeitet, sich fast vollständig integrieren lässt und nur eine externe Spule sowie einige preiswerte keramische Kondensatoren benötigt. Weiterhin enthält der Artikel genaue Informationen für den Schaltungsentwurf. Schliesslich werden mehrere vollständige Empfänger zusammen mit einer Auswahl geeigneter NF-Verstärker vorgestellt.

Fortschritte bei der Optimierung magnetischer Bauelemente für Schaltnetzteile

Der Entwurf von Transformatoren und Drosseln für Schaltnetzteile wird nunmehr gut beherrscht. Die angegebenen Entwurfsverfahren führen zu voraussagbarem Verhalten und zu einer unkomplizierten Optimierung des Entwurfs. Die bei der Ausarbeitung dieser Verfahren gewonnenen Erkenntnisse sind beim Entwurf der Ferritkerne selbst verwendet worden, was zu einer neuen Reihe von Kernen, Spulenkörpern und Montage-Zubehör geführt hat – dem ETD-System.

Signalkonverter für Roboter-Steuerungen

Im den Masse wie die Funktionen Messwertaufnahme, digitale Datenverarbeitung und Bewegung kombiniert werden, besitzen die meisten industriellen Roboter im Grunde eine ähnliche Architektur. Die wesenlichen Unterschiede, die den Preis beeinflussen, sind Geschwindigkeit und Vielseitigkeit. Eine sorgfältige Spezifikation der Messwertaufnahme und Bewegungsfunktionen in Anpassung an die geplante Verwendung des Roboters ist notwendig. Sie beeinflusst entscheidend die Wahl der A/D- und D/A-Wandler und das endgültige Preis/Leistungsverhältnis.

Réseaux de portes CMOS – une logique sur mesure à portée de la main

Cet article dcrit une nouvelle gamme de réseaux de porte CMOS au silicium. Cette gamme bénéficie d'un progiciel de CAO complet qui permet aux concepteurs de systèmes logiques de contrôler également la conception du circuit intégré. Cet article donne également des détails sur la structure interne des réseaux ainsi qu'une description du progiciel de CAO et des caractéristiques de fonctionnement.

Transmission de données

Parallèlement à l'augmentation du nombre des ordinateurs en service ainsi que de leur vitesse et de leur volume de travail, il s'est avéré de plus en plus nécessaire de transmettre les données produites en des lieux plus nombreux et sur des distances plus longues. Divers éléments, dispositifs, techniques et systèmes ainsi que diverses normes et procédures, sont inhérents au processus de transmission des données. Leur bonne compréhension peut aider les utilisateurs de l'informatique à tirer pleinement parti des systèmes de transmission actuellement disponibles.

Le détecteur magnétorésistif

Un petit dispositif permettant de détecter les variations d'un champ magnétique. Développement récent dans la mesure des variations de champs magnétiques, le détecteur magnétorésistif (MRS) est une alternative intéressante aux détecteurs plus classiques à effet Hall. Ce dispositif comprend quatre barrettes en permalloy disposées en pont de Wheatstone dont la sortie fournit une mesure du champ magnétique dominant. Etant donné que même d'infimes mouvements de composants mobiles dans des machines peuvent engendrer des modifications mesurables du champ magnétique, le MRS peut être utilisé comme détecteur de position sensible dans des équipements d'instrumentation et de régulation et dans des systèmes d'allumage électronique.

Circulateurs et isolateurs pour la réduction de l'intermodulation dans les émetteurs

Les circulateurs et les isolateurs sont extrêmement efficaces pour réduire l'intermodulation entre des émetteurs utilisant des fréquences très proches. Ils sont particulièrement utiles lorsque les produits de l'intermodulation tombent dans des zones du spectre de fréquence éliminées par kilohertz et non pas par mégahertz des fréquences requises. Cet article décrit le fonctionnement des circulateurs/isolateurs, examine leurs applications dans les systèmes d'émission et propose certaines recommandations pratiques.

Une radio f.m. complète sur une puce

Cet article décrit un nouveau système de réception f.m. superhétérodyne presque entièrement intégré qui n'exige qu'une bobine externe et quelques condensateurs céramiques peu coûteux. Outre des informations de conception approfondies, on trouvera une présentation de plusieurs récepteurs complets ainsi qu'une sélection d'amplificateurs audio adaptés.

Progrès dans l'optimisation des composants magnétiques SMPS

La conception des transformateurs et inductances pour les alimentations à découpage est désormais bien comprise. Les méthodes de conception publiées vont dans le sens de performances prévisibles et d'une optimisation nette de la conception. L'expérience acquise lors de l'élaboration de ces méthodes a été appliquée à la conception des noyaux en ferrite eux-mêmes. Le résultat est une nouvelle gamme de matériel – noyaux, mandrins et accessoires de montage – le système ETD.

Convertisseurs de données pour la robotique

Dans la mesure où ils réunissent les fonctions de détection, de traîtement numérique des données et de locomotion, la plupart des robots industriels partagent une architecture similaire pour l'essentiel. Les différences majeures qui affectent le coût résident dans la vitesse, la résolution et la souplesse d'emploi. La spécification des fonctions correctes de détection et de locomotion, par rapport à la tâche prévue du robot, a une influence déterminante sur le choix des convertisseurs A/N et N/A et sur le rapport coût/performances final.

Redes de puertas CMOS – el camino más rapido hacia la lógica semi-custom

Este artículo describe una nueva familia de redes de puertas CMOS de silicio. Esta familia está soportada por una colección de programas de fácil manejo para diseño ayudado por ordenador, que permite a los diseñadores de sistemas lógicos mantener un control del diseño del circuito integrado. Se dan detalles de la estructura interna de las redes junto con una descripción de la colección de programas y de los datos de funcionamiento.

Comunicación de datos

Con el aumento del número de ordenadores en uso y de la velocidad y volumen de sus salidas, ha aumentado la necesidad de transmitir sus salidas a más puntos y a mayores distancias. Inherente al proceso de comunicación de datos existen diversos elementos, dispositivos, técnicas y sistemas, así como estándares y procedimientos, cuya comprensión puede ayudar a los usuarios de los servicios de ordenador a conocer los sistemas de comunicaciones disponibles actualmente.

El sensor magnetoresistivo – un dispositivo sensitivo para detectar variaciones de campo magnético

El sensor magnetoresistivo (MRS) es un desarrollo reciente que mide variaciones de campo magnético, y proporciona una atractiva alternativa a los sensores convencionales de efecto Hall. El dispositivo contiene cuatro cintas permalloy dispuestas para formar un puente de Wheatstone – la salida del cual proporciona una medida del campo magnético. Ya que incluso un movimiento muy pequeño de los componentes que actuan en la maquinaria puede crear variaciones medibles en el campo magnético, el sensor magnetoresistivo puede actuar como sensor de posición sensitivo en instrumentación y equipos de control y en sistemas electrónicos de ignición.

Circuladores y aisladores para reducir la intermodulación de transmisores

Los circuladores y aisladores son muy efectivos para reducir la intermodulación entre transmisores que trabajan en frecuencias muy cercanas. Son particularmente útiles cuando los productos de intermodulación caen en zonas del espectro de frecuencia a una distancia de las frecuencias deseadas del orden de los kilociclos mas que del orden de los megacidos. Este artículo describe el funcionamiento del circulador/aislador, se estudia su utilización en sistemas de transmisión y se dan algunas recomendaciones de operación.

Radio f.m. completa en un chip

Este artículo describe un nuevo sistema superheterodino de recepción de f.m. que está casi totalmente integrado y sólo requiere una bobina externa y algunos condensadores cerámicos baratos. Se da la información detallada del diseño y se presentan algunas radios completas y una selección de los amplificadores de audio adecuados.

Progresos en la optimizacion de componentes magnéticos para fuentes de alimentación conmutadas

El diseño de transformadores y choques para fuentes de alimentación conmutadas es ya bien conocido. Las rutinas de diseño publicadas se hacen para un funcionamiento predecible y para una optimización del diseño sin complicaciones. Los conocimientos obtenidos a partir de la preparación de estas rutinas han sido aplicados al diseño de los propios núcleos de ferrita. El resultado es una nueva gama de núcleos, formadores de bobina y accesorios de montaje – el sistema ETD.

Convertidores de datos para robótica

Por el hecho de que combinan las funciones de sensado, procesado digital de datos y locomoción, la mayoría de los robots industriales tienen la arquitectura fundamentel similar. Las diferencias importantes que afectan al costo son: velocidad, resolución y versatilidad. La correcta especificación de las funciones de sensado y locomoción en relaciñon con la tarea para la que ha sido diseñado el robot, tiene una influencia decisiva en la selección de convertidores A/D y D/A y en la definitiva relación costo/prestaciones.

Authors

Lout P. M. Bracke, born 1948 in Eindhoven, took his degree in electrical engineering at Eindhoven Polytechnic and, after two years with Philips cable television group, continued his studies at the University of Technology, Eindhoven. Since 1980 he has worked for the Electronic Components and Materials Division as a member of the magnetic materials development group of the ceramics laboratory.

Alex Goldberger gained his BSEE degree at the City College of New York and his MSEE at the Polytechnic Institute of Brooklyn. He has worked in integrated circuits since 1969 and was design manager for the first large-scale integrated circuit for data communications. As applications manager for the microprocessor division of Signetics Corporation, Sunnyvale, California, he is responsible for product applications support, new product planning, and technical marketing support for microprocessor products.

Rob Croes, born in Nijmegen, graduated in electrical engineering at 's Hertogenbosch in 1963. After military service he joined the IC development group of Philips Electronic Components and Materials Division, Nijmegen, where he worked on the design of bipolar digital ICs and is now involved in development of CMOS gate arrays and the new high-speed CMOS family.

Werner Golombek was born in Beuthen, Germany, in 1931. He studied electrical engineering at the Technical Universities of Hannover and Darmstadt, receiving his Dip. Ing. in 1957. The same year he joined Valvo, initially working in the Quality Laboratory for Professional Tubes, Hamburg. He is now quality manager for Professional Tubes, and since 1976 he has also been responsible for circulator development and production.

U. Dibbern studied physics at Hamburg University, receiving his doctorate in 1965. He joined Philips Research, Hamburg the same year, initially working on gas discharge devices, and subsequently on non-impact printers, speech synthesis, data processing, and since 1980, on sensors.

Michael Hufschmidt was born at Solingen, Germany, in 1947. He studied at Tübingen and Bochum and, after gaining his doctorate in nuclear physics, joined Valvo in Hamburg where he is now product marketing manager for radio, audio, and industrial integrated circuits.

Wim van Dooremolen was born in Eindhoven, The Netherlands, in 1937 and joined Philips in 1956 to work on ultra-short-wave transmitting tubes. Since 1965 he has been working in the radio/audio section of the central application laboratory of the Electronic Components and Materials Division, where he is currently engaged in the design and application of bipolar integrated radio circuits.

August Petersen was born near Flensburg, Germany, in 1937, and graduated in physics from the University of Kiel in 1964. The same year he joined Valvo Applications Laboratory, Hamburg, initially working on applications of passive components, especially piezo-electric ceramics. As a member of the Industrial Electronics Group, he is currently responsible for developing sensor control circuitry.

Philips Electronic Components & Materials

Philips Electronic Components and Materials Division (Elcoma) embraces a group of companies with sales and manufacturing facilities in every major component market. Together we offer OEMs the greatest in-depth support in component technologies, in systems application and in the widest range of components. Fundamental support in providing the latest technologies comes from Philips Research Laboratories - recognised throughout the world for their contributions to science and industry.

The components and materials we supply cover the entire range of present-day electronics.

DISPLAY SYSTEMS

B & W tv display systems
Colour tv display systems
Data graphic display systems

INTEGRATED CIRCUITS

Bipolar analogue
Consumer circuits
● video & radio/audio circuits

Industrial circuits
● opamps ● voltage regulators
● comparators ● D/A & A/D converters
● amplifiers ● interface circuits

Bipolar digital
Standard logic families
● TTL/STTL ● ECL 10K/100K

LSI circuits
● gate arrays ● interface circuits

8-bit Microprocessors

Memories
● RAMs/PROMs ● Fuse logic

NMOS
8 and 16-bit Microprocessors & peripherals

Logic systems
● video & radio/audio circuits
● text decoders

ROM memories

CMOS
Standard logic families

LSI circuits
● gate arrays ● clock circuits

8-bit Microprocessors

Hybrid integrated circuits
LF, VHF, UHF & microwave circuits
D/A converters
Proximity switches
Custom-designed circuits

ELECTRO-OPTICAL DEVICES

Image intensifier devices
Infra-red image detectors
Camera tubes
Imaging devices

SEMICONDUCTORS

Small-signal diodes
Medium and high-power diodes
Controlled rectifiers
LF & HF small-signal transistors
LF & HF power transistors
Microwave semiconductors
Opto-electronic semiconductors
Semiconductors for hybrid ICs
Semiconductor sensors

PROFESSIONAL TUBES

Industrial cathode-ray tubes
Photomultiplier tubes
Geiger Müller tubes
Transmitting tubes
Microwave devices
Reed switches

MATERIALS

Ferroxcube products
Permanent magnets
Piezoelectric products
White ceramic products

PASSIVE COMPONENTS

Ceramic, film and foil capacitors
Electrolytic capacitors
Fixed resistors
Variable capacitors
Potentiometers and resistor trimmers
Non-linear resistors
Delay lines
Piezoelectric quartz devices

ASSEMBLIES

Electric motors
Loudspeakers
Tuners
Connectors
Printed circuit boards
Variable transformers
Thumbwheel switches
Industrial microcomputer systems
Microwave sub-assemblies

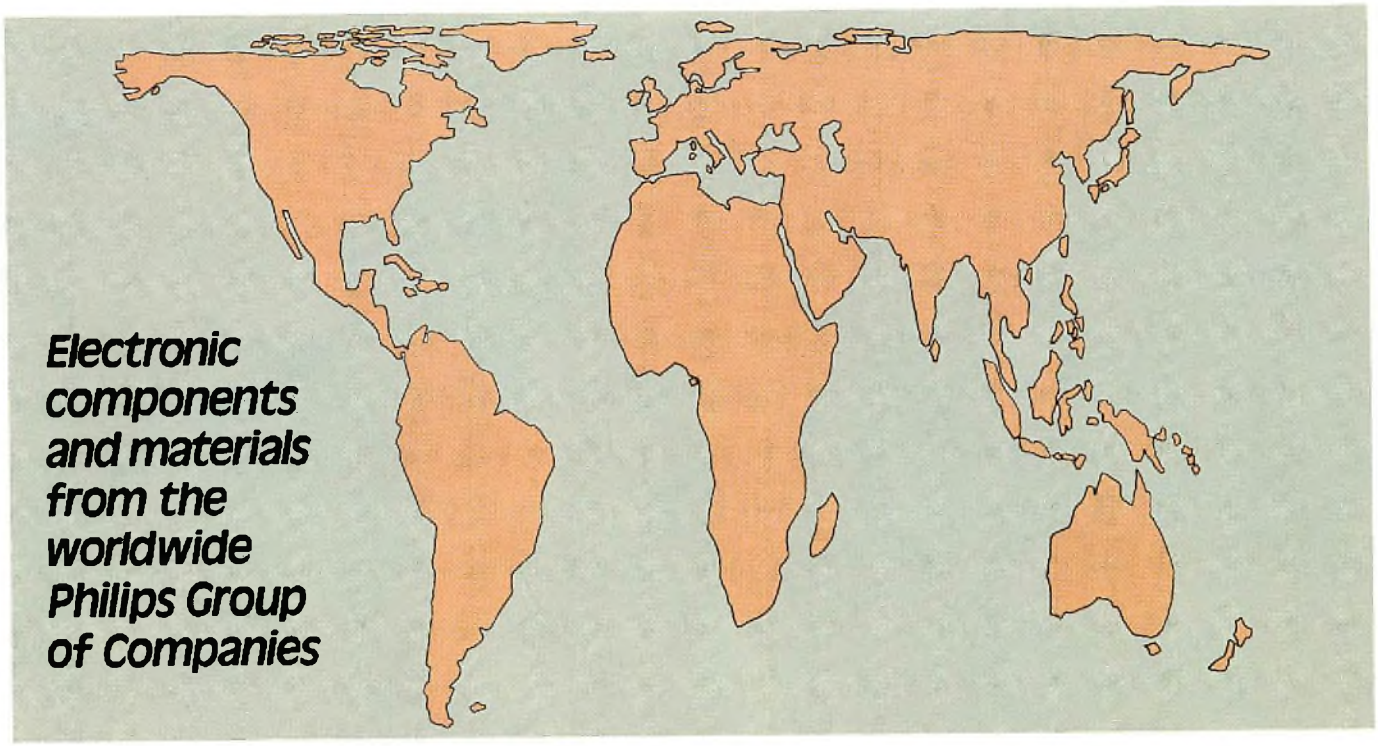

Argentina: PHILIPS ARGENTINA S.A., Div. Elcoma, Vedia 3892, 1430 BUENOS AIRES, Tel. 541-7141/7242/7343/7444/7545.
Australia: PHILIPS INDUSTRIES HOLDINGS LTD., Elcoma Division, 67 Mars Road, LANE COVE, 2066, N.S.W., Tel. 427 08 88.
Austria: ÖSTERREICHISCHE PHILIPS BAUELEMENTE Industrie G.m.b.H., Triester Str. 64, A-1101 WIEN, Tel. 62 91 11.
Belgium: N.V. PHILIPS & MBLE ASSOCIATED, 9, rue du Pavillon, B-1030 BRUXELLES, Tel. (02) 242 74 00.
Brazil: IBRAPE, Caixa Postal 7383, Av. Brigadeiro Faria Lima, 1735 SAO PAULO, SP, Tel. (011) 211-2600.
Canada: PHILIPS ELECTRONICS LTD., Electron Devices Div., 601 Milner Ave., SCARBOROUGH, Ontario, M1B 1M8, Tel. 292-5161.
Chile: PHILIPS CHILENA S.A., Av. Santa Maria 0760, SANTIAGO, Tel. 39-4001.
Colombia: SADAPE S.A., P.O. Box 9805, Calle 13, No. 51 + 39, BOGOTA D.E. 1., Tel. 600 600.
Denmark: MINIWATT A/S, Emdrupvej 115A, DK-2400 KOBENHAVN NV., Tel. (01) 69 16 22.
Finland: OY PHILIPS AB, Elcoma Division, Kaivokatu 8, SF-00100 HELSINKI 10, Tel. 172 71.
France: R.T.C. LA RADIOTECHNIQUE-COMPELEC, 130 Avenue Ledru Rollin, F-75540 PARIS 11, Tel. 355-44-99.
Germany: VALVO, UB Bauelemente der Philips G.m.b.H., Valvo Haus, Burchardstrasse 19, D-2 HAMBURG 1, Tel. (040) 3296-0.
Greece: PHILIPS S.A. HELLENIQUE, Elcoma Division, 52, Av. Syngrou, ATHENS, Tel. 9215111.
Hong Kong: PHILIPS HONG KONG LTD., Elcoma Div., 15/F Philips Ind. Bldg., 24-28 Kung Yip St., KWAI CHUNG, Tel. (0)-24 51 21.
India: PEICO ELECTRONICS & ELECTRICALS LTD., Elcoma Div., Ramon House, 169 Backbay Reclamation, BOMBAY 400020, Tel. 295144.
Indonesia: P.T. PHILIPS-RALIN ELECTRONICS, Elcoma Div., Panim Bank Building, 2nd Fl., Jl. Jend. Sudirman, P.O. Box 223, JAKARTA, Tel. 716 131.
Ireland: PHILIPS ELECTRICAL (IRELAND) LTD., Newstead, Clonskeagh, DUBLIN 14, Tel. 69 33 55.
Italy: PHILIPS S.p.A., Sezione Elcoma, Piazza IV Novembre 3, I-20124 MILANO, Tel. 2-6752.1.
Japan: NIHON PHILIPS CORP., Shuwa Shinagawa Bldg., 26-33 Takanawa 3-chome, Minato-ku, TOKYO (108), Tel. 448-5611.
(IC Products) SIGNETICS JAPAN LTD., 8-7 Sanbancho Chiyoda-ku, TOKYO 102, Tel. (03)230-1521.
Korea: PHILIPS ELECTRONICS (KOREA) LTD., Elcoma Div., Philips House, 260-199 Itaewon-dong, Yongsan-ku, C.P.O. Box 3680, SEOUL, Tel. 794-4202.
Malaysia: PHILIPS MALAYSIA SDN. BERHAD, No. 4 Persiaran Barat, Petaling Jaya, P.O.B. 2163, KUALA LUMPUR, Selangor, Tel. 77 44 11.
Mexico: ELECTRONICA, S.A. de C.V., Carr. Mexico-Toluca km. 62.5, TOLUCA, Edo. de Mexico 50140, Tel. Toluca 91(721)613-00.
Netherlands: PHILIPS NEDERLAND, Marktgroep Elonco, Postbus 90050, 5600 PB EINDHOVEN, Tel. (040) 79 33 33.
New Zealand: PHILIPS ELECTRICAL IND. LTD., Elcoma Division, 110 Mt. Eden Road, C.P.O. Box 1041, AUCKLAND, Tel. 605-914.
Norway: NORSK A/S PHILIPS, Electronica Dept., Sandstuveien 70, OSLO 6, Tel. 68 02 00.
Peru: CADESA, Av. Alfonso Ugarte 1268, LIMA 5, Tel. 326070.
Philippines: PHILIPS INDUSTRIAL DEV. INC., 2246 Pasong Tamo, P.O. Box 911, Makati Comm. Centre, MAKATI-RIZAL 3116, Tel. 86-89-51 to 59.
Portugal: PHILIPS PORTUGESA S.A.R.L., Av. Eng. Duarte Pacheco 6, LISBOA 1, Tel. 68 31 21.
Singapore: PHILIPS PROJECT DEV. (Singapore) PTE LTD., Elcoma Div., Lorong 1, Toa Payoh, SINGAPORE 1231, Tel. 25 38 811.
South Africa: EDAC (Pty.) Ltd., 3rd Floor Rainer House, Upper Railway Rd. & Ove St., New Doornfontein, JOHANNESBURG 2001, Tel. 614-2362/9.
Spain: MINIWATT S.A., Balmes 22, BARCELONA 7, Tel. 301 63 12.
Sweden: PHILIPS KOMPONENTER A.B., Lidingövägen 50, S-11584 STOCKHOLM 27, Tel. 08/67 97 80.
Switzerland: PHILIPS A.G., Elcoma Dept., Allmendstrasse 140-142, CH-8027 ZURICH, Tel. 01-488 22 11.
Taiwan: PHILIPS TAIWAN LTD., 3rd Fl., San Min Building, 57-1, Chung Shan N. Rd, Section 2, P.O. Box 22978, TAIPEI, Tel. (02)-5631717.
Thailand: PHILIPS ELECTRICAL CO. OF THAILAND LTD., 283 Silom Road, P.O. Box 961, BANGKOK, Tel. 233-6330-9.
Turkey: TÜRK PHILIPS TICARET A.S., EMET Department, Inonu Cad. No. 78-80, ISTANBUL, Tel. 43 59 10.
United Kingdom: MULLARD LTD., Mullard House, Torrington Place, LONDON WC1E 7HD, Tel. 01-580 6633.
United States: (Active Devices & Materials) AMPEREX SALES CORP., Providence Pike, SLATERSVILLE, R.I. 02876, Tel. (401) 762-9000.
(Passive Devices) MEPCO/ELECTRA INC., Columbia Rd., MORRISTOWN, N.J. 07960, Tel. (201)539-2000.
(Passive Devices & Electromechanical Devices) CENTRALAB INC., 5855 N. Glen Park Rd., MILWAUKEE, WI 53201, Tel. (414)228-7380.
(IC Products) SIGNETICS CORPORATION, 811 East Arques Avenue, SUNNYVALE, California 94086, Tel. (408) 739-7700.
Uruguay: LUZILECTRON S.A., Avda Uruguay 1287, P.O. Box 907, MONTEVIDEO, Tel. 91 43 21.
Venezuela: IND. VENEZOLANAS PHILIPS S.A., Elcoma Dept., A. Ppal de los Ruices, Edif. Centro Colgate, CARACAS, Tel. 36 05 11.

For all other countries apply to: Philips Electronic Components and Materials Division, Corporate Relations & Projects, Building BAE-3, P.O. Box 218, 5600 MD EINDHOVEN, The Netherlands, Tel. +31 40 72 33 04, Telex 35000 phtc nl/nl be vec.

Printed in The Netherlands

9398 703 80011